Dissertation

submitted to the
Combined Faculties for the Natural Sciences and for Mathematics
of the Ruperto-Carola University of Heidelberg, Germany
for the degree of
Doctor of Natural Sciences

presented by

Andreas Matern, M.Sc.

born in Lahr (Schwarzwald), Germany

Oral examination:_____

Flavin uptake and metabolism in *Listeria monocytogenes* and FMN riboswitches as targets for riboflavin analogs

Referees: Prof. Dr. Michael Wink
Prof. Dr. Matthias Mack

"An expert is a person who has found out by his own painful experience all the mistakes that one can make in a very narrow field."

Nils Bohr

This work is dedicated to my family.

Abstract

The riboflavin analog roseoflavin – an antibiotic produced by the bacteria *Streptomyces davawensis* and *Streptomyces cinnabarinus*, and the key intermediate of the roseoflavin biosynthesis, 8-demthyl-8-amino riboflavin which is an antibiotic as well, are both known to have a growth inhibiting effect on the human pathogen *Listeria monocytogens*. The adverse effect of roseoflavin on *L. monocytogenes* has been proposed to be a result of its interaction with the FMN riboswitch *Rli96*, regulating expression of the riboflavin transporter gene *lmo1945*. Whether flavin analogs, such as roseoflavin and 8-demethyl-8-amino riboflavin, are assimilated by *L. monocytogenes* through the riboflavin transporter protein Lmo1945 has not yet been known. In addition, the conversion of flavin analogs into cofactor analogs by flavokinase/FAD synthetase enzymes from *L. monocytogenes* has not been investigated. The functional analysis of the effect of the cofactor analogs on the FMN riboswitch *Rli96* could help to elucidate how flavin analogs affect riboflavin auxotrophic bacteria, including *L. monocytogenes*.

Through heterologous expression of Lmo1945 in a riboflavin transporter deficient *Bacillus subtilis* strain, the role of Lmo1945 in the uptake of riboflavin and roseoflavin was confirmed. Two enzymes, catalyzing the conversion of riboflavin into the cofactors flavin mononucleotide (FMN) and flavin adenine dinucleotide (FAD) have been identified by sequence analysis. The bifunctional flavokinase/FAD synthetase Lmo1329 and the unique monofunctional FAD

synthetase Lmo0728 were purified and kinetically characterized. Additionally, their involvement in the generation of the cofactor analogs roseoflavin mononucleotide (RoFMN), 8-demethyl-8-amino riboflavin mononucleotide (AFMN), roseoflavin adenine dinucleotide (RoFAD) and 8-demethyl-8-amino riboflavin adenine dinucleotide (AFAD) were shown *in vitro*. Notably, the bifunctional enzyme Lmo1329 did not convert the roseoflavin derived cofactor RoFMN into RoFAD.
In vivo reporter gene assays and *in vitro* transcription/translation experiments showed that the FMN riboswitch *Rli96*, and consequently the expression of the riboflavin transporter gene *lmo1945*, is negatively affected by FMN and RoFMN but not by AFMN.

With the FMN riboswitch *Rli96*, the riboflavin transporter Lmo1945, the bifunctional flavokinase/FAD synthetase Lmo1329 and the monofunctional FAD synthetase Lmo0728, the key mechanisms of riboflavin uptake and metabolism in *L. monocytogenes* were identified and characterized. Particularly, the FAD synthetase Lmo0728 is the first monofunctional FAD synthetase that has been described in bacteria.

As a second part of this thesis a novel reporter system for *in vivo* studies of translational riboswitches in *Streptomyces* species was evaluated. However, the system proved to not be suitable for the desired application, i.e. the confirmation of previously obtained *in vitro* data. Several attempts to adapt and optimize the system failed which turned out to be due to the complexity of the natural expression platform in streptomycetes.

Zusammenfassung

Von dem Riboflavinanalogon Roseoflavin – einem Antibiotikum das von den Bakterien *Streptomyces davawensis* und *Streptomyces cinnabarinus* produziert wird sowie von 8-Demethyl-8-Amino-Riboflavin, einem wichtigen Zwischenprodukt der Roseoflavinbiosynthese, ist bekannt, dass sie auf das humanpathogene Bakterium *Listeria monocytogenes* eine wachstumshemmende Wirkung haben. Die hemmende Wirkung von Roseoflavin auf *L. monocytogenes* wurde seinem Einfluss auf den FMN Riboswitch *Rli96*, der die Expression des Ribflavintransportergens *lmo1945* reguliert, zugeschrieben. Ob auch Flavinanaloga, wie Roseoflavin und 8-Demethyl-8-Amino-Riboflavin, von *L. monocytogenes* mittels des Riboflavintransporters Lmo1945 aufgenommen werden, war bislang nicht bekannt. Auch die Umsetzung von Flavinanaloga zu Cofaktoranaloga durch Flavokinasen/FAD synthetasen in *L. monocytogenes* wurde bisher noch nicht untersucht. Die funktionelle Charakterisiereng der Interaktion zwischen Cofaktoranaloga und dem FMN Riboswitch *Rli96* könnte dazu beitragen, den Einfluss von Flavinanaloga auf riboflavinauxotrophe Bakterien wie *L. monocytogenes* besser zu verstehen.

Durch die heterologe Expression von Lmo1945 in einem spezialisierten *Bacillus subtilis* Stamm konnte die Rolle von Lmo1945 als funktioneller Transporter für Riboflavin und Roseoflavin bestätigt werden. Zwei Enzyme, die die Umsetzung von Riboflavin in die Cofaktoren Flavinmononukleotid (FMN) und Flavin-Adenin-Dinukleotid (FAD) katalysieren, konnten durch Sequenzvergleiche identifiziert werden. Die bifunktionelle Flavokinase/FAD syn-

thetase Lmo1329 und die monofunktionelle FAD synthetase Lmo0728 wurden aufgereiningt und anschließend bezüglich ihrer kinetischen Eigenschaften charakterisiert. Weiterhin konnte ihre Rolle in der Biosynthese der Cofaktoranaloga Roseoflavinmononukleotid (RoFMN), 8-Demethyl-8-Amino-Riboflavinmononukleotid (AFMN), Roseoflavin-Adenin-Dinkleotid (RoFAD) und 8-Demethyl-8-Amino-Riboflavin-Adenin-Dinukleotid (AFAD) durch *in vitro* Experimente aufgezeigt werden. Bemerkenswert war, dass die bifunktionelle Flavokinase/FAD synthetase Lmo1329 RoFMN nicht in RoFAD umsetzt. Mittels eines *in vivo* Reportersystems und gekoppelten *in vitro* Transkriptions-/Translationsexperimenten konnte gezeigt werden, dass der FMN Riboswitch *Rli96*, und infolgedessen auch die Expression des Riboflavintransportergens *lmo1945* von FMN und RoFMN, jedoch nicht von AFMN beeinträchtigt wurde.

Somit konnten mit dem FMN Riboswitch *Rli96*, dem Riboflavintransporter Lmo1945, der bifunktionellen Flavokinase/FAD synthetase Lmo1329 und der monofunktionellen FAD synthetase Lmo0728 die zentralen Mechanismen im Riboflavinstoffwechsel von *L. monocytogenes* aufgezeigt und charakterisiert werden. Besonderes Augenmerk fällt dabei auf die FAD synthetase Lm0728, die als erste bakterielle monofunktionelle FAD synthetase beschrieben wurde.

In einem zweiten Teil dieser Arbeit wurde ein neuartiges Reportersystem für die *in vivo* Charakterisierung von translationalen Riboswitches in Streptomyceten evaluiert. Jedoch stellte sich das System für die gewünschte Anwendung, der Verifizierung von vorherigen *in vitro* Experimenten, als ungeeignet heraus. Mehrere Optimierungs- und Anpassungsversuche blieben aufgrund der natürlichen Komplexität der Expressionsplattform in Streptomyceten erfolglos.

Acknowledgements

Firstly, I would like to express my sincere gratitude to my advisor Prof. Dr. Matthias Mack for offering me a place in his group, his continued support of my work and his interest in my own ideas on the project.

Besides my advisor, I would like to thank Prof. Dr. Michael Wink and Prof. Dr. Luise Krauth-Siegel for their investment in my thesis and their guidance as my thesis advisory committee as well as Prof. Dr. Rüdiger Rudolph for completing my examination commision.

My sincere thanks also goes to Prof. Dr. Jörgen Johansson for the stimulating discussions and for providing me with bacterial strains necessary for my experiments.

I thank my fellow labmates Ahmed Boumezbeur, Birgit Hobl, Frank Jankowitsch, Tobias Jung, Valentino Konjik, Christian Kühm, Simone Langer, Petra Ludwig, Danielle Pedrolli and Julia Schwarz for the great atmosphere in the lab. Also I thank everyone working in the MIB/BIC labs who has supported my work with technical assistance or by sharing their experience with me.

Last but not the least, I would like to thank my family: my parents who planted the seed of curiosity that made me become the scientist I am today, my wife Sanja for her unconditional love and her support when I needed it the most, and my daughter Laura for teaching me something new every day.

Contents

List of Figures

List of Tables

Abbreviations

5′–UTR	5′–Untranslated region
AF	8-Amino-8-demethyl-riboflavin
AFAD	8-Amino-8-demethyl-riboflavin adenine dinucleotide
AFMN	8-Amino-8-demethyl-riboflavin mononucleotide
Amp	Ampicillin
Apr	Apramycin
Carb	Carbenicillin
Cm	Chloramphenicol
FAD	Flavin adenine dinucleotide
FADS	FAD synthetase
FK	Flavokinase
FMN	Flavin mononucleotide
Kan	Kanamycin
MBP	Maltose Binding Protein
RF	Riboflavin
RFN	FMN riboswitch element
RoF	Roseoflavin
RoFAD	Roseoflavin adenine dinucleotide
RoFMN	Roseoflavin mononucleotide
Tsr	Thiostrepton

1 Introduction

1.1 Flavins and Flavoenzymes

Riboflavin (vitamin B_2; RF) (figure 1.3 on page 9) is the universal precursor for the phosphorylated cofactors riboflavin 5′-phosphate (flavin mononucleotide, FMN) and flavin adenine dinucleotide (FAD) that are essential metabolites in all types of organisms. Riboflavin is synthesized *de novo* by plants and many microorganisms. Animals and also some species of bacteria, however, rely solely on the uptake of riboflavin (Gerdes et al., 2002). FMN and FAD serve as cofactors for so-called flavoenzymes that are involved in a wide range of biochemical reactions, such as dehydrogenations, one- and two-electron transfer from and to redox centers, light emission, the activation of oxygen for oxidation and hydroxylation (Massey, 1995; Fraaije and Mattevi, 2000). The biochemical utility of riboflavin derived cofactors in flavoenzymes relies on the redox activity of the isoalloxazine ring system, which is able to assume three different redox states: the oxidized or quinone state, the one-electron reduced or semiquinone (radical) state, and the two-electron reduced (fully reduced) or hydroquinone state (Massey, 1994; Abbas and Sibirny, 2011). In a study that included 374 flavoenzymes from 22 species throughout all domains of life, Macheroux et al. reported more than 90% of flavoenzymes being oxidoreductases, while less than 10% of flavoenzymes catalyzed non-redox reactions. They also found that the majority of flavoenzymes used FAD as cofactor (75%), while 25% utilized FMN (Macheroux et al., 2011).

1.2 Biosynthesis and Transport of Riboflavin

Riboflavin is synthesized in bacteria, fungi and plants from guanosine-5′-triphosphate (GTP) and two molecules of ribulose-5-phosphate. The biosynthetic pathway has been described in detail by Fischer and Bacher. It involves a set of enzymes consisting of GTP cyclohydrolase II (EC 3.5.4.25), 3,4-dihydroxy-2-butanone-4-phosphate synthase (EC 4.1.99.12), diaminohydroxyphosphoribosylaminopyrimidine deaminase (EC 3.5.4.26), 5-amino-6-(5-phosphoribosylamino)uracil reductase (EC 1.1.1.193), lumazine synthase (EC 2.5.1.78) and riboflavin synthase (EC 2.5.1.9) (Bacher et al., 2000; Fischer and Bacher, 2005).

In procaryotes functionally related genes are often located in close proximity to each other on the chromosome (Demerec and Hartman, 1959; Overbeek et al., 1999). If expression of such clusters is controlled by the same promoter and regulated by an operator (i.e. repressor or activator), they are referred to as operons (Jacob and Monod, 1961). Genes involved in the biosynthesis of riboflavin have been found to form operons (*rib*-operon) in many bacterial species, e.g. *Bacillus subtilis* (Perkins and Pero, 2001), *Fusobacterium nucleatum* (Serganov et al., 2009) and *S. davawensis* (Grill et al., 2007). The expression of genes from *rib*-operons is typically modulated by the interaction of FMN with the aptamer portion of an FMN riboswitch, located directly upstream of the operon (Gelfand et al., 1999; Vitreschak et al., 2002). FMN riboswitches re described in more detail in section 1.4. However, in other species, such as *Escherichia coli*, the genes involved in riboflavin biosynthesis are scattered throughout the chromosome (Neidhardt, 1994), while some bacterial species do not possess riboflavin biosynthetic genes at all, and thus are unable to synthesize riboflavin *de novo*, including the pathogenic species *L. monocytogenes* and *Enterococcus faecalis* (Fischer and Bacher, 2005).

Riboflavin uptake in bacteria is mediated by a surprisingly high number of different types of riboflavin transport systems. The membrane-embedded substrate-binding subunit (EcfS) RibU of an energy-coupling factor (ECF) transporter system has been described for *Lactococcus lactis* (Burgess et al., 2006) and for *B. subtilis* (Vogl et al., 2007). A RibU orthologue was predicted in *L. monocytogenes* downstream of an FMN riboswitch (Mansjö and Johansson,

2011). The structure of RibU from *L. monocytogenes* was resolved recently, although no functional characterization was performed (Karpowich et al., 2015). A different class of energy independent riboflavin transporter proteins, such as RibM from *S. davawensis* (Grill et al., 2007; Hemberger et al., 2011) and *C. glutamicum* (Vogl et al., 2007) that are homologues of the nicotinamide riboside permease protein PnuC from *Haemophilus influenzae* have been described (Sauer et al., 2004). Deka et al. have identified another riboflavin transport mechanism present in riboflavin auxotrophic pathogenic spirochetes such as *Treponema pallidum*. They have identified the ATP-binding casette (ABC) type riboflavin transport system RfuABCD with the riboflavin binding component RfuA (Deka et al., 2013). The genes *impX* in *Fusobacterium nucleatum* and *rfnT* in *Mesorhizobium loti, Sinorhizobium meliloti* and *Agrobacterium tumefaciens* were predicted to be putative riboflavin transporters due to their location downstream of the conserved FMN riboswitch motif and the prediction of transmembrane domains (Vitreschak et al., 2002). It was speculated that only Gram-positve bacteria feature riboflavin transport systems, while Gram-negative bacteria rely solely on the endogenous *de novo* synthesis of riboflavin (Abbas and Sibirny, 2011). However, García Angulo et al. were able to identify and characterize the riboflavin transporter RibN in the Gram-negative soil bacterium *Rhizobium leguminosarum*. Furthermore RibN orthologues were found in the Gram-negative species *Ochrobactrum anthropi* and *Vibrio cholerae* (García Angulo et al., 2013).

With the increasing number of available complete genome sequences from bacteria, Gutiérrez-Preciado et al. recently were able to identify the two new putative riboflavin transporter genes *ribZ* in *Clostridium difficile* and *ribV* in *Mesoplasma florum*. They were able to confirm the riboflavin transporter activity of RibZ from *C. difficile* as well as of the previously uncharacterized putative transporters RibXY from *Chloroflexus aurantiacus*, ImpX from *F. nucleatum* and RfnT from *O. anthropi* (Gutiérrez-Preciado et al., 2015).

Eukaryotic riboflavin transporter proteins have been identified in yeast (Reihl and Stolz, 2005) and also in mammals, namely in humans and rats (Yonezawa et al., 2008; Yao et al., 2010). However, none of those proteins is similar to any known bacterial riboflavin transporter.

1.3 Synthesis of the Flavin Cofactors FMN and FAD

After riboflavin has been either *de novo* synthesized, or taken up by transporters, all organisms are faced with the necessity to convert it into its metabolic active forms, the cofactors FMN and FAD. The irreversible conversion of riboflavin and ATP to FMN and ADP is catalyzed by flavokinases (FK, EC 2.7.1.26). In a second, reversible reaction, FMN is further metabolized under the consumption of ATP to FAD and pyrophosphate by FAD synthetases (FADS, EC 2.7.7.2) (Fischer and Bacher, 2005). Efimov et al. proposed a steady-state kinetic mechanism for the bifunctional flavokinase/FAD synthetase (FK/FADS) from *Corynebacterium ammoniagenes*, and they suggested that FMN has to be released after its synthesis in order to rebind to a different domain of the enzyme where it is then adenylylated (Efimov et al., 1998). A reaction scheme of the two reactions is given in figure 1.1.

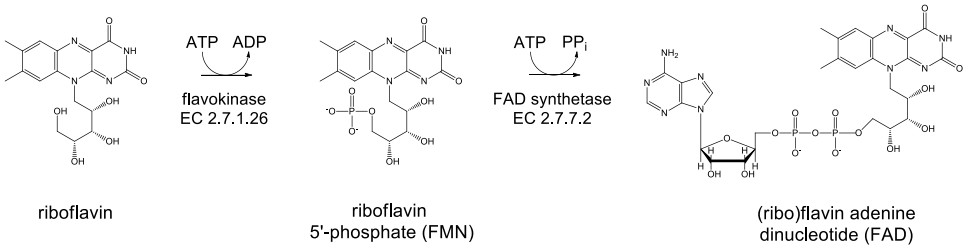

Figure 1.1: Riboflavin is converted into the cofactors FMN and FAD. Reaction scheme for the conversion of riboflavin and ATP to FMN and ADP, catalyzed by flavokinase (EC 2.7.1.26) and the formation of FAD and pyrophosphate from FMN and ATP, catalyzed by FAD synthetase (EC 2.7.7.2).

In bacteria both reactions are typically catalyzed by bifunctional enzymes, first described by Manstein and Pai for the bifunctional flavokinase/FAD synthetase from *Brevibacterium ammoniagenes*, while in eukaryotes like in the yeast *Saccharomyces cerevisiae*, and also in humans, the two reactions are catalyzed by two independent enzymes (Manstein and Pai, 1986; Wu et al., 1995; Santos et al., 2000; Karthikeyan et al., 2003; Brizio et al., 2006). The monofunctional flavokinase RibR from *B. subtilis*, first described by Solovieva et al., was found recently to interact with both FMN riboswitches to synchronize the sulfur and riboflavin metabolism in in *B. subtilis* (Solovieva et al., 1999; Pedrolli et al., 2015a). In the archaeon *Methanocaldococcus jannaschii* a monofunctional FAD synthetase (RibL) was identified and characterized by Mashhadi et al.. RibL, in

contrast to bacterial FAD synthetases, does not catalyze the reverse reaction of FAD and pyrophosphate to FMN and ATP. Furthermore, RibL activity is inhibited by pyrophosphate (Mashhadi et al., 2010). To this date, however, no monofunctional bacterial FAD synthetase has been characterized.

1.4 FMN Riboswitches

Riboswitches are protein independent regulatory elements, residing in the 5′-untranslated region (5′-UTR) of messenger RNAs (mRNA) and can be found throughout all three domains of life (Barrick and Breaker, 2007). Riboswitches typically consist of two elements, an aptamer that binds a specific ligand molecule (e.g. a metabolite) and an expression platform, which controls expression of the downstream gene(s) by conformational changes upon binding of the ligand to the aptamer (Wickiser et al., 2005). The two most important mechanisms for the riboswitch mediated control of gene expression are the termination of transcription and the prevention of translation initiation (Winkler et al., 2002; Vitreschak et al., 2002). Binding of the ligand to the aptamer leads to the formation of a secondary structure in the expression platform that prevents expression of the downstream gene(s) (figure 1.2). However, other mechanisms of riboswitch mediated regulation of gene expression have been described and were reviewed by Breaker as well as by Serganov and Nudler (Breaker, 2012; Serganov and Nudler, 2013). Also an FMN riboswitch featuring a combination of transcription termination and sequestration of the ribosomal binding site (RBS), regulating the expression of the 3,4-dihydroxy-2-butanone-4-phosphate synthase gene *ribB* in *E. coli* was described recently (Pedrolli et al., 2015b). Although most riboswitches sense only a single metabolite, more intricate riboswitch conformations, so called *tandem riboswitches* have been identified. Tandem riboswitch arrangements feature two independent aptamers, each binding a distinct ligand, and expression platforms, so that the binding of only one of the ligands is sufficient to repress the expression of the downstream gene(s) (Sudarsan et al., 2006; Coppins et al., 2007).

FMN riboswitches, also referred to as RFN-elements, are riboswitches featuring an FMN binding aptamer. They are typically found upstream of genes involved in riboflavin biosynthesis or riboflavin transport. The presence of a regulatory region, formerly designated as "*ribO*", between the P_{rib} promoter and the first gene of the cluster *ribDG*, coding for the bifunctional enzyme RibDG

(EC 3.5.4.26 and EC 1.1.1.193) of *B. subtilis* has first been reported by Kil et al. (1992). However, Kil et al. speculated that the regulatory mechanism relied on binding of the protein RibC to the *ribO* region. Mack et al. were able show that RibC was not involved in the regulation of the *rib*-operon in *B. subtilis*. They speculated that the regulation of riboflavin biosynthesis genes occurred in the absence of a protein factor (Mack et al., 1998). Through comparative sequence analysis Gelfand et al. (1999) were able to identify this regulatory region to be highly conserved throughout several branches of bacteria. Gelfand et al. identified the association of the regulatory properties of the conserved region with RNA folding, as they stated that it could fold into a conserved structure with five hairpins and referred to it as "RFN-element". They also described the association of the RFN-element with genes involved in riboflavin biosynthesis and genes similar to *ypaA* of *B. subtilis* that has later been reported to encode the riboflavin transporter protein RibU (Kreneva et al., 2000; Vogl et al., 2007).

The term "riboswitch" was first introduced by Nahvi et al. and readily accepted by others (Nahvi et al., 2002; Winkler et al., 2002; Mironov et al., 2002). From a more extensive alignment of in total 58 RFN-elements found upstream of riboflavin operons, single riboflavin biosynthesis genes and putative riboflavin transporters respectively, Vitreschak et al. were able to derive two FMN-mediated regulatory mechanisms of the RFN-elements. Downstream of the FMN binding aptamer they identified hairpin structures, that either were followed by runs of uracil bases and thus were considered transcription terminators (figure 1.2–B) or hairpins that include the RBS of the downstream gene and like so interfere with the translation initiation (figure 1.2–C). In addition, all RFN-elements of the alignment were found capable of forming alternative structures where the base stem of the aptamer could pair with parts of the regulatory hairpin and in this way form either an anti-terminator or an anti-sequestor secondary structure respectively (figure 1.2–A) (Vitreschak et al., 2002).

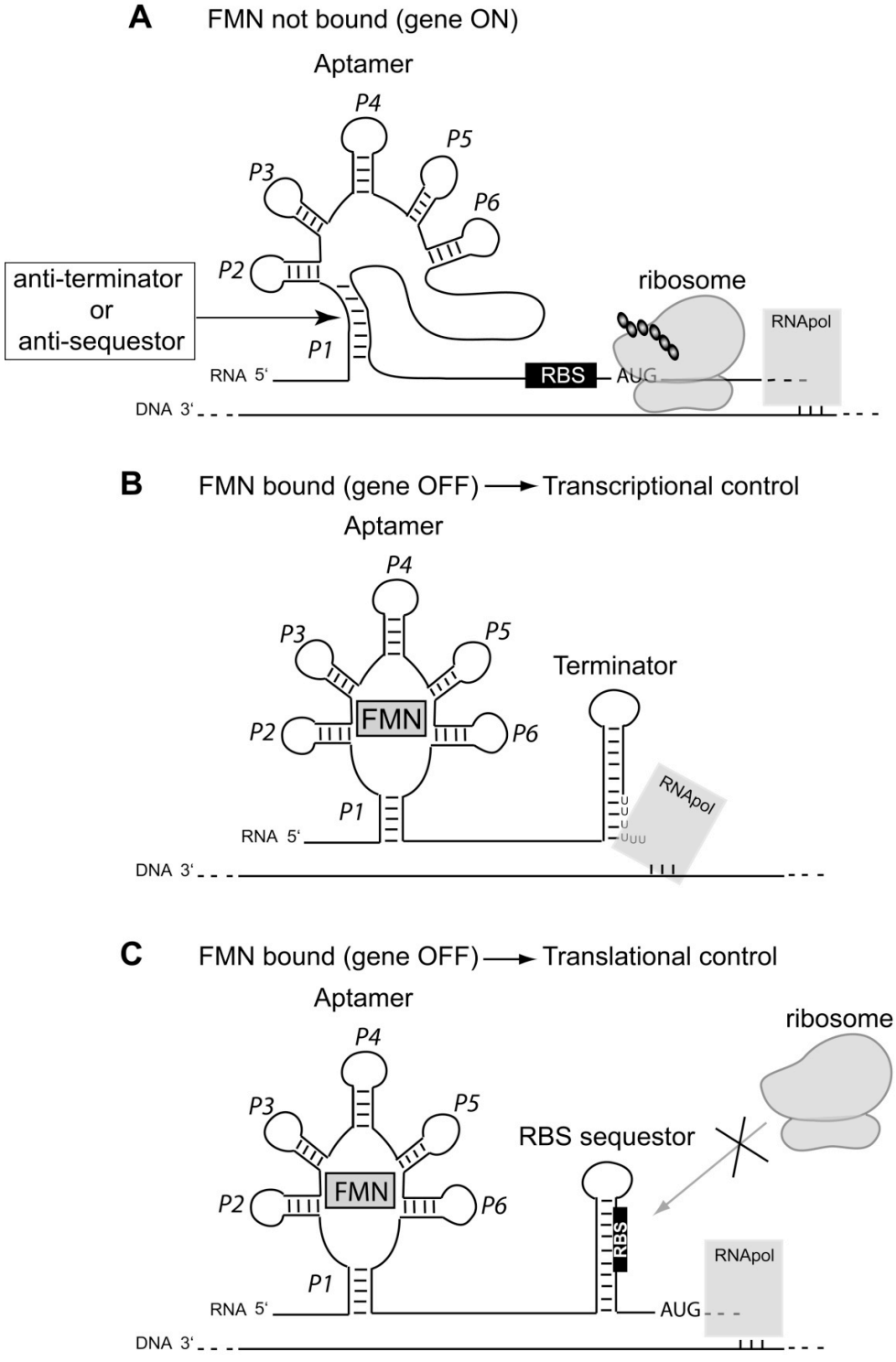
A
FMN not bound (gene ON)
Aptamer
P4
P5
P3
P6
P2
anti-terminator
or
anti-sequestor
P1
ribosome
RNApol
RNA 5'
RBS
AUG
DNA 3'
B
FMN bound (gene OFF) → Transcriptional control
Aptamer
P4
P3
P5
Terminator
FMN
P2
P6
P1
RNApol
RNA 5'
DNA 3'
C
FMN bound (gene OFF) → Translational control
Aptamer
ribosome
P4
P3
P5
RBS sequestor
FMN
P2
P6
RBS
P1
RNApol
RNA 5'
AUG
DNA 3'

Figure 1.2: Mechanisms of FMN riboswitch mediated gene regulation. FMN riboswitch mediated regulation mechanisms, as proposed by Vitreschak et al. (2002) and confirmed by Serganov et al. (2009). Figure adapted from Pedrolli and Mack (2014).
A: At low FMN concentrations (or in the absence of FMN) the aptamer does not bind the regulating metabolite and adopts the anti-termination or anti-sequestor secondary structure. Transcription is able to proceed, translation may initiate and protein synthesis occurs.
B: At high FMN concentrations the aptamer binds the metabolite which leads to the formation of the terminator hairpin downstream of the aptamer, causing transcription termination and dissociation of RNA-polymerase from the DNA-template.
C: Alternatively at high FMN concentrations the aptamer binds the metabolite and allows the RBS sequestor hairpin to form. Although transcription still proceeds, protein synthesis does not occur since the ribosome cannot access the ribosomal binding site (RBS).

It has been predicted by Vitreschak et al. (2002) that expression of riboflavin biosynthesis genes and transporters in Gram-positive bacteria (including *Streptomyces spp., Bacillus spp., Listeria spp.)* were regulated by transcription attenuation, while expression of the corresponding genes in Gram-negative bacteria (e.g. *E. coli*) would be regulated by prevention of translation initiation. However, this general statement does not hold true regarding the FMN riboswitches of the bacterial species that were in the focus of this work. In *B. subtilis*, one FMN riboswitch regulates expression of the riboflavin biosynthesis operon through transcription termination and a second FMN riboswitch controls expression of *ribU* coding for the riboflavin transporter RibU by sequestration of the RBS (Winkler et al., 2002; Sklyarova and Mironov, 2014). In *S. coelicolor*, *S. davawensis* and also other *Strepotmyces* species an FMN riboswitch controls expression of the riboflavin synthase gene *ribB* through translation inhibition (Grill et al., 2007; Pedrolli et al., 2012). The FMN riboswitch *Rli96* upstream of the riboflavin transporter gene *lmo1945* of *L. monocytogenes* has been reported to terminate transcription in the presence of FMN (Mansjö and Johansson, 2011).

1.5 Flavin Analogs and Their Potential as Novel Antimicrobial Drugs

The riboflavin analog roseoflavin is the only known naturally occurring flavin analog with antibiotic properties (Otani et al., 1974). Roseoflavin is produced by the two closely related *Streptomyces* species, *S. davawensis* and *S. cinnabarinus* (Jankowitsch et al., 2011, 2012). Jankowitsch et al. demonstrated that

roseoflavin is synthesized in *S. davawensis* from riboflavin via the intermediate flavin analog 8-amino riboflavin (figure 1.3). A recombinant *S. davawensis* strain, lacking the gene *rosA*, coding for the N,N-8-amino-8-demethyl-D-riboflavin dimethyltransferase RosA was shown to be roseoflavin deficient and accumulated 8-amino riboflavin instead (Jankowitsch et al., 2011). Schwarz et al. recently were able to the key enzyme of roseoflavin biosynthesis in *S. davawensis*. They describe the enzyme RosB, catalyzing the first steps in the biosynthesis of roseoflavin, starting from FMN (Schwarz et al., 2016).

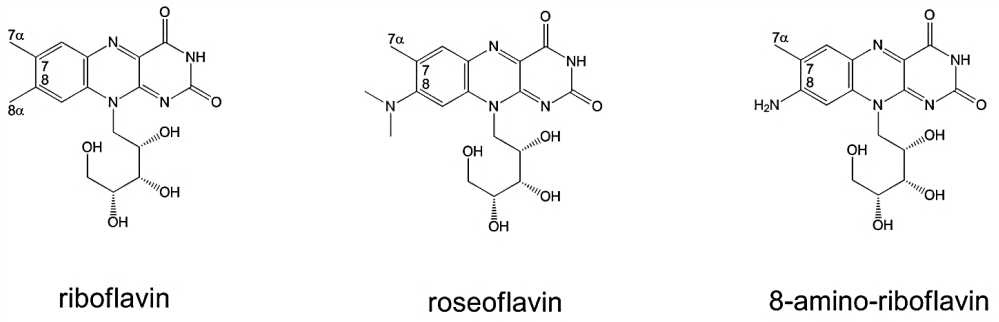

Figure 1.3: Structures of ribofalvin, roseoflavin and 8-amino riboflavin. The structures of 7,8-dimethyl-10-(D-1′-ribityl)isoalloxazine (riboflavin, RF; vitamin B_2), 8-dimethylamino-8-demethyl-riboflavin (roseoflavin, RoF) and 8-amino-8-demethyl-riboflavin (8-amino riboflavin, AF).

The antibiotic effect of both, roseoflavin and 8-amino riboflavin, was attributed to their phosphorylated forms as cofactor analogs roseoflavin mononucleotide/8-demethyl-8-amino riboflavin mononucleotide (RoFMN/AFMN) and their adenylylated forms roseoflavin adenine dinucleotide/8-demethyl-8-amino riboflavin adenine dinucleotide (RoFAD/AFAD) (Grill et al., 2008; Pedrolli et al., 2011). The conversion of roseoflavin and 8-amino riboflavin to the respective cofactor analogs is catalyzed by flavokinase and FAD synthetase enzymes respectively, analog to the conversion of riboflavin to FMN and FAD (figure 1.4). The bifunctional flavokinase/flaviFAD synthetase RibC from *B. subtilis* (unpublished experimental data) and the monofunctional human FAD synthetase (Pedrolli et al., 2011), however, did not accept AFMN as a substrate and consequently did not synthesize the cofactor analog AFAD.

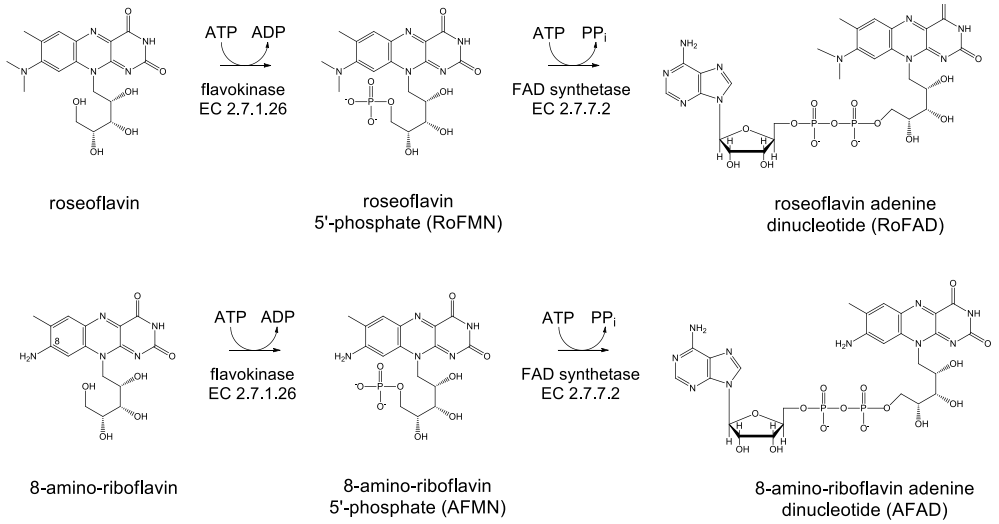

Figure 1.4: Flavin analogs are converted into cofactor analogs. The biosynthesis of the cofactor analogs roseoflavin mononucleotide (RoFMN), roseoflavin adenine dinucleotide (RoFAD), 8-demethyl-8-amino riboflavin mononucleotide (AFMN) and 8-demethyl-8-amino riboflavin adenine dinucleotide (AFAD).

Although the cofactor analogs derived from roseoflavin and 8-amino riboflavin exhibit considerably different physicochemical properties to FMN an FAD, including redox potential or hydrophobicity, they are thought to still form holoenzymes with most of the flavo-apoenzymes present in the cell (Walsh et al., 1978; Otani et al., 1997; Langer et al., 2013a). However, cofactor analog bound holoenzymes were reported to be less or not active at all (Grill et al., 2008; Langer et al., 2013b). Which of the altered properties of the cofactor analogs is responsible for the reduced activity of flavoenzymes remains unclear and might also be different for individual enzymes. Binding of cofactor analogs to flavoenzymes might not only affect the catalyzed reaction directly but could also interfere with multimerization or change the overall structure in a nonbeneficial way (Pedrolli et al., 2014).

In addition to the above described effects of cofactor analogs on the activity of flavoenzymes, FMN riboswitches have been identified as secondary, non-protein targets for the flavin analog roseoflavin (Blount and Breaker, 2006; Ott et al., 2009; Lee et al., 2009). Mansjö and Johansson were able to demonstrate that roseoflavin in the growth medium affected the FMN riboswitch mediated gene expression of the gene *lmo1945* in *L. monocytogenes*. However, roseoflavin was found to also stimulate the expression of genes connected to virulence and infection abilities in *L. monocytogenes* (Mansjö and Johansson, 2011). With

a coupled *in vitro* transcription/translation assay Pedrolli et al. were able to show that the cofactor analog RoFMN, and not roseoflavin, interacts with the FMN riboswitch aptamer in roseoflavin sensitive *Streptomyces* species.

1.6 Streptomycetes

Streptomycetes are Gram-positive, aerobic soil bacteria. They comprise all members of the genus *Streptomyces* within the phylum of actinobacteria (Waksman and Henrici, 1943). Known *Streptomyces* species feature a single, linear chromosome of approximately 8 – 10 Mbp in length, with a notably high G+C content of typically > 70% (Kieser et al., 2000). The morphology of streptomycetes is similar to that of eucaryotic filamentous fungi. Streptomycetes in their natural habitat grow as a vegetative mycelium consisting of branching hyphae. They spread through spores that form on aerial hyphae, as a response to diminishing nutrient supply of the substrate. The similarities of streptomycetes to fungi are hypothesized to originate from the independent adaptation to the same ecological niches and lifestyle, i.e. the involvement of both in the degradation of unsoluble biomass, like lignocellulose or chitin (Hodgson, 2000; Hopwood, 2006; Flärdh and Buttner, 2009).

In contrast to most other bacteria, streptomycetes differentiate into complex, multicellular mycelia. The developmental life cycle and differentiation is shown exemplary for *S. coelicolor* in figure 1.5. After germination of spores in favorable environmental conditions, germ tubes are formed that develop into vegetative hypha. Unlike in rod-shaped bacteria, as e.g. *E. coli* and *B. subtilis*, the hyphal growth of streptomycetes occurs through tip extension and is not associated with the bacterial actin homologue MreB. The individual cells do not separate completely but merely form hyphal cross-walls between each other. When streptomycetes are faced with limitation of nutrients, they initiate the development of aerial hyphae. To enable the aerial hyphae to break the surface tension of the aqueous environment of the mycelium and to grow into the air, their surface is coated with the hydrophobic surfactant peptide SapB. The aerial hyphae later differentiate from apically growing cells into spores. Other than endospores formed by *Bacillus* species, the spores of streptomycetes are less resistant to harsh environmental conditions. They can, however, survive extended periods of desiccation (Flärdh and Buttner, 2009).

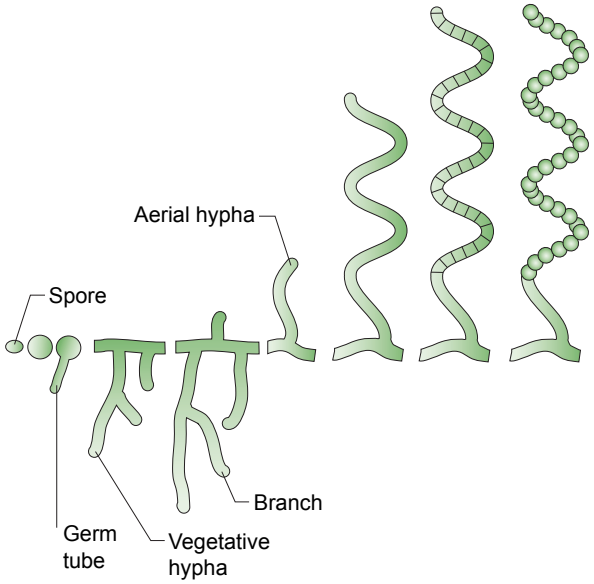

Figure 1.5: The developmental life cycle of *S. coelicolor*. After germination, a germ tube emerges from a spore and develops into a vegetative hypha. Hyphae grow by tip extension and branch into a vegetative mycelium that spreads into the substrate. Aerial hypha break the surface tension of the aqueous environment of the substrate and grow into the air. The aerial hyphae differentiate into a long chain of prespore compartments, which then develop thick spore walls. Figure adapted from Flärdh and Buttner (2009).

Throughout the past, streptomycetes have been studied in-depth, especially due to their capability to produce a great variety of secondary metabolites, including several compounds of pharmaceutical relevance like antifungals, antivirals, antitumorals, antihypertensives, immunosuppressants and most important antibiotics. The production of antibiotic substances by streptomycetes is assumed to be part of a defense mechanism, possibly triggered by nutrient limitation, in the phase of aerial mycelium formation. Most antibiotics in streptomycetes are species specific, and also affect other members of the genus (Procópio et al., 2012).

S. coelicolor is the genetically best characterized representative of streptomycetes and is widely used in genetic studies. The analysis of its genome sequence, presented over one decade ago by Bentley et al., revealed that the chromosome of streptomycetes features a central "core" region, comprising approximately half of the genome's size, containing the origin of replication (oriC) and nearly all essential genes coding for enzymes involved in cell division, DNA replication, transcription, translation and amino-acid biosynthesis. The more variabel outer regions of the chromosome are referred to as "arms" and carry genes with

non-essential functions, from the secondary metabolism including antibiotic production (Bentley et al., 2002).

The genes involved in riboflavin biosynthesis have been found to be clustered in streptomycetes and form an operon controlled by an FMN riboswitch (Vitreschak et al., 2002). The arrangement of the riboflavin biosynthesis genes in the *rib*-operon in streptomycetes, however, is different from other Gram-positive bacteria like *B. subtilis*. The *rib*-operon in streptomycetes interestingly includes the gene *ribM*, coding for the energy independent riboflavin transporter RibM, while the gene *ribG*, coding for the bifunctional riboflavin specific deaminase/reductase RibG (EC 3.5.4.26 and EC 1.1.1.193), was found in a secondary location on the chromosomes of *S. coelicolor*, *S. avermitilis* and *S. davawensis* (Grill et al., 2007).

The FMN riboswitch upstream of the *rib*-operon in the streptomycetes *S. davawensis* and *S. coelicolor* was shown to regulate the expression of the riboflavin synthase gene *ribB* by prevention of translation initiation through sequestration of the *ribB*-RBS (see figure 1.6-A). This mechanism is different from other FMN riboswitches, e.g. the *ribG* FMN riboswitch of *B. subtilis*, which regulate the expression of the *rib*-operon through transcription termination. The FMN riboswitch of *S. davawensis*, in contrast to the one of *S. coelicolor*, respectively, is able to discriminate between FMN and its roseoflavin derived analog RoFMN. Opposite to what was observed for *S. coelicolor*, the FMN riboswitch of *S. davawensis* showed upregulation of the expression of its downstream gene when confronted with RoFMN. Pedrolli et al. were able to interchange this property by the exchange of a single nucleotide in the sequence coding for the aptamer of the FMN riboswitch. Exchange of the nucleotide on position 61 in the alignment shown in figure 1.6-B from A to G in *S. davawensis* confers sensitivity to RoFMN, while the exchange from G to A in *S. coelicolor* renders the FMN riboswitch RoFMN insensitive. The single nucleotide A61 in the FMN riboswitch provides resistance to the antibiotic flavin analog roseoflavin to *S. davawensis* (Pedrolli et al., 2012).

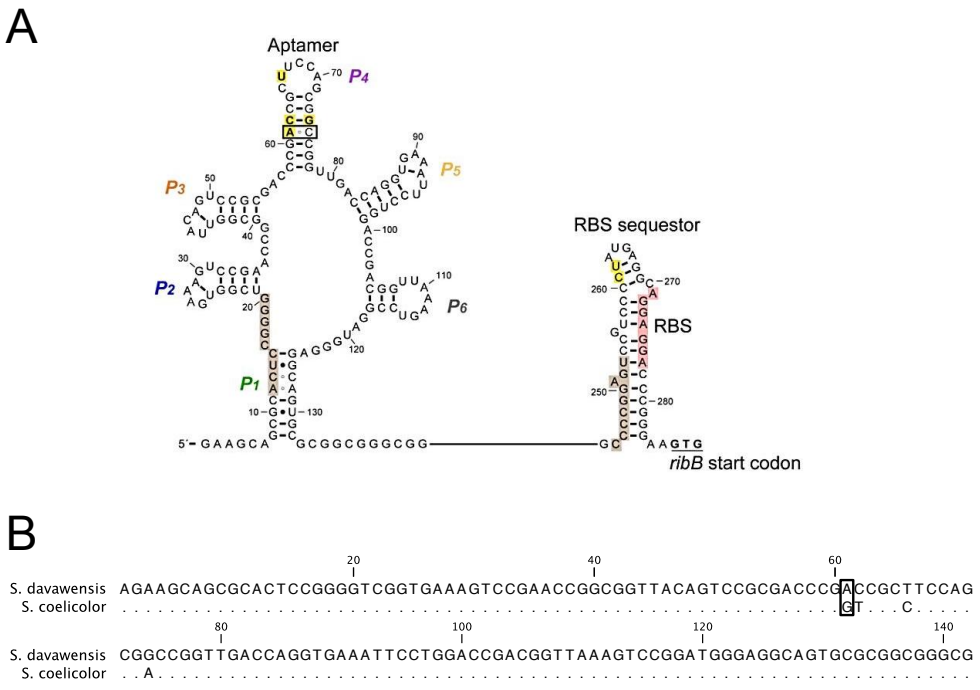

Figure 1.6: The translational *ribB* FMN riboswitch in *Streptomyces* spp. A: Secondary structure of the *ribB* FMN riboswitch from *S. davawensis*. Stem loops of the aptamer are labeled P1 – P6; nucleotides different to *S. coelicolor* highlighted in yellow; nucleotide 61 marked by black box; nucleotides highlighted in brown are paired in the absence of FMN and form the anti-sequestor structure; RBS highlighted in red; *ribB*-start codon underlined. B: Alignment of the DNA sequence coding for the aptamer portion of the *ribB* FMN riboswitch of *S. davawensis* and *S. coelicolor*. Identical nucleotides are shown as points; nucleotide 61 marked by black box. Figure adapted from Pedrolli et al. (2012).

1.7 *Listeria monocytogenes*

Listeria monocytogenes is an opportunistic foodborne pathogen causing listeriosis, a potentially fatal infection causing meningitis, meningoencephalitis, sepsis, abortion, perinatal infections, and gastroenteritis. It is one of ten species in the Gram-positive genus *Listeria*. *L. monocytogenes* is an aerobic, facultative anaerobic, rod-shaped and non-sporulating bacterium. It contains a circular chromosome of 2.9 Mbp in length with a relatively low G+C content of 39%. *Listeria* species are close relatives to species of the genera *Bacillus*, *Clostridium*, *Enterococcus*, *Streptococcus*, and *Staphylococcus*. Comparison of the complete genome sequences of two *Listeria* species (*L. monocytogenes* and *L. innocua*) with

the genome of *B. subtilis* revealed a close relationship that suggests a common ancestor of the three species (Vázquez-Boland et al., 2001; Glaser et al., 2001; Liu, 2008). *Listeria* species can be found in a variety of natural environments, such as soil, vegetation and fresh water. Silage, sewage as well as human and animal feces have also been shown to contain *L. monocytogenes* (Farber and Peterkin, 1991). A continuous fecal-oral enrichment of *L. monocytogenes* in domesticated ruminants (e.g. sheep and cattle) and the consumption of spoiled silage can result in herd outbreaks (Vázquez-Boland et al., 2001). In most animals, including humans, infection with *L. monocytogenes* occurs almost exclusively through the ingestion of contaminated food. The bacteria have developed to withstand acidic conditions in the stomach and elevated salt concentrations found in the small intestine.

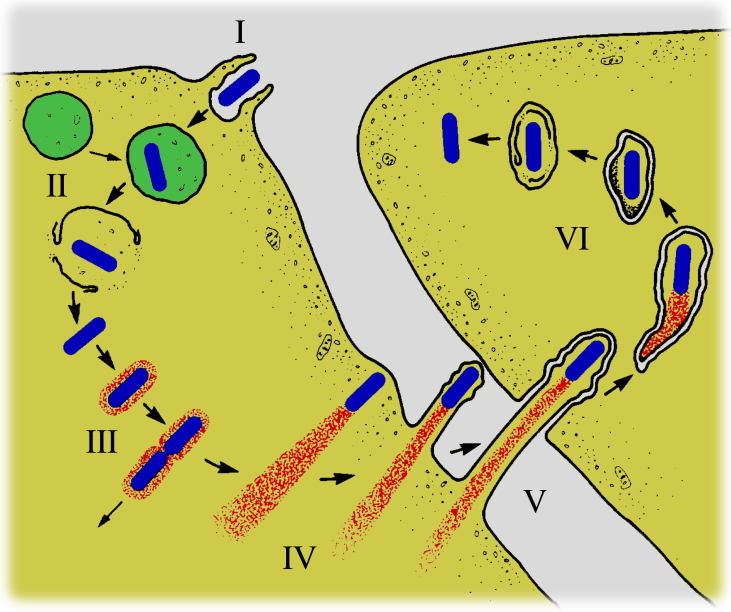

Figure 1.7: The intracellular life cycle of *L. monocytogenes*. (I) invasion factor (InlA, InlB) mediated internalization of *L. monocytogenes* by an intestinal epithelial cell; (II) lysis of the phagocytic vacuole through hemolysin, listeriolysin (LLO) and phospholipases; (III) replication and ActA induced nucleation of host actin filaments; (IV) formation of a polar actin tail; (V) formation of pseudopod, invading neighboring cell; (VI) release of *L. monocytogenes* into the cytoplasm after lysis of double membrane vacuole by LLO and phospholipases. Color legend - yellow: cytoplasm of the epithelial cell; green: phagocytic vacuole; blue: *L. monocytogenes* cell; red: polar actin tail. Figure adapted from Tilney and Portnoy (1989).

In the gastrointestinal tract *L. monocytogenes* adheres to the epithelial cells of the mucosa before crossing the intestinal barrier by invasion of enterocytes

(Schuppler and Loessner, 2010). The different stages of the invasion and the intracellular life cycle of *L. monocytogenes* are shown in figure 1.7.

The bacterium enters the host cell with the help of the two surface associated invasion factors InlA and InlB. Inside the host cell, it escapes from the phagolysosome by lysis of the phagocytic vacuole. After being released into the cytoplasm, *L. monocytogenes* starts replication and recruits host cell actin using the actin assembly-inducing protein ActA. Polar localization of ActA and continuos actin polymerization results in a directional movement of the bacterium. A pseudopod with the bacterium at the tip is formed when it reaches the plasma membrane. Inside this pseudopod *L. monocytogenes* enters neighboring cells. A double membrane vacuole is formed after penetration of the membrane of the neighboring cell, which is lysed similar to the phagocytic vacuole subsequent to primary invasion. This mechanism of cell-to-cell invasion allows *L. monocytogenes* to spread without leaving the host cells' cytoplasm (Liu, 2008; Schuppler and Loessner, 2010).

From the gastrointestinal tract *L. monocytogenes* spreads via the mesenteric lymph nodes to its primary target organs, the liver and the spleen where, in immunocompetent, healthy adults, the infection typically is contained and resolved by the host's immune system in a subclinical course. In immunocompromised hosts (e.g. through HIV infection, in cancer patients, after organ transplantation or liver cirrhosis), newborns or pregnant women the infection cannot be contained effectively in the primary target organs and the bacteria are released into the bloodstream which can lead to localized infections in the brain or the fetoplacental unit causing a clinical form of listeriosis (Liu, 2008).

Additionally to its adaptation to the adverse conditions in the stomach and the small intestine, *L. monocytogenes* is not only capable to tolerate a pH range from 3.0 to 9.5 and salt concentrations as high as 10%, it is also able to survive in a temperature range from 0 to 45 °C. Especially the growth at refrigeration temperatures (growth rate ~ 0.5 – 1 d^{-1} at 4 °C) poses enormous problems to the food industry. *L. monocytogenes* can survive on foods that were processed to extend shelf-life (e.g. smoked fish and raw meat saussages) but also on other foods that are consumed without being cooked before consumption (e.g. dairy products, vegetables and fruits) (Liu, 2008).

L. monocytogenes is one of the deadliest food-borne pathogens with a death-rate of approximately 30% in the clinical stage. However, the incidence of clinical listeriosis is relatively low with only about 3 – 5 cases per million persons

per year in the United States and Europe (Liu, 2008). *Listeria* species were shown to be naturally sensitive to tetracyclines, aminoglycosides, penicillins (except for oxacillin), frst- and second-generation cephalosporins (cefaclor, cefazolin, loracarbef) and chloramphenicol while they showed resistance to most 'modern' cephalosporins (cefetamet, cefixime, ceftibutene, ceftazidime, cefdinir, cefpodoxime, cefotaxime, ceftriaxone, cefuroxime) (Troxler et al., 2000). Hansen et al. found that the the antibiotic susceptibility of *L. monocytogenes* has not changed throughout the second half of the 20th century in a study of *L. monocytogenes* strains from human isolates, collected during the period 1958 to 2001 in Denmark (Hansen et al., 2005). However, multi-resitant isolates of *L. monocytogenes* have been reported elsewhere and pose the risk of a potential spread of multi-resistant *L. monocytogenes* (Poyart-Salmeron et al., 1990; Tsakris et al., 1997; Haubert et al., 2016).

Under laboratory conditions *Listeria spp.* require the addition of three vitamins (riboflavin, biotin and thiamin), the cofactor lipoate as well as six amino acids (leucine, isoleucine, arginine, methionine, valine and cysteine) into chemically defined growth media to enable growth (Premaratne et al., 1991). Since the biosynthetic pathways for all amino acids could be identified in the genome of *L. monocytogenes*, the amino acid auxotrophy was attributed to possible repression under laboratory conditions. The biosynthetic pathways for the biosynthesis of all four vitamins, however, were found to be missing completely or partially in *L. monocytogenes* (Glaser et al., 2001).

From the *Rfam database collection of RNA families* one FMN riboswitch (*Rli96*) was identified upstream the gene *lmo1945*. Since the putative gene product Lmo1945 shows high similarity to the riboflavin transporter RibU from *B. subtilis*, *lmo1945* was assumed to encode a riboflavin transport protein as well (Griffiths-Jones et al., 2003, 2005; Toledo-Arana et al., 2009; Mansjö and Johansson, 2011). The secondary structure of *Rli96*, suggested in figure 1.8, is based on the Rfam alignment to the covariance model of the FMN riboswitch family (Rfam-Accession: RF00050) and thermodynamic data obtained through the *Mfold webserver for nucleic acid folding and hybridization prediction* (Zuker, 2003).

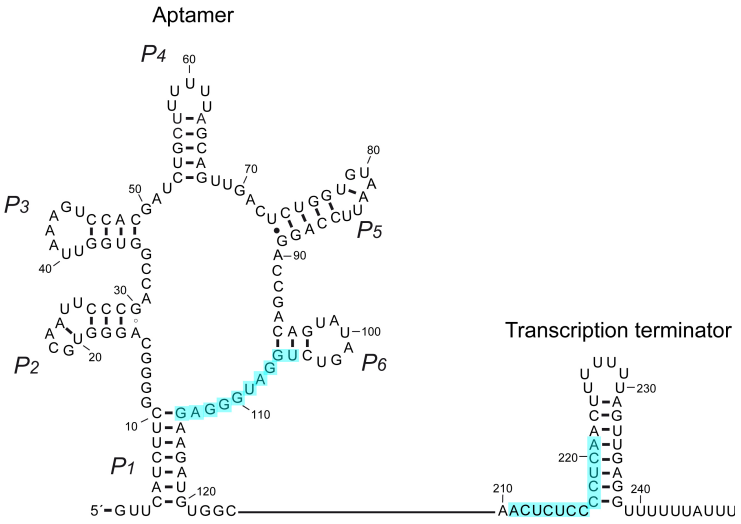

Figure 1.8: The transcriptional FMN riboswitch *Rli96* from *L. monocytogenes*. Suggested secondary structure of *Rli96* featuring the FMN binding aptamer and the transcription terminator loop. The bases highlighted in blue are predicted to pair in the absence of FMN to form an anti-terminator loop, enabling transcription to proceed. The suggested secondary structure is based on the alignment of *Rli96* to the FMN riboswitch family (Rfam-Accession: RF00050) and thermodynamic data obtained through the *Mfold webserver* (Griffiths-Jones et al., 2003; Zuker, 2003).

1.8 Objectives of the Work

The main objective of this work was to gain insight into the flavin metabolism of *L. monocytogenes*. Particularly, the focus was on how toxic flavin analogs are metabolized and their possible use as antimicrobials against the human pathogen. This included answering the question if the riboflavin transport protein Lmo1945 was also responsible for the uptake of riboflavin analogs into the cells and to which extent the intracellular concentrations of riboflavin derived cofactors are related to the response of the FMN riboswitch *Rli96*, controlling the expression of Lmo1945, to cofactor analogs. In addition, the identification and characterization of enzymes producing cofactors from riboflavin and its analogs in *L. monocytogenes* were approached.

Furthermore, an *in vivo* reporter system for the characterization of translationally controlled riboswitches from *Streptomyces* species was evaluated.

2 Materials

2.1 Buffers and Solutions

For the preparation of all buffers and solutions ultrapure water, prepared with *Millipore Milli-Q® Gradient A10* was used. All buffers and solution that were used for HPLC-MS or FPLC applications were filtered through 0.2 μm after preparation and degassed for 20 min in an ultrasonic bath prior to use.
If not stated differently, the pH was adjusted to the given values with concentrated (i.e. > 1 M) hydrochloric acid or sodium hydroxide respectively.

2.1.1 Stock Solutions for Buffer Preparation

Table 2.1: 0.5 M EDTA stock solution; pH 8.0.

Compound	Amount	Final Conc.
Na_2EDTA	93.05 g	0.5 M
NaOH (solid)	approx. 10.14 g[a]	
H_2O	ad 500 ml	

[a] Pre-calculated amount for pH 8.0

Table 2.2: 5 M NaCl stock solution; pH not adjusted.

Compound	Amount	Final Conc.
NaCl	292.2 g	5 M
H_2O	ad 1000 ml	

Table 2.3: 0.5 M monobasic sodium phosphate stock solution; pH not adjusted

Compound	Amount	Final Conc.
$NaH_2PO_4 \cdot H_2O$	69.0 g	0.5 M
H_2O	ad 1000 ml	

Table 2.4: 0.5 M dibasic sodium phosphate stock solution; pH not adjusted

Compound	Amount	Final Conc.
$Na_2HPO_4 \cdot 2H_2O$	89.0 g	0.5 M
H_2O	ad 1000 ml	

Table 2.5: 0.5 M sodium phosphate buffer; various pH.

pH	monobasic stock (0.5 M)	dibasic stock (0.5 M)
6.0	877 ml	123 ml
6.5	685 ml	315 ml
7.0	390 ml	610 ml
7.5	160 ml	840 ml
8.0	53 ml	947 ml

Table 2.6: 1 M Tris-HCl stock solution; pH 7.5.

Compound	Amount	Final Conc.
Tris base	121.1 g	1 M
H_2O	ad 1000 ml[a]	

[a] Water added to approx. 800 ml, pH adjusted with conc. HCl, volume adjusted with water to 1000 ml after the solution has cooled off to room temperature.

Table 2.7: 10x Tris-glycine buffer for SDS-PAGE; pH 8.6 $\pm$ 0.2 not adjusted.

Compound	Amount	Final Conc.
Glycine	144 g	1.92 M
Tris base	30.3 g	250 mM
SDS	10 g	1% m/v
H_2O	ad 1000 ml	

Table 2.8: Towbin buffer[a]; pH 8.6 ± 0.2 not adjusted.

Compound	Amount	Final Conc.
Glycine	14.41 g	192 mM
Tris base	3.03 g	25 mM
Methanol	200 ml	20% v/v
H_2O	ad 1000 ml	

[a] not autoclavable, stored af 4 °C

Table 2.9: GES lysis buffer; pH 8

Compound	Amount	Final Conc.
Guanidinium thiocyanate	5.91 g	5 M
EDTA 0.5 M	2 ml	0.1 M
N-Lauroylsarcosine	0.05 g	0.5% m/v
H_2O	ad 10 ml[a]	

[a] Guanidinium thiocyanate and EDTA were mixed with approx. 8 ml H_2O at 65 °C. Laurylsarcosine was added and the volume was adjusted to 10 ml after the solution has cooled off to room temperature.

Table 2.10: GusA extraction buffer; pH 7

Compound	Amount	Final Conc.
Sodium phosphate 0.5 M; pH 7[a]	100 ml	50 mM
DTT	0.771 g	5 mM
Triton-X 100	1 ml	0.1% v/v
H_2O	ad 1000 ml	

[a] see table 2.5

2.1.2 Buffers for FPLC and HPLC-MS

Table 2.11: Buffer A for IMAC; pH 7.5.

Compound	Amount	Final Conc.
Sodium phosphate 0.5 M; pH 7.5[a]	100 ml	50 mM
NaCl 5 M	60 ml	300 mM
Imidazole 2 M	10 ml	20 mM
H_2O	ad 1000 ml	

[a] see table 2.5

Table 2.12: Buffer B for IMAC; pH 7.5.

Compound	Amount	Final Conc.
Sodium phosphate 0.5 M; pH 7.5[a]	100 ml	50 mM
NaCl 5 M	60 ml	300 mM
Imidazole 2 M	100 ml	200 mM
H_2O	ad 1000 ml	

[a] see table 2.5

Table 2.13: Buffer A for AEX; pH 8.0.

Compound	Amount	Final Conc.
Tris-HCl 1M	20 ml	20 mM
NaCl 5M	5 ml	25 mM
H_2O	ad 1000 ml	

Table 2.14: Buffer B for AEX; pH 8.0.

Compound	Amount	Final Conc.
Tris-HCl 1M	20 ml	20 mM
NaCl 5M	100 ml	500 mM
H_2O	ad 1000 ml	

Table 2.15: Buffer A for MBPTrap; pH 7.4.

Compound	Amount	Final Conc.
Tris-HCl 1M	20 ml	20 mM
NaCl 5M	40 ml	200 mM
EDTA 0.5 M	2 ml	1 mM
H_2O	ad 1000 ml	

Table 2.16: Buffer B for MBPTrap; pH 7.4.

Compound	Amount	Final Conc.
Tris-HCl 1M	20 ml	20 mM
NaCl 5M	40 ml	200 mM
EDTA 0.5 M	2 ml	1 mM
Maltose	3.42 g	10 mM
H_2O	ad 1000 ml	

Table 2.17: Ammonium formate buffer for HPLC-MS; pH 3.7.

Compound	Amount	Final Conc.
Ammonium formate	2.53 g	20 mM
Formic acid	1.84 ml	20 mM
H_2O	ad 2000 ml	

2.1.3 Antibiotics and Inducer

Stock solutions of antibiotics that were prepared with ultrapure water were sterilized by passing through a syringe filter (RC, 0.2 μm). The stocks were stored in aliquots of 1 ml at $-20\,^{\circ}$C in sterilized MCTs. To reach the working concentration in the culture media, appropriate volumes of the stock solution were added to the media directly before inoculation.
For solid media containing agar-agar, the antibiotic stock solution was added after the temperature of the media was below 55 °C.

Table 2.18: Antibiotics used for selection of *E. coli*.

Antibiotic	Stock conc. ($^{mg}/_{ml}$)	Working conc. ($^{\mu g}/_{ml}$)
Apramycin	50	50
Ampicillin	100	100
Carbenicillin	100	100
Chloramphenicol[a]	34	34
Kanamycin	100	50
Nalidixic acid[b]	25	25

[a]Stock in 96% EtOH
[b]Stock in 0.15 M NaOH

Table 2.19: Antibiotics used for selection of *B. subtilis*.

Antibiotic	Stock conc. ($^{mg}/_{ml}$)	Working conc. ($^{\mu g}/_{ml}$)
Chloramphenicol[a]	30	5
Erythromycin	10	1
Kanamycin	100	5 - 10

[a]Stock in 96% EtOH

Table 2.20: Antibiotics used for selection of *Streptomyces* spp.

Antibiotic	Stock conc. ($^{mg}/_{ml}$)	Working conc. ($^{\mu g}/_{ml}$)
Apramycin	50	50
Hygromycin	50	25
Thiostreptone[a]	50	50

[a]Stock in DMSO

Table 2.21: Compunds used for induction of protein production.

Compund	Stock conc.	Working conc.
IPTG	1 M	0.1 - 1 mM
Thiostreptone[a]	50 $^{mg}/_{ml}$	10 $^{\mu g}/_{ml}$

[a]Stock in DMSO

2.2 Media

For the preparation of growth media ultrapure water was used by default. The media were heat sterilized for 20 min at 121 °C (Varioklav® 75S, H+P Labortechnik, Habermoos). If not stated differently, the pH was adjusted to the given values with concentrated (i.e. > 1 M) hydrochloric acid or sodium hydroxide respectively.

Table 2.22: Lysogeny Broth (LB); pH 7.2 (Sambrook and Russell, 2001).

Compound	Amount	Final Conc.
Tryptone	10 g	10 g/l
Yeast extract	5 g	5 g/l
NaCl	10 g	10 g/l
H_2O	ad 1000 ml	

Table 2.23: Lysogeny Agar (LA); pH 7.2 (Sambrook and Russell, 2001).

Compound	Amount	Final Conc.
Tryptone	10 g	10 g/l
Yeast extract	5 g	5 g/l
NaCl	10 g	10 g/l
Agar-agar	15 g	15 g/l
H_2O	ad 1000 ml	

Table 2.24: SOC Medium; pH 6.8 - 7.0 (Hanahan, 1983).

Compound	Amount	Final Conc.
Tryptone	2 g	20 g/l
Yeast extract	0.5 g	5 g/l
NaCl	1 g	10 mM
KCl[a] 1 M	0.25 ml	2.5 mM
$MgCl_2$[a] 1 M	1 ml	10 mM
Glucose[b] 2 M	1 ml	20 mM
H_2O	ad 100 ml	

[a] filter sterilized (0.2 μm cellulose acetate) and added after autoclaving
[b] glucose stock solution was autoclaved separately

Table 2.25: GYT Medium; pH 7.2 (Tung and Chow, 1995).

Compound	Amount	Final Conc.
Tryptone	2.5 g	2.5 g/l
Yeast extract	1.25 g	1.25 g/l
Glycerol[a] 50% (v/v)	200 ml	10% (v/v)
H_2O	ad 1000 ml	

[a] autoclaved separately

Table 2.26: 2 xYT Medium; pH 7.0.

Compound	Amount	Final Conc.
Tryptone	16 g	16 g/l
Casamino acids	10 g	10 g/l
NaCl	5 g	5 g/l
H_2O	ad 1000 ml	

Table 2.27: Tryptic Soy Broth (TSB); pH 7.3.

Compound	Amount	Final Conc.
Casein peptone (pancreatic)	17 g	17 g/l
Soya peptone (papain)	3 g	20 g/l
Glucose	2.5 g	2.5 g/l
NaCl	5 g	5 g/l
KH_2PO_4	2.5 g	2.5 g/l
H_2O	ad 1000 ml	

Table 2.28: Yeast Starch Nutrient Broth (YS); pH 7.2 (Kieser et al., 2000).

Compound	Amount	Final Conc.
Yeast extract	2 g	2 g/l
Soluble potato strach	10 g	10 g/l
H_2O	ad 1000 ml	

Table 2.29: Mannitol Soy Sporulation Medium (MS); pH 7.2 (Kieser et al., 2000).

Compound	Amount	Final Conc.
Mannitol	20 g	20 g/l
Soybean flour[a]	20 g	20 g/l
Agar-agar	15 g	15 g/l
H_2O	ad 1000 ml	

[a] dissolved in hot tap water

Table 2.30: 10 x Spizizen Minimal Salts (SMS); pH 7.2 (Spizizen, 1958).

Compound	Amount	Final Conc.
Ammonium sulfate	20 g	20 g/l
K_2HPO_4	140 g	140 g/l
KH_2PO_4	60 g	60 g/l
Sodium citrate (dihydrate)	10 ml	10 g/l
Magnesium sulfate (heptahydrate)	2 g	2 g/l
H_2O	ad 1000 ml	

Table 2.31: Spizizen Minimal Medium (SMM); pH 7.2 (Spizizen, 1958).

Compound	Amount	Final Conc.
10 x Spizizen Minimal Salts	100 ml	10% (v/v)
Glucose 50% (w/v)	10 ml	0.5 g/l
L-Tryptohan 5 mg/ml	10 ml	50 mg/l
100 xTrace elements[a]	10 ml	1 x
H_2O	ad 1000 ml	

[a] Trace elements are not included in the original recipe by Spizizen (1958). 100 xTrace elements solution according to Cutting (1990).

2.3 Kits and Enzymes

Table 2.32: Kits, Enzymes, Ladders and Dyes

Product	Supplier
GeneJet™ Plasmid Miniprep Kit	Thermo Scientific
GeneJet™ Genomic DNA Purification Kit	Thermo Scientific
GeneJet™ Gel Extraction Kit	Thermo Scientific
Mini-PROTEAN® TGX™ Any kD™	BioRad
His·Tag® AP Western Reagents	Merck Millipore
E. coli T7 S30 Extract System for Circular DNA	Promega
T4 DNA Ligase	Thermo Scientific
FastAP™ Alkaline Phosphatase	Thermo Scientific
KAPAHiFi™ DNA Polymerase	KAPA Biosystems
DreamTaq DNA Polymerase	Thermo Scientific
Fast Digest™ Restriction Enzymes	Thermo Scientific
Type IIs Restriction Enzymes	Thermo Scientific
GeneRuler 1 kb Plus DNA Ladder	Thermo Scientific
PageRuler™ Plus Prestained Protein Ladder	Thermo Scientific
PageBlue™ Protein Staining Solution	Thermo Scientific

2.4 Oligonucleotides and Plasmids

A comprehensive list of all oligonucleotides and plasmids used in this work, including their relevant genetic features and resistance markers is given in tables 2.33 and 2.34, respectively. A selection of plasmids that were constructed and used throughout this work is described in more detail, including a graphical representation of the relevant genetic features in the following sections.

2.4.1 Plasmids for the *xylE* Reporter System

The plasmids pAM01, pAM023, pAM673, pAM893 and pAM893a were constructed to provide a reporter platform in *Streptomyces* spp. for an *in vivo* test system for translational riboswitches, based on the expression of the reporter gene *xylE*. The backbone of all plasmids shown in figure 2.1 was the integrative vector pSET152 constructed by Bierman et al. (1992). Hence, all the plasmids feature an *oriT* region that allows for conjugally transfer from *E. coli* to *Streptomyces* spp., as well as the $int^{\phi C31}$ region, that allows site-specific integration of

the plasmid at the bacteriophage ϕC31 attachment site in streptomycetes.

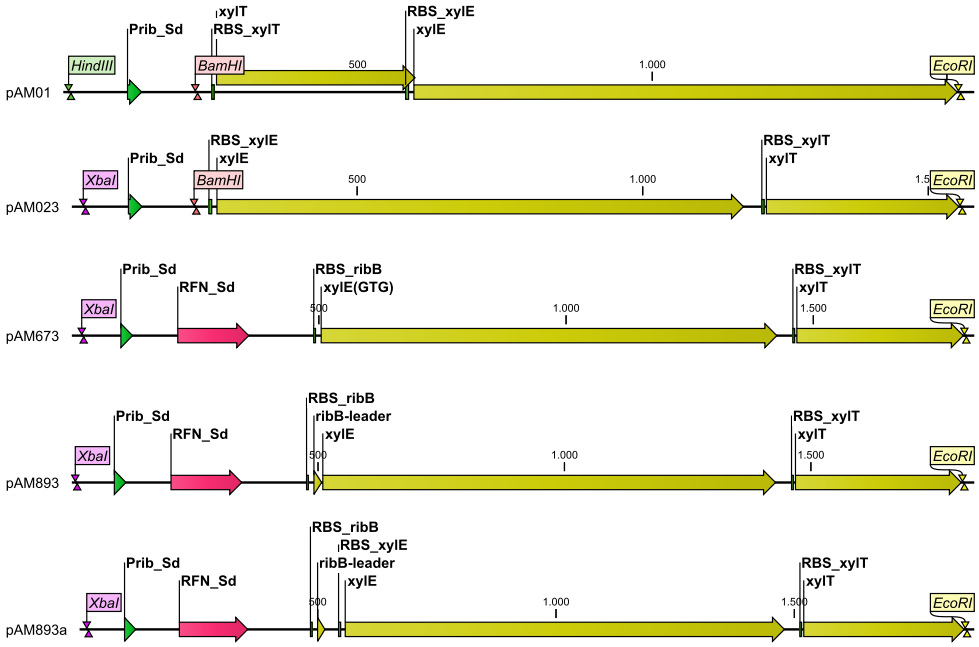

Figure 2.1: Integrative plasmids for the *xylE* reporter system. The pSET152 derived plasmids pAM01, pAM023, pAM673, pAM893 and pAM893a.

The plasmid pAM01 features the P_{rib} promoter region of *S. davawensis* upstream of the two genes *xylT* and *xylE* in their overlapping configuration that was amplified from the promoter probe plasmid pIPP1. In contrast to pIPP1 the plasmid pAM01 provides two unique restriction sites *HindIII* and *BamHI* upstream of the reporter region, that allows for directional insertion of putative promoter fragments.

The plasmid pAM023 features the same elements as pAM01 where the coding sequences for *xylT* and *xylE* have been separated and their sequential arrangement has been inverted so that *xylE* is placed upstream of *xylT*.

The plasmid pAM673 features a translational fusion of the he P_{rib} promoter, the FMN riboswitch and the ribosomal binding site RBS_{ribB}, including the GTG start codon of *ribB* from *S. davawensis* replacing the ATG start codon of *xylE*. The placement of *xylT* is identical as on pAM023.

The plasmid pAM893 includes adjacent to RBS_{ribB} the six leading codons of *ribB* merging directly into the coding sequence of *xylE*.

The plasmid pAM893a features a 34 nt sequence between the six leading codons of *ribB* from *S. davawensis* and the ATG start codon of *xylE*. This sequence contains the original ribosomal binding site RBS_{xylE}. The placement of *xylE*, *xylT* and the respective ribosomal binding sites is identical to the plasmid pAM023.

2.4.2 Plasmids for the *gusA* Reporter System

The plsamids pMgus01 and pAMgus04 were constructed based on the work of Myronovskyi et al. (2011). With the plasmid pGUSHL4aadA Myronovskyi et al. provided a platform for translational fusions in streptomycetes to the reporter gene *gusA* from *E. coli*. The gene *gusA* is coding for the enzyme β-glucuronidase (GusA) that tolerates large C- and N-terminal fusions and hydrolyzes several β-glucuronides (e.g. p-Nitrophenyl β-D-glucopyranoside (PNPG)).

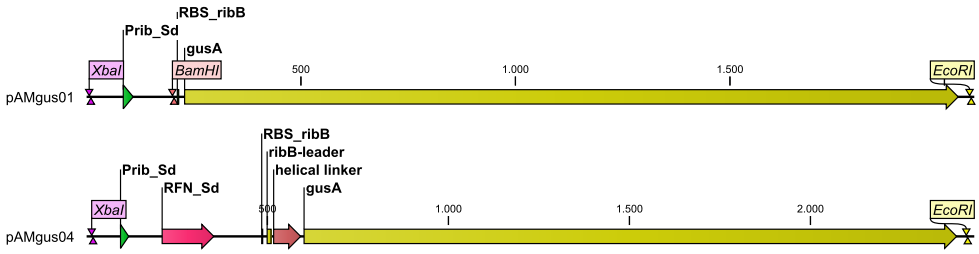

Figure 2.2: Integrative plasmids for the *gusA* reporter system. The pSET152 derived plasmids pAMgus01 for transcriptional fusions and pAMgus04 for translational fusions with *gusA*.

The plasmid pAMgus01 features the P_{rib} promoter region of *S. davawensis*, the ribososmal binding site RBS_{ribB} upstream of *gusA*. Therefore pAMgus01 functions as a *gusA* based promoter probe plasmid similar to pSETgus (kindly provided by Andriy Luzhetskyy, Helmholtz Institute for Pharmaceutical Research, Saarbrücken, Germany).

The plasmid pAMgus04 consists of a 492 nt long sequence from *S. davawensis*, including the P_{rib} promoter, the FMN riboswitch, the ribosomal binding site RBS_{ribB} as well as the six leading codons of *ribB*, that is fused in-frame to the coding sequence for the helical linker HL4 and the downstream gene *gusA*.

2.4.3 Lmo0728 Expression Plasmids

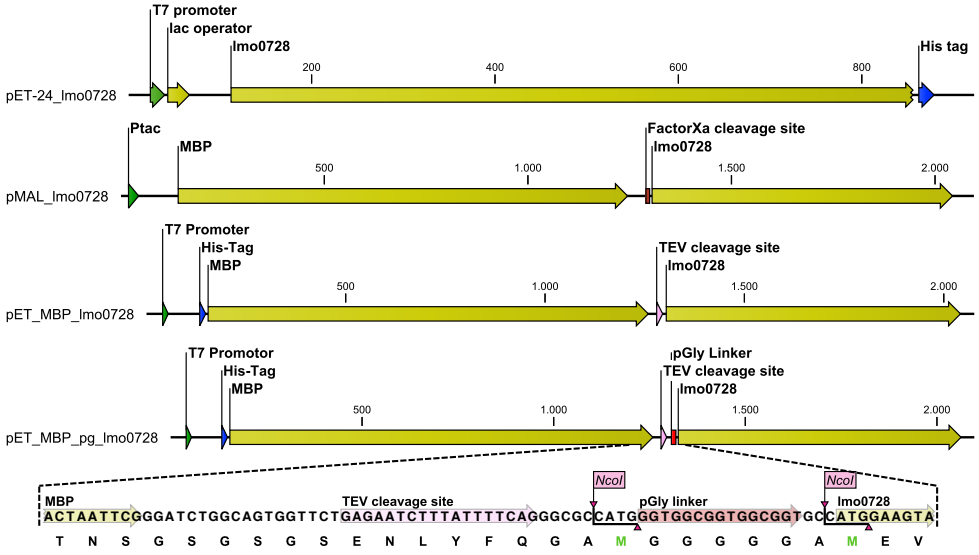

Figure 2.3: Lmo0728 expression plasmids. The plasmids were used for the heterologous expression of different Lmo0728-fusion proteins. pET-24_lmo0728, pMAL_0728, pET-MBP-0728 and pET-MBP-pg-0728 with sequence detail.

The plasmid pET-24_lmo0728 features the coding sequence of *lmo0728* cloned into pET-24a(+), digested with *XbaI/XhoI*. The protein Lmo0728-His expressed from this vector possesses a C-terminal His-tag.

The plasmid pMAL_lmo0728 features a fusion of *malE* and *lm0728*, separated by a spacer, coding for the FactorXa recognition sequence. The expression is controlled by the IPTG inducible, synthetic P_{tac} promoter.

The plasmid pET-MBP-lmo0728 was constructed by replacing *egfp* in the plasmid pET-MBP-1a with the coding sequence of *lmo0728*. The plasmid provides an expression platform for a N-terminally His-tagged MBP-Lmo0728 fusion protein. The two domains are separated by by a spacer sequence, coding for the TEV protease recognition sequence.

The plasmid pET-MBP-pg-lmo0728 was derived from pET-MBP-lmo0728 through insertion of a 25 nt long linker into the unique *NcoI* restriction site upstream of *lmo0728*. The linker features the codons GGT and GGC, both coding for glycine, in an alternating manner. The introduction of the glycine spacer alleviates the access of the TEV protease to the dedicated cleavage site.

Table 2.33: Oligonucleotides used in this work. Restriction sites underlined.

Name	Sequence ($5' \rightarrow 3'$)	Application
F-lmo0728.NheI	ATTATTGCTAGCGAAGTATCGCATGTAACG	pET-24_lmo0728, pET-28_lmo0728
R-lmo0728.XhoI	ATTACTCGAGCTCGGAAAGTTCGTTTTCA	pET-24_lmo0728
F-lmo1329atg.NheI	AATAATGCTAGCATGAAGACGATATACTTACA	pET-24_lmo1329
R-lmo1329.NotI	AATATAGCGGCCGCATCTTCTAATTTAGCAA	pET-24_lmo1329
R-lmo0728taa.XhoI	TATCCTCGAGTTACTCGGAAAGTTCGTTTTCA	pET-28_lmo0728
F-lmo0728.EcoRV	TATAGATATCATGGAAGTATCGCATGTAAC	pMAL_lmo0728
R-lmo0728taa.BamHI	TATCGGATCCTTACTCGGAAAGTTCGTTT	pMAL_lmo0728, pET-MBP-lmo0728
F-lmo0728.NcoI	ATAGCCATGGAAGTATCGCATGTAAC	pET-MBP-lmo0728
FL-pGly.NcoI	CATGGGTGGCGGTGGCGGTGC	linker for pET-MBP-pg-lmo0728
RL-pGly.NcoI	CATGGCACCGCCACCGCCACC	linker for pET-MBP-pg-lmo0728
F-lmo1945.BamHI	ATATATGGATCCATGAAGAATTATTCAATGAA	pHT01_lmo1945
R-lmo1945.AatII	ATTGACGTCTTAATGGCTTATTTCTTGTTGTCTTTT	pHT01_lmo1945
F-Rli96.EcoRI	CGCGAATTCATAAATAAAACCAGCTAATT	pDG268_Rli96
R-Rli96.BamHI	CGCGGATCCGAATATTTTCTTACAATTTT	pDG268_Rli96
F-Rli96.HindII	CGCAAAGCTTATAAATAAAACCAGCTAATT	pT7luc_Rli96
R-Rli96.NotI	ATATATGCGGCCGCTCATTGAATAATTCTTCATTG	pT7luc_Rli96
F-PribSc.BamHI	GGGGGATCCA GTCGGTTCCT CTCCACGGA	pIPP1_PribSc/(AS)
R-PribSc.BamHI	GGGGGATCCCACGGCCAGTGTGCCACGCC	pIPP1_PribS/(AS)

Name	Sequence ($5' \rightarrow 3'$)	Application
F-PribSd.BamHI	GGGGGATCCGTCGGTTCCTCTCCACGGAA	pIPP1_PribSd/(AS)
R-PribSd.BamHI	GGGGGATCCCAGGGCCAGTGTGCCACGCC	pIPP1_PribSd/(AS), pAM01, pAM023, pAMgus01, pAMgus02, pAMgus03, pAMgus04
F-PribSc.XbaI	ATATATTCTAGAAGTCGGTTCCTCTCCACGGA	pAM152ScxE
F-PribSd.XbaI	ATATATTCTAGAGTCGGTTCCTCTCCACGGAA	pAM152SdxE, pAM01, pAM023, pAMgus01, pAMgus02, pAMgus03, pAMgus04
R-ribB.BamHI	ATATATGGATCCGACGATTCCGGTGAACACTT	pAM152ScxE, pAM152SdxE
F-xylE.BamHI	ATATATGGATCCAACAAAGGTGTAATGCG	pAM152ScxE, pAM152SdxE
R-xylE.EcoRI	ATATATGAATTCTCAGGTCAGCACGGTCATGAAT	pAM152ScxE, pAM152SdxE, pAM01
F-xylT.HindIII	ATATAAGCTTTCCGTCATGTTTAGTGTATC	pAMxT
R-xylT.XbaI	ATATATTCTAGATCATGACGTCACCTCTTCAT	pAMxT, pAM01
F-xylT.BamHI	ATATGGATCCTCCGTCATGTTTAGTGTATC	pAM01
F-xylE.BamHI	ATATGGATCCAACCTGACAACATGAACTAT	pAM023, pAM453a, pAM893a
R-xylE.NotI	ATATGCGGCCGCTCAGGTCAGCACGGTCATG	pAM023, pAM453/a, pAM673, pAM893/a
F-xylT.NotI	ATATGCGGCCGCTCCGTCATGTTTAGTGTATC	pAM023, pAM453/a, pAM673, pAM893/a
R-xylT.EcoRI	ATATATGAATTCTCATGACGTCACCTCTTCAT	pAM023, pAM453/a, pAM673, pAM893/a

Name	Sequence ($5' \rightarrow 3'$)	Application
F-xylEatg.BsaI	ATATGGTCTCGAAATGAACAAAGGTGTAATGCG	pAM453/a
R-RFNatg.BsaI	ATATGGTCTCGATTTCCCGGGTCCTCCTGCCTCAT	pAM453/a
F-xylEgtg.BsaI	ATATGGTCTCGAAGTGAACAAAGGTGTAATGCG	pAM673
R-RFNgtg.BsaI	ATATGGTCTCGACTTCCCGGGTCCTCCTGCCTCAT	pAM673
F-xylE.BsaI	ATATGGTCTCATCAACAAAGGTGTAATGCGA	pAM893/a
R-ribB.BsaI	ATTAGGTCTCATTGACGATTCCGGTGAACACTT	pAM893/a
R-RFNSd.BamHI	TAGCGGATCCTTCCCGGGTCCTCCTGCCTCAT	pAM453a
R-ribB2.BamHI	ATTAGGATCCGACGATTCCGGTGAACACTT	pAM893a
R-gusA.NotI	ATATGCGGCCGCTTATCACTGCTTCCCGC	pAMgus01, pAMgus02, pAMgus03, pAMgus04
F-gusA.BsaI	ATATGGTCTCAAGTGCTGCGGCCCGTCGAAACC	pAMgus01
F-HL4.BsaI	ATATGGTCTCAAGTGCTCGCCGAGGCCGCCGC	pAMgus02
F-ribBHL4.BsaI	ATATGGTCTCACGTCCTCGCCGAGGCCGCCGC	pAMgus03, pAMgus04
R-ribB2.BsaI	ATATGGTCTCAGACGATTCCGGTGAACACTT	pAMgus04
FL-RBSribB.BamHI	GATCCAGGCAGGAGGACCCGGGA	linker for pAMgus01, pAMgus02
RL-RBSribB.BamHI	CACTTCCCGGGTCCTCCTGCCTG	linker for pAMgus01, pAMgus02
FL-ribB.BamHI	GATCCAGGCAGGAGGACCCGGGAAGTGTTCACCGGAAT	linker for pAMgus03
RL-ribB.BamHI	GACGATTCCGGTGAACACTTCCCGGGTCCTCCTGCCTG	linker for pAMgus03

Table 2.34: Plasmids used in this work

Name	Relevant Features	Resistance	Reference
pET-24a(+)	P_{T7}, MCS, C-His	Kan	Novagen (2002)
pET-28a	P_{T7}, MCS, N-His / C-His	Kan	Novagen (2002)
pET-24_lmo0728	modified pET-24a(+), *lmo0728*-His	Kan	This work
pET-24_lmo1329	modified pET-24a(+), *lmo1329*-His	Kan	This work
pET-28_lmo0728	modified pET-28a, His-*lmo0728*	Kan	This work
pMAL-c5x	*malE* (MBP-), Factor Xa cleavage site, MCS	Amp	NEB
pMAL_lmo0728	modified pMAL-c5x, MBP-*lmo0728*	Amp	This work
pET-MBP-1a	modified pET-24d, P_{T7}, N-His-MBP, TEV cleavage site, *eGFP*	Kan	EMBL[a]
pET-MBP-lmo0728	modified pET-MBP-1a, *eGFP* replaced by *lmo0728*	Kan	This work
pET-MBP-pg-lmo0728	modified pET-MBP-0728, featuring a spacer, coding for 5 Glycines, between the TEV recognition site and *lmo0728*	Kan	This work
pSET152	IncPα oriT, pUC18 oriV, *lacZ*α, int$^{\phi C31}$	Apr	Bierman et al. (1992)
pUB307	RP1 derivate, conjugative, broad-host-range helper plasmid	Kan	Bennett et al. (1977)
pR9406	modified pUB307, *cat* replaced with *bla*	Amp	Jones et al. (2013)
pUWloriTaph	pUC18 oriV, pIJ101 oriV, IncPα oriT, P_{ermE}	Kan, Tsr	Blaesing et al. (2005)
pIPP1	derived from pXE4 and pSET152, *xylE*, *xylT*	Apr, Amp	Jones (2011)
pIPP1_PribSc	P_{rib} of *S. coelicolor* in *BamHI*-site of pIPP1	Apr, Amp	This work

[a]EMBL-made plasmid by Gunter Stier

Name	Relevant Features	Resistance	Source
pIPP1_PribSc(AS)	P_{rib} of *S. coelicolor* in anti sense orientation in *BamHI*-site of pIPP1	Apr, Amp	This work
pIPP1_PribSd	P_{rib} of *S. davawensis* in *BamHI*-site of pIPP1	Apr, Amp	This work
pIPP1_PribSd(AS)	P_{rib} of *S. davawensis* in anti sense orientation in *BamHI*-site of pIPP1	Apr, Amp	This work
pAM152ScxE	pSET152 derived, translational fusion of P_{rib}-RFN-RBS-*ribB*[b] from *S. coelicolor* with *xylE* amplified from pIPP1 (no start codon)	Apr	This work
pAM152SdxE	pSET152 derived, translational fusion of P_{rib}-RFN-RBS-*ribB*[b] from *S. davawensis* with *xylE* amplified from pIPP1 (no start codon)	Apr	This work
pAMxT	pUWloriTaph derived, P_{ermE}, *xylT*	Kan, Tsr	This work
pAM01	pSET152 derived, P_{rib} from *S. davawensis*, *xylT-xylE* fragment from pIPP1	Apr	This work
pAM023	pSET152 derived, P_{rib} from *S. davawensis*, *xylE*, *xylT*	Apr	This work
pAM453[c]	pSET152 derived, translational fusion of P_{rib}-RFN-RBS_{ribB} from *S. davawensis* and *xylE*, *xylT*	Apr	This work
pAM453a[c]	pAM453 derivate, where *xylE* is led by its native RBS_{xylE}	Apr	This work
pAM673[c]	pSET152 derived, translational fusion of P_{rib}-RFN-RBS_{ribB} from *S. davawensis* and $xylE_{GTG}$, *xylT*	Apr	This work

[b] Leading 6 codons of the *ribB*-gene incl. GTG start codon
[c] *Golden Gate Cloning*

Name	Relevant Features	Resistance	Source
pAM893[c]	translational fusion of P_{rib}-RFN-RBS-*ribB*[b] from *S. davawensis* with *xylE* (w/o start codon), *xylT*	Apr	This work
pAM893a[c]	pAM893 derivate, where *xylE* is led by its native RBS_{xylE}	Apr	This work
pSETgus	pSET152 derivate, P_{tipA}, *gusA*[d]	Apr	Myronovskyi et al. (2011)
pGUSHL4aadA	pTESa derivate, MCS, *gusA*[d] fused to helical linker HL4[e]	Apr	Myronovskyi et al. (2011)
pAMgus01[c]	pSET152 derived, P_{rib} from *S. davawensis*, RBS_{ribB}, *gusA*[d]	Apr	This work
pAMgus02[c]	pSET152 derived, P_{rib} from *S. davawensis*, RBS_{ribB}, HL4[e]-*gusA*[d]	Apr	This work
pAMgus03[c]	pSET152 derived, P_{rib} from *S. davawensis*, RBS_{ribB}-*ribB*[b]-HL4[e]-*gusA*[d]	Apr	This work
pAMgus04[c]	pSET152 derived, translational fusion of P_{rib}-RFN-RBS_{ribB}-*ribB*[b] from *S. davawensis* with HL4[e]-*gusA*[d]	Apr	This work
pHT01	ColE1 oriV, *lacI*, P_{grac}, MCS	Amp, Cm	Mobitec (2012)
pHT01_lmo1945	pHT01 derivate, *lmo1945* from *L. monocytogenes*	Amp, Cm	This work
pDG148	pUB110 oriV, pBR322 oriV, P_{spac}, MCS, P_{pen}, *lacI*	Amp, Kan	Stragier et al. (1988)
pDG148_ribU	pGD148 derived, *ribU* from *B. subtilis*	Amp, Kan	Ott et al. (2009)
pDG268	3′–*amyE*, MCS, *lacZ*, *cat*, 5′–*amyE*	Amp, Cm	Antoniewski et al. (1990)
pDG268_RFNbs	modified pDG268, P_{rib}-RFN from *B. subtilis* upstream of *lacZ*	Amp, Cm	Ott et al. (2009)

[d]Codon optimized for *Streptomyces spp.*
[e]Ref: Arai et, al. Protein Eng. 14(8) 2001

Name	Relevant Features	Resistance	Source
pDG268_Rli96	modified pDG268, *Rli96* from *L. monocytogenes* upstream of *lacZ*	Amp, Cm	This work
pT7luc	P_{T7}, MCS, *luc* from *P. pyralis*	Amp	Promega
pT7luc_RFNbs	P_{T7}, RFN from *B. subtilis* upstream of *luc*	Amp	Pedrolli et al. (2012)
pT7luc_Rli96	P_{T7}, *Rli96* from *L. monocytogenes* upstream of *luc*	Amp	This work

2.5 Strains

A comprehensive list of all bacterial strains used in this work, including their relevant genetic features is given in table 2.35.

2.5.1 *B. subtilis* Strains for β-galactosidase Activity Assay

The *B. subtilis* strains Bs::RFNbs and Bs::Rli96 were generated by double crossover integration of plasmids derived from pDG268 (Cutting, 1990). The strains feature the putative riboswitch sequence including its upstream promoter controlling the expression of *lacZ*. The reporter gene *lacZ* is coding for the enzyme β-galactosidase (LacZ, EC 3.2.1.23). The basic structure of the plasmids used for this assay is shown in figure 2.4. The double crossover integration into the amylase locus *amyE* of *B. subtilis* allows for screening with an amylase production assay (section 3.11.4).

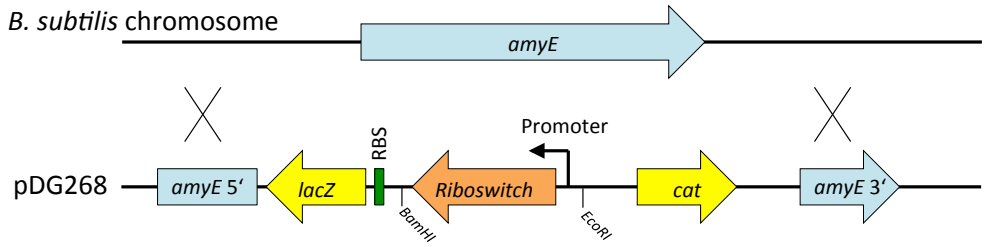

Figure 2.4: Integrative plasmids for the *lacZ* reporter system. Double crossover integration of pDG268 derived riboswitch test plasmids into the *amyE* locus of the chromosome of *B. subtilis*. Figure altered from Ott et al. (2009).

Bs::RFNbs and Bs::Rli96 were used to test the effect of flavins on the *in vivo* expression of the reporter gene *lacZ*. Both strains additionally carry a plasmid with the riboflavin transporter gene *ribU* under the control of a constitutive promoter to ensure the flavin uptake of the cells is not reduced due to regulatory effects in the host. The β-galactosidase activity assay is described in section 3.11.3.

2.5.2 The *L. monocytogenes* FMN Riboswitch Mutant Strain M1

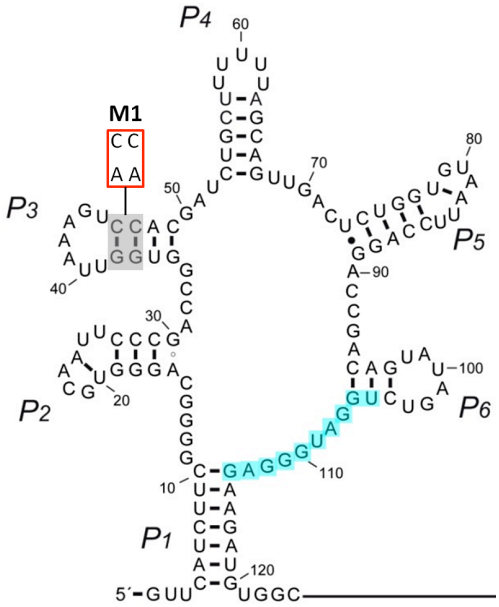

Figure 2.5: The deregulated FMN riboswitch mutant strain M1. Aptamer portion of the FMN riboswitch *Rli96* from *L. monocytogenes* (see also figure 1.8 on page 18). The replacement of nucleotides G37/G38 (grey) by A37/A37 (red box) in the aptamer generated the FMN riboswitch variant M1, which did not terminate the transcription when riboflavin or roseoflavin was added to the medium (Mansjö and Johansson, 2011).

The *L. monocytogenes* mutant strain M1 was kindly provided by Jörgen Johansson (Laboratory for Molecular Infection Medicine Sweden (MIMS), Department of Molecular Biology, Umeå University, Umeå, Sweden). It was created by Mansjö and Johansson (2011) by replacing two nucleotides (GG to AA) in the aptamer region of the FMN riboswitch *Rli96* (figure 2.5). The mutant strain M1 was able to grow better in the presence of roseoflavin when compared to the wild type. Mansjö and Johansson demonstrated in a northern blot experiment that *lmo1945* was transcribed in the M1 strain in the presence of 100 μM riboflavin and roseoflavin respectively. This was in contrast to the wild type, where they only observed a terminated fragment (*Rli96*) under the same conditions.

Table 2.35: Bacterial Strains used in this work

Name	Relevant Features	Reference/Source
E. coli		
Top10	host for plasmid propagation	Invitrogen
	F$^-$ *mcr*A Δ(*mrr-hsd*RMS-*mcr*BC) ϕ80*lac*ZΔM15 Δ*lac*X74 *rec*A1 *ara*D139 Δ(*ara-leu*)7697 *gal*U *gal*K *rps*L (Str^R) *end*A1 *nup*G λ-	
BL21(DE3)	host for recombinant protein production	Invitrogen
	F$^-$ *ompT hsdS*$_B$ (r$_B^-$ m$_B^-$) *gal dcm* (DE3)	
Rosetta(DE3)	host for recombinant protein production	Invitrogen
	F$^-$ *ompT hsdS*$_B$ (r$_B^-$ m$_B^-$) *gal dcm lacY1* (DE3), pRARE	
ER2523	host for recombinant protein production	NEB
	fhuA2 [lon] ompT gal sulA11 R(mcr-73::miniTn10--TetS)2 [dcm] R(zgb-210::Tn10--TetS) endA1 Δ(mcrC-mrr)114::IS10	
ET12567	*dam-13::Tn9*, *dcm-6*, *hsdM*, pUB307	MacNeil et al. (1992)
GM2163	*dam−*, *dcm−*	NEB
L. monocytogenes		
EGDe	wild type	Johansson
M1	*L. monocytogenes* EGDe with G37/G38 replaced by A37/A37 in *Rli96*	Mansjö and Johansson (2011)

Name	Relevant Features	Reference/Source
B. subtilis		
Marburg 168	wild type	DSMZ
BsΔribU	Δ*ribU::kan*^{R}	Hemberger et al. (2011)
BsΔribUB	Δ*ribU::kan*^{R} Δ*ribB::erm*^{R}	Hemberger et al. (2011)
Bs::RFNbs	*amyE::RFNbs-lacZ*	Ott et al. (2009)
Bs::Rli96	*amyE::Rli96-lacZ*	This work
S. davawensis		
JSCC #768	wild type	JSCC
S. coelicolor		
DSM #40233	wild type	DSMZ
Sc::pIPP1	*S. coelicolor* with integrated pIPP1	This work
Sc::PribSc	*S. coelicolor* with integrated pIPP1_PribSc	This work
Sc::PribScAS	*S. coelicolor* with integrated pIPP1_PribSc(AS)	This work
Sc::PribSd	*S. coelicolor* with integrated pIPP1_PribSd	This work
Sc::PribSdAS	*S. coelicolor* with integrated pIPP1_PribSd(AS)	This work
Sc::pSET152	*S. coelicolor* with integrated pSET152	This work
Sc::ScxE	*S. coelicolor* with integrated pAM152ScxE	This work
Sc::SdxE	*S. coelicolor* with integrated pAM152SdxE	This work

Name	Relevant Features	Reference/Source
Sc::pAM01	*S. coelicolor* with integrated pAM01	This work
Sc::pAM023	*S. coelicolor* with integrated pAM023	This work
Sc::pAM453	*S. coelicolor* with integrated pAM453	This work
Sc::pAM453a	*S. coelicolor* with integrated pAM453a	This work
Sc::pAM673	*S. coelicolor* with integrated pAM673	This work
Sc::pAM893	*S. coelicolor* with integrated pAM893	This work
Sc::pAM893a	*S. coelicolor* with integrated pAM893a	This work

3 Methods

3.1 Cultivation of Microorganisms

3.1.1 Cultivation of *E. coli*

E. coli was cultivated under oxic conditions in baffled glass Erlenmeyer flasks in Lysogeny Broth (LB) at 37 °C on an orbital shaker at 180 rpm. For cultivation on solid media, *E. coli* was grown on Lysogeny Agar (LA) at 37 °C. Antibiotics were added to the growth media from sterile filtered stock solutions. Stock and working concentrations of all used antibiotics are given in table 2.18.
E. coli ER2523 was cultivated for recombinant production of MBP fusion proteins in LB with addition of 0.2% (m/v) glucose to repress the expression of amylase genes from the host genome.

3.1.2 Preparation of Chemically Competent *E. coli*

For preparation of chemically competent *E. coli* 50 ml of LB were inoculated from an overnight culture of the desired strain to an OD_{600} of 0.03. When the optical density reached 0.4, the incubation was stopped and the cells was harvested by centrifugation (10 min, 3000 x g, 4 °C). The supernatant was discarded, the cells were resuspended carefully in 20 ml pre-chilled, ice cold $CaCl_2$ (0.1 M) solution and put on ice for 20 min and afterwards centrifuged as before. The cells were resuspended in 2 ml of the ice cold $CaCl_2$ solution and 660 μl of sterile glycerol (60% v/v) were added. The chemically competent cells were aliquoted on ice to volumes of 50 μl and frozen by immersion in liquid nitrogen. The frozen aliquots were stored for later use at -80 °C (Cohen et al., 1972; Sambrook and Russell, 2001).

3.1.3 Preparation of Electrocompetent *E. coli*

For the preparation of electrocompetent *E. coli* 1 l (4 x 250 ml) LB medium was inoculated from an overnight culture of the desired strain to an OD_{600} of 0.03 and incubated at 37 °C and 180 rpm. When the OD_{600} of the cultures reached 0.4, they were put on ice for 30 min and afterwards the cells were harvested by centrifugation (15 min, 5000 x g, 4 °C). The cells were carefully resuspended in 500 ml of ice cold, sterile ultra pure water and once again centrifuged as before. The cells were resuspended in 250 ml ice cold glycerol (10% v/v) and through repeated centrifugation and resuspension in glycerol (10% v/v) the volume was reduced to 10 ml. After a final centrifugation step the cells were resuspended in 1 ml ice cold GYT and aliquoted on ice to volumes of 50 μl and frozen by immersion in liquid nitrogen and stored at -80 °C(Elvin and Bingham, 1991; Sambrook and Russell, 2001; Miller and Nickoloff, 1995).

3.1.4 Transformation of Chemically Competent *E. coli*

For the transformation of chemically competent *E. coli* the frozen cells were thawed on ice for 10 min. For each transformation 100 - 500 ng of plasmid DNA or 5 μl of a ligation reaction were added to the vial and mixed gently by tapping. The mixture was incubated on ice for 30 min and subsequently incubated for 30 s at 42 °C by immersion in a water bath. After the heat shock, the vial was placed on ice for 2 min and 250 μl pre-warmed (37 °C) SOC media were added. The vial was incubated at 37 °C for 1 h with horizontal shaking at 225 rpm. Following incubation, two volumes per reaction (20 μl and 200 μl) were spread onto selective LA plates containing the appropriate antibiotics. The plates were incubated overnight at 37 °C.
The success of the transformation was confirmed by either colony PCR or purification of plasmid DNA from resistant colony and subsequent restriction analysis or sequencing of the obtained plasmid DNA.

3.1.5 Transformation of Electrocompetent *E. coli*

For the transformation of electrocompetent *E. coli* the frozen cells were thawed on ice for 10 min. For each reaction 10 - 100 ng of plasmid DNA or 2 μl of a ligation reaction were added to the vial and mixed gently by tapping. The mixture was transferred into a pre chilled electroporation cuvette with 0.1 cm gap width (Bio-Rad Laboratories). The electroporation was carried out in a Gene Pulser® II Electroporation System (Bio-Rad Laboratories) set to a voltage

of 2.5 kV, capacitance of 25 μF and sample resistance of 200 Ω. Immediately after the pulse 250 μl of pre-warmed (37 °C) SOC media were added into the cuvette. The mixture was transferred into a 1.5 ml testtube and incubated at 37 °C for 1 h with horizontal shaking at 225 rpm. Following incubation, two volumes per reaction (20 μl and 200 μl) were spread onto LA plates containing the appropriate antibiotic for plasmid selection. The plates were incubated overnight at 37 °C.

3.1.6 Triparental Mating

Triparental mating was used to move the plasmids pAMxT and pR9406 into the non-methylating *E. coli* strain GM2163.

Table 3.1: Strains used for Triparental Mating

Strain	Plasmid	Resistance
E. coli Top10	pAMxT	Kan
E. coli DH5α	pR9406	Amp
E. coli GM2163		Cm

From each strain given in table 3.1 an overnight culture was diluted 1:100 and grown into exponential phase. When the OD_{600} reached 0.4 the respective culture was harvested by centrifugation (5 min, 3500 x g, 4 °C) and washed twice with fresh LB to remove residual antibiotics that might disturb the mating process, and finally resuspended in 500 μl fresh LB. Since the growth rates may vary for different strains, the resuspended cells were stored on ice until the cells from all cultures were available. For the mating process 10 μl of each strain were added to the same spot on an LA plate and incubated for 16 h at 37 °C. To select for single colonies of *E. coli* GM2163 containing pAMxT and the helper plasmid pR9406, material from each of the spots was streaked onto an LA plate containing kanamycin, ampicillin and chloramphenicol and incubated over night at 37 °C. Single colonies were picked and tested by colony PCR to verify the uptake of both plasmids.
The resulting strain *E. coli* GM2163 (pAMxT, pR9406) was used for the transformation of *S. coelicolor* (wt, Sc::pSET152, Sc::ScxE, Sc::SdxE) by conjugation.

3.1.7 Cultivation of Streptomycetes

Liquid cultures of *Streptomyces* spp. were grown under oxic conditions in baffled glass Erlenmeyer flasks on an orbital shaker at 180 rpm. *S. coelicolor* was cultivated in TSB at 30 °C while *S. davawensis* cultures were typically grown in YS at 37 °C. For the production of sporulating cultures, streptomycetes were grown on MS agar plates at 30 °C until the aerial mycelium was clearly visible.

3.1.8 Preparation of a Spore Suspension from *S. coelicolor*

For the preparation of a spore suspension, 200 μl of a mid-exponential liquid culture of *S. coelicolor* were spread on MS agar plates and incubated at 30 °C until the surface was completely covered with sporulating mycelium (up to 96 h). Per milliliter of spore suspension, 3 - 10 of such plates were prepared. Each plate was covered with 9 ml sterile water containing 0.1% (v/v) Tween20 and a sterile cell scraper was used to scrape off spores and mycelia from the surface of the MS agar. The liquid from all plates was pooled in a sterile tube and mixed for 1 min with a vortex mixer to separate the spores from the mycelium. The liquid was then passed through sterile cotton, to separate the mycelium from the spore suspension, and subsequently centrifuged (5 min, 3500 x g, 4 °C). The spores were resuspended in 1 ml sterile glycerol (20% (v/v)) and stored at -80 °C. The titer of viable spores in the spore suspension was determined by spreading 100 μl of relevant dilutions (10^{-6} - 10^{-9}) on MS agar plates (Kieser et al., 2000).

3.1.9 Transformation of *S. coelicolor* by Conjugation

A donor strain of *E. coli* GM2163 with the helper plasmid pUB307 containing also the oriT-plasmid (e.g. pSET152 or a plasmid derived from it) was prepared beforehand through electrotransformation of *E. coli* GM2163 (pUB3017) with the oriT-plasmid.
A culture with the volume of 50 ml of the donor strain was grown in LB, containing chloramphenicol, kanamycin and apramycine to select for the host and both plasmids, to an OD_{600} of 0.4. The cells were harvested by centrifugation (5 min, 2500 x *g*, 4 °C) and washed twice with fresh LB without antibiotics and finally resuspended in 0.5 ml of fresh LB.
A volume of 50 μl of a *S. coelicolor* spores suspension (approx. 10^{10} spores per ml) were added to 500 μl of 2 x YT and incubated for 10 min at 50 °C to promote

germination of the spores. After the spore suspension had cooled off to room temperature, 500 μl of the *E. coli* donor strain suspension were added. The mixture was inverted several times to ensure proper suspension of donor cells and recipient spores. The whole volume (1000 μl) was spread on one MS agar plate and incubated at 30 °C for 16 - 20 h.
After this first incubation phase, each plate was overlaid with 1 ml of water containing a total amount of 0.5 mg nalidixic acid and 1 mg of apramycine. The liquid was spread carefully on the surface of the plates. The plates were further incubated at 30 °C for up to 5 days until exconjugant colonies of *S. coelicolor* formed on the plates. The exconjugants were isolated and grown on MS agar plates containing 25 μg/ml nalidixic acid and 50 μg/ml apramycine. The correct integration of the oriT-plasmid was verified by colony PCR (Kieser et al., 2000).

3.1.10 Cultivation of *L. monocytogenes*

L. monocytogenes was cultivated under oxic conditions in liquid cultures of brain heart infusion medium (BHI) at 37 °C in baffled glass Erlenmeyer flasks on an orbital shaker at 180 rpm. For cultivation on solid media, *L. monocytogenes* was grown on BHI agar or LA at 37 °C.

3.2 Purification of Chromosomal DNA

For the purification of chromosomal DNA the *Genomic DNA Purification Kit* (Thermo Scientific) was used according to the included instructions. When the chromosomal DNA of Gram-positive bacteria (e.g. *Streptomyces* spp., *Bacillus* spp.) was isolated, the cell pellet was treated with lysozyme (5 mg/ml) for 30 min at 30 °C prior to the addition of the lysis buffer.

3.3 Purification of Plasmid DNA

For the purification of plasmid DNA from an over night culture of *E. coli*, the *GeneJET^{TM} Plasmid Miniprep Kit* (Thermo Fisher Scientific) was used according to the manufacturers recommendations. The plasmid DNA was eluted from the column with 30 μl elution buffer (supplied with the kit). The concentration of the plasmid DNA was determined using a *NanoVue^{TM} Plus Spectrophotometer* (GE Healthcare) and was stored at -20 °C.

3.4 Polymerase Chain Reaction

Polymerase chain reaction (PCR) was used for the amplification of DNA fragments from chromosomal or plasmid DNA for subsequent recombination, sequencing or for confirmation of successful DNA uptake. For subsequent digest and recombination of PCR products modifying oligonucleotides (primers) including recognition sequences for restriction enzymes adjacent to an approximately 20 – 25 nt long sequence, homolog to the template were used.

Table 3.2: PCR reaction mixture using KAPAHiFi^{TM} DNA polymerase.

	Volume	Final conc.
Nuclease free water	ad 25 μl	
5 x KAPAHiFi^{TM} Fidelity Buffer	5 μl	1 x
dNTP mix (10 mM)	0.5 μl	200 μM each
Forward primer (10 μM)	1.25 μl	0.5 μM
Reverse primer (10 μM)	1.25 μl	0.5 μM
Template DNA	0.5 μl	as needed[a]
KAPAHiFi^{TM} DNA Polymerase	0.5 μl	0.02 $^{U}/_{\mu l}$

[a] $\leq$ 10 ng plasmid DNA per reaction; $\leq$ 100 ng genomic DNA per reaction

When the amplified DNA fragments were to be used in cloning experiments, the engineered enzyme *KAPAHiFi^{TM} DNA Polymerase* (KAPA Biosystems) was used. The constitution of one 25 μl reaction mixture is given in table 3.2. The amplification was carried out in a *C1000^{TM} Thermal Cycler* (Bio-Rad) according to the cycling conditions given in table 3.3.

Table 3.3: Standard cycling conditions for the amplification of DNA fragments using KAPAHiFi^{TM} DNA polymerase in KAPAHiFi^{TM} Fidelity Buffer.

	Temperature	Time	Cycles
Initial Denaturation	95 °C	5:00 min	1
Denaturation	98 °C	0:20 min	25
Annealing[a]	65 °C	0:15 min	
Extension	72 °C	0:30 $^{min}/_{kb}$	
Final Extension	72 °C	5:00 min	1

[a] An annealing temperature of 65 °C was chosen by default. If the reaction failed, a gradient ranging from 60 – 78 °C was applied to determine the optimal annealing temperature.

Prior to subsequent recombination in molecular cloning experiments, the correct sizes of the respective PCR products were determined through agarose gel electrophoresis (section 3.5). If necessary the correct nucleotide sequences were verified through sequencing (Eurofins Genomics GmbH, Ebersberg, Germany).

3.4.1 Colony PCR

Colony PCR was used for the fast verification whether a transformation reaction was successful. Resistant colonies were picked after over night incubation and suspended in 50 μl sterile nuclease free water. This suspension was used as a template in the colony PCR reaction mixture given in table 3.4. The reaction conditions are given in table 3.5. The reaction products were analyzed by agarose gel electrophoresis. The amplification of a DNA fragment with the expected size was considered to indicate a successful transformation, however, the verification of the sequence was done by sequencing (Eurofins Genomics GmbH, Ebersberg, Germany).

Table 3.4: Colony PCR reaction mixture using DreamTaq^{TM} DNA polymerase.

	Volume	Final conc.
Nuclease free water	ad 20 μl	
10 x DreamTaq Green Buffer	2 μl	1 x
dNTP mix (10 mM)	0.4 μl	200 μM each
Forward primer (10 μM)	1 μl	0.5 μM
Reverse primer (10 μM)	1 μl	0.5 μM
Template (colony suspension)	1 μl	
DreamTaq^{TM} DNA Polymerase	0.1 μl	5 $^{U}/_{\mu l}$

Table 3.5: Cycling conditions for colony PCR using DreamTaq^{TM} DNA polymerase.

	Temperature	Time	Cycles
Initial Denaturation	95 °C	3:00 min	1
Denaturation	94 °C	0:30 min	30
Annealing	$T_m - 5$ °C	0:30 min	
Extension	72 °C	1:00 $^{min}/_{kb}$	
Final Extension	72 °C	5:00 min	1

3.5 Separation of DNA Fragments by Agarose Gel Electrophoresis

The separation of DNA fragments by agarose gel electrophoresis was carried out to verify the presence of DNA fragments of a certain size in a solution (e.g. after plasmid DNA purification, PCR, restriction digest or ligation).
Agarose (1% m/v) was dissolved in TAE buffer by heating the mixture in a microwave oven until the agarose dissolved completely. The warm solution was carefully poured into a gel rack, and a comb was placed 5 - 10 mm from one end of the gel to form the loading pockets of the gel. After the gel hardened completely, the the comb was removed and the gel was transferred into the buffer tank of a gel electrophoresis cell (Bio-Rad Laboratories). The buffer tank of the cell was filled with TAE buffer until the gel was covered completely.
The DNA samples were mixed with 6 fold DNA loading dye (Thermo Scientific) and loaded into the pockets of the gel. As a reference 3 μl GeneRuler 1 kb Plus DNA Ladder (Thermo Scientific) was loaded in at least one pocket of each gel. For the separation of the DNA fragments a constant potential of 90 V was applied for 45 min.
After the electrophoresis the gel was immersed in a ethidium bromide solution (1 $\mu g/ml$) and stained under constant agitation for at least 20 min. The stained gel was documented using a GelDoc^{TM} XR system (Bio-Rad Laboratories).

3.6 Molecular Cloning

For the recombination of DNA molecules *FastDigest^{TM}* restriction enzymes (Thermo Scientific) were used to digest PCR products and plasmid DNA (table 3.6). To reduce the recircularization rate during the ligation reaction, the alkaline phosphatase *FastAP^{TM}* (Thermo Scientific) was added to the digest reaction of cloning vectors. The digest was typically incubated 20 min immersed into a water bath at 37 °C.

After the digest the DNA fragments were, if necessary, separated by agarose gel electrophoresis (section 3.5) and purified using the *GeneJet^{TM} Gel Extraction* kit (Thermo Scientific) or purified directly after the digest with the *GeneJet^{TM} PCR Purification* kit (Thermo Scientific).

Table 3.6: Restriction digest reaction mixture.

	Plasmid DNA	PCR product
DNA	2 μl ($\leq$ 1 μg)	2 μl (~0.2 μg)
10 x FastDigest® buffer	2 μl	10 μl
FastDigest™ enzyme	1 μl	1 μl
FastAP™ Alkaline Phosphatase[a]	1 μl	–
Water	ad 20 μl	ad 30 μl

[a] FastAP™ was used for dephosphorylation of plasmid DNA to prevent recircularization during ligation.

The purified DNA fragments were then combined in a ligation reaction (table 3.7) using *T4 DNA Ligase* (Thermo Scientific). In one ligation reaction mixture up to three PCR products were combined with one linearized vector. The ligation reaction was typically incubated for 1 h at room temperature. For transformation of chemically competent *E. coli* cells, 5 μl of the ligation reaction were added directly to one aliquot (50 μl) of competent cells (section 3.1.4).

Table 3.7: Reaction mixture for the ligation of purified vector DNA and insert(s).

	sticky ends	blunt ends
Vector DNA	20 – 100 ng	20 – 100 ng
Insert DNA	molar ratio 5:1	molar ratio 5:1
50% PEG 4000 solution	–	2 μl
10 x T4 DNA Ligase buffer	2 μl	2 μl
T4 DNA Ligase	0.2 μl (1 U)	1 μl (5 U)
Water	ad 20 μl	ad 20 μl

3.6.1 Cloning with Linkers

The Linker DNA was ordered as two separate single stranded oligonucleotides. Both oligonucleotides were aliquoted with nuclease free water to a concentration of 100 μM. Prior to the annealing reaction, the oligonucleotides were diluted 10-fold in TE buffer (10 mM Tris-HCl, 1 mM EDTA, pH 8.0). One volume of each was added to a test tube and heated to 98 °C and held at that temperature for 10 min. The mixture was allowed to cool off slowly (~2 h) while remaining in the heating block. The annealed linker DNA was added to

the ligation reaction in a molar ratio of 100:1 over the vector DNA. If the vector DNA was treated with *FastAP*^{TM} during the digest reaction, the linker DNA had to be phosphorylated prior to the ligation reaction. Phosphorylation of the linker DNA was carried out using *T4 Polynucleotide Kinase* (T4 PNK, Thermo Scientific). The phosphorylation reaction (table 3.8) was incubated at 37 °C for 20 min and subsequently inactivated at 75 °C (10 min) before it was added to a ligation reaction.

Table 3.8: Reaction mixture for linker dephosphorylation.

	Volume
Linker DNA (5 μM)	10 μl (~50 pmol)
10 x reaction buffer A	2 μl
ATP (10 mM)	2 μl
T4 Polynucleotide Kinase	1 μl (10 U)
Water	ad 20 μl

3.6.2 Golden Gate Cloning

The cloning strategy described as *Golden Gate Cloning* was based on the work of Engler et al. (2008). In this method, type IIs restriction enzymes were employed to digest the PCR products prior to ligation. Since type IIs restriction enzymes feature non-palindromic, asymmetric recognition sites and cleave DNA at a defined distance from them, their use facilitates the seamless assembly of two or more PCR products in a ligation reaction. This was of great use for the creation of translational fusions, as the ligation product did not contain the recognition sequence and thus did not introduce additional codons into the translated sequence.

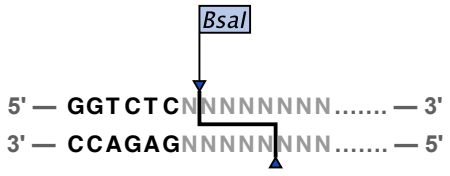

Figure 3.1: The type IIs restriction enzyme *BsaI*. Recognition sequence (black) and cleavage site (arrows) of the type IIs restriction enzyme *BsaI*. Bases denoted as 'N' can be chosen arbitrarily to form user designed overhangs.

Throughout this work the enzyme *BsaI* (Thermo Scientific) was used. Figure 3.1 shows the recognition sequence and the cleavage site of *BsaI*. The bases denoted as 'N' can be chosen freely to design user defined overhangs, which then recombine seamless with homolog overhangs of other assembly parts.

3.7 Separation of Proteins by Polyacrylamide Gel Electrophoresis

Purified proteins and cell free extracts were separated according to their electrophoretic mobility, i.e. a function of the molecular weight, using denaturing sodium dodecyl sulfate polyacrylamide gel electrophoresis (SDS-PAGE). Typically 15 μl of each sample were mixed 1+1 with 2 x denaturing SDS sample buffer and incubated at 95 °C for 5 min using a *C1000^{TM} Thermal Cycler* (Bio-Rad Laboratories). After cooling off to room temperature the samples were centrifuged briefly.
Up to 20 μl per sample were applied to an *Any kD^{TM} Mini-PROTEAN® TGX^{TM} Precast Protein Gel* (Bio-Rad Laboratories). On each gel at least one lane was loaded with 10 μl *PageRuler^{TM} Plus Prestained Protein Ladder* (Thermo Scientific) to serve as a reference for protein size. For the separation the gel was mounted in a *Mini-PROTEAN® Tetra Cell System* (Bio-Rad Laboratories) filled with Tris-Glycin buffer and a direct current with constant voltage was applied (100 V for 10 min, then 150 V for 45 min). After the electrophoresis, the gel was either stained with PageBlue^{TM} Protein Staining Solution (Thermo Scientific) and documented by scanning or further processed as described in section 3.8.

3.8 Western-Blot

For the western-blot analysis, the polyacrylamide gel was not stained after the SDS-PAGE, but the proteins were transferred electrophoretically from the gel onto a nitrocellulose membrane in a semi-dry transfer procedure using a *Trans-Blot® SD Cell* (Bio-Rad Laboratories) with a constant current of 0.04 A for 1 h. For the detection of His-tagged proteins, the *His·Tag® AP Western Reagents* kit (Merck Milipore) was used as described in the included user's manual (Novagen, 2011).

3.9 Recombinant Protein Production

The production of recombinant proteins was carried out in *E. coli* BL21(DE3) or *E. coli* Rosetta(DE3) with pRARE[a]. The plasmids with the genetic information coding for the proteins of interest were pET derivates where the expression of the gene of interest is controlled by the IPTG inducible promoter P_{T7}.
For the protein production 50 – 200 ml of LB, supplemented with all necessary antibiotics, were inoculated with material from a 10 ml overnight culture to an initial OD_{600} of 0.03. When the OD_{600} reached 0.4, the protein production was induced by addition of IPTG to a final concentration of 1 mM. The production phase lasted usually 3 – 5 h and was carried out at 37 °C.
Alternatively, the induction could be delayed until OD_{600} reached 0.8 and IPTG concentration could be lowered down to 0.1 mM. Also the temperature during the production phase could be lowered to 20, 25 or 30 °C with prolonged production times of 16 – 24 h. The cells were harvested by centrifugation (8000 x g, 10 min, 4 °C) and stored at -20 °C upon lysis and subsequent purification of the recombinantly produced proteins.

[a] encodes tRNAs for the in *E. coli* rarely used codons AGA and AGG (arginine), GGA (glycine), AUA (isoleucine), CUA (leucine), CCC (proline)

3.10 Protein Purification (FPLC)

For the purification of recombinantly produced proteins, the Fast Protein Liquid Chromatography (FPLC) system *ÄKTApurifier UPC-900* (GE Healthcare) with an additional sample collector (FRAC-920) was applied. The system was controlled manually via the UNICORN software package. Additionaly to the user-set parameters, such as flow rate and buffer constitution, the system pressure, the conductivity and the UV absorption at 280 nm (relative protein concentration) were monitored and recorded continuously throughout the purification process.

3.10.1 Immobilized Metal Ion Affinity Chromatography (IMAC)

For the purification of HIs-tagged proteins, prepacked nickel-sepharose columns *HisTrap™ HP* (GE Healthcare) with a column volume (CV) of 5 ml were used. Up to 50 ml of cell free extract were applied to the column with a 50 ml superloop, which allowed the introduction of larger samples into the pressurized fluid system. The flow rate during sample application was typically 5 $^{ml}/_{min}$ and was adjusted when necessary, to not exceed the recommended

maximal system pressure of 0.3 MPa given in the column's specifications.
After sample application, the column was washed with at least 10 CV *Buffer A for IMAC* (20 mM Imidazole) until the UV signal at 280 nm returned to a stable baseline. The elution of proteins bound to the column was performed through a linear gradient of *Buffer B for IMAC* (200 mM Imidazole) over 10 CV. The fractionation of the eluate was controlled manually to separate the occurring peaks into independent samples.
Prior to freezing of protein samples, the imidazole was removed by gel filtration (see section 3.10.4) to avoid protein precipitation.

3.10.2 Affinity Purification of MBP-tagged Fusion Proteins

For the purification of MBP fusion proteins expressed from pMAL-c5X derivates in *E. coli* ER2524, prepacked dextrin sepharose columns *MBPTrap*^{TM} *HP* (GE Helthcare) with column volumes of 1 and 5 ml were used. The samples were loaded in binding buffer (*Buffer A for MBPTrap*) as described in section 3.10.1 and eluted from the column with a linear gradient or in a step elution profile with *Buffer B for MBPTrap* (10 mM maltose).
Buffer exchange after the purification was necessary if subsequent protease treatment, AEX or IMAC purification were carried out.

3.10.3 Anion Exchange Chromatography (AEX)

For the separation of proteins based on their net surface charge the anion exchange column *HiTrap*^{TM} *Q FF* (GE Healthcare) prepacked with Q sepharose, a strong anion exchange matrix, featuring quaternary amine ligands with a column volume of 1 ml were used. The samples were loaded to the column in *Buffer A for AEX* (20 mM Tris-HCl, 25 mM NaCl, pH 8.0) and eluted with a linear gradient over 20 CV to *Buffer B for AEX* with higher ionic strength (20 mM Tris-HCl, 500 mM NaCl, pH 8.0). Alternatively, a linear gradient over 10 CV to 50% (v/v) *Buffer B for AEX* and a subsequent step elution profile with an immediate increase to 100% (v/v) *Buffer B for AEX* was applied, to gain a better focus on the proteins eluting at higher concentrations.

3.10.4 Gel Filtration Size Exclusion Chromatography (SEC)

For desalting and buffer exchange of previously purified protein samples a *HiPrep 26/10 Desalting* (GE Healthcare) column, prepacked with the cross-linked dextran matrix *Sephadex G-25 Fine* and a column volume of 53 ml, was

applied. The samples were injected via a 10 ml sample loop. The successful buffer exchange was monitored by observation of two separated peaks for the absorption and conductivity signal respectively.

3.11 Enzyme Activity Assays

3.11.1 Catechol 2,3–dioxygenase (XylE) Activity Assay

The catechol 2,3–dioxygenase activity (EC 1.13.11.2) of the reporter enzyme XylE was assayed by measuring the increasing absorption of the sample at 375 nm due to the conversion of pyrocatechol and oxygen into 2–hydroxymuconate semialdehyde (2–HMS) (see figure 3.2).

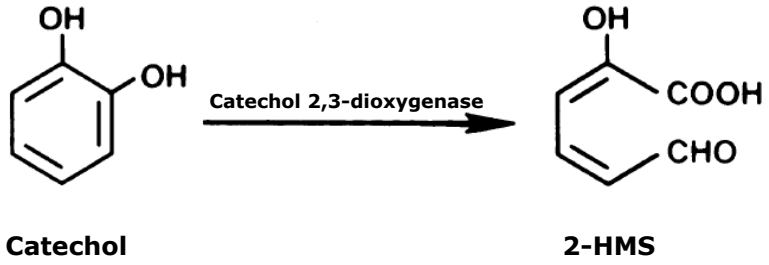

Figure 3.2: The conversion of catechol into 2–HMS. The conversion of catechol (colorless) and oxygen into 2–HMS (yellow) is catalyzed by the catechol 2,3–dioxygenase XylE. Specific XylE activity is used to measure expression of the reporter gene *xylE*. Figure adapted from Zukowski et al. (1983).

To assay the catechol 2,3–dioxygenase activity in the cell free extract of *Streptomyces* spp., the mycelia were harvested by centrifugation (3,000 x g for 10 min at 4 °C) and washed twice with 20 mM potassium phosphate buffer pH 7.2. The cells were resuspended in an appropriate volume of sample buffer (100 mM potassium phosphate, 20 mM EDTA, pH 7.5) and lysed twice with a *TS Series Benchtop Cell Disruptor System* (Constant Systems Ltd.) and put on ice for 15 min prior to centrifugation (8,000 x g for 10 min at 4 °C) and subsequent ultracentrifugation (108,000 x g for 30 min at 4 °C). The protein concentration of the samples was determined with the method described by Bradford (1976). For each sample 2.9 ml assay buffer (100 mM potassium phosphate, 0.2 mM pyrocatechol, pH 7.5) were prewarmed to 30 °C in a cuvette. To start the reaction 100 μl of the respective sample (i.e. cell free extract) were added to the substrate and mixed by stirring. The abance at 375 nm was recorded for 6 min in intervals of 20 s in a spectrophotometer. If the absorption exceeded

the measurable range or the change in absorption did not increase in a linear fashion, the sample had to be diluted and the measurement was repeated.

$$A_{\text{XylE}} = \frac{dE_{375\,\text{nm}}}{dt} \cdot \frac{1}{\epsilon_{\text{2–HMS}} \cdot d} \cdot \frac{V_{\text{total}}}{V_{\text{sample}}} \cdot \frac{1}{c_{\text{Protein}}} \cdot DF \tag{3.1}$$

A_{XylE}	specific XylE activity in the sample [$^{\text{mmol}}/_{\text{min·mg}}$]
$\frac{dE_{375\,\text{nm}}}{dt}$	change of the extinction at 375 nm over the recorded time [$^{1}/_{\text{min}}$]
$\epsilon_{\text{2–HMS}}$	molar attenuation coefficient of 2–HMS; $\epsilon_{\text{2–HMS}} = 4.4 \cdot 10^4\,{}^{\text{l}}/_{\text{mol·cm}}$
d	pathlength of the cuvette; $d = 1\,\text{cm}$
V_{total}	total volume of the assay; $V_{\text{total}} = 3\,\text{ml}$
V_{sample}	volume of the sample in the assay; $V_{\text{sample}} = 0.1\,\text{ml}$
c_{Protein}	Protein concentration of the sample determined after Bradford $^{\text{mg}}/_{\text{ml}}$
DF	dilution factor; $DF = 100$ for 1:100 dilution of the sample

The specific catechol 2,3–dioxygenase activity A_{XylE} calculated according to equation 3.1 results the amount of 2–HMS in mmol that was formed in the reaction per minute relative to the total protein concentration of the sample. Since enzymatic activity is commonly denoted in enzyme units (U) where 1 U is defined as the amount of enzyme necessary for the conversion of 1 μmol substrate per minute, the results of equation 3.1 have to be multiplied with a factor of 1000 in order to obtain a result for the specific activity with the dimension $^{\text{U}}/_{\text{mg}}$.

Qualitative Colorimetric XylE Plate Assay A qualitative XylE assay can be performed by spraying approximately 1 ml of a 0.5 M aqueous pyrocatechol solution onto an agar plate with grown colonies. Colonies producing XylE exhibit a yellow stained halo around the colony. This assay has to be performed on duplicate plates, since the colonies can not be picked for recultivation after the assay (Ingram et al., 1989; Jones, 2011).

3.11.2 β-glucuronidase (GusA) Activity Assay

To assay the GusA activity of a cell free extract from a liquid culture in a spectrophotometer, the cells were harvested by centrifugation (10 min, 3500 xg, 4 °C) and resuspended in 20 mL of extraction buffer (50 mM NaPB pH 7, 5 mM DTT, 0.1% (v/v) Triton-X 100) and lysed with a *TS Series Benchtop Cell Disruptor System* and stored on ice until centrifugation (8,000 x g for 10 min at 4 °C) and subsequent ultracentrifugation (108,000 x g for 30 min at 4 °C). The protein

concentrations of the samples were determined after Bradford (1976).
A volume of 750 μl (1 - 5 μg total protein) of the cell free extract was pre-incubated in a cuvette for 15 min at 28 °C. To start the reaction, 80 μl of the substrate (0.2 M PNPG) were added to the cuvette. The absorption at 415 nm was recorded over 30 min in intervals of 20 s. The specific GusA activity of the sample was calculated similar to the XylE activity (equation 3.1).
Since the accurate measurement of enzyme activity requires the 4-nitrophenol product of the reaction to be fully deprotonated, i.e. pH > 9.2, the absorbance values of the real time measurements of the reaction in phosphate buffer at pH 7 were used to calculate the specific activity GusA activity in GUS Units (GU) where the molar attenuation coefficient of the product was not taken into account. So that 1 GU $\stackrel{\text{def}}{=}$ 1 $A_{415nm} \cdot min^{-1} \cdot mg^{-1}$ (Myronovskyi et al., 2011).

3.11.3 β-galactosidase (LacZ) Activity Assay

The β-galactosidase (LacZ) activity assay was performed as described by Ott et al. (2009). *B. subtilis* strains with integrated pDG268 derivates were cultivated in SMM at 37 °C until the optical density reached 0.4. Flavins (riboflavin, roseoflavin or 8-amino riboflavin) were added to a final concentration of 50 and 100 μM, respectively. Cultivation was continued for 4.5 h at 37 °C. The cells were harvested by centrifugation (10 min, 4000 x g, 4 °C) and washed 3 times with PM buffer (100 mM sodium phosphate, 1 mM magnesium sulfate, pH 7.8) and finally resuspended in 0.05 volumes of PM. To disrupt the cells, 1 ml of the resuspended cells was mixed with 1.2 g glass beads (0.3 mm diameter) in a 1.5 ml test tube and treated 5 min at maximum speed in a vibratory tube mill. The lysate was cleared by centrifugation (10 min, 13000 x g, 4 °C) and the specific LacZ activity of the supernatant was determined.
To assay the specific LacZ activity of a sample, 800 μl ortho-Nitrophenyl-β-galactoside (ONPG) substrate (2 $^{mg}/_{ml}$) were prewarmed to 37 °C. To start the reaction, 50 μl of the sample were added to the substrate. The change in absorbance at 415 nm was recorded with a spectrophotometer over 5 min.

3.11.4 Amylase Production Assay

The successful integration of pDG268 derived plasmids into the chromosome of *B. subtilis* resulted in disruption of the gene *amyE*. The loss of amylase activity after transformation with pDG268 derivates indicated the double crossover integration into the locus *amyE* had been successful. To test the generated

strains for amylase activity, single colonies were picked and cultivated on LA supplemented with 1% (m/v) potato starch. After approximately 24 h the plates were flooded with 1 ml Lugol's iodine solution. Colonies with intact *amyE* gene exhibited an unstained halo around them, due to the absence of stainable amylose in the growth medium, while colonies with disrupted *amyE* were fully stained and no halo was visible (O'Kane et al., 1986; Cutting, 1990).

3.11.5 Coupled *In Vitro* Transcription/Translation Luciferase Activity Assay

The coupled *in vitro* transcription/translation (TK/TL) luciferase activity assay was performed as described by Pedrolli et al. (2012). The assay mixture (TK/TL mix) was prepared by combining the *T7 extract solution*, the *S30 premix* and the *amino acid mix* from the *E. coli T7 S30 Extract System for Circular DNA Kit* (Promega) in the proportion 3:4:1 (v/v/v). To 8 μl TK/TL mix, 1 μl from a 10 x flavin stock solution (nuclease free water as control) and 1 μl plasmid solution (0.2 – 10 $^{ng}/_{\mu l}$) were added and incubated by immersion into a water bath at 30 °C for 5 min. To stop the reaction, the vial was placed on ice and 90 μl stop solution (1 $^{mg}/_{ml}$ BSA, 2 mM DTT, 25 mM Tris-phosphate, pH 7.8) were added to the reaction mixture.
To assay luciferase activity, 50 μl *Luciferase Assay Reagent* (provided with the kit) were mixed with 10 μl of the sample. Luminescence was determined from the resulting mixture in a *Tecan Genios Pro microplate reader* (Tecan) at 26 °C. If the luminescence level reached saturation, the sample was diluted appropriately with an aqueous BSA (1 $^{mg}/_{ml}$) solution.

3.11.6 Flavokinase/FAD synthetase Activity Assay

Flavokinase and FAD synthetase activity was determined with an enzyme activity assay based on the work of Pedrolli et al. (2011). The reaction mixture was set up as given in table 3.9. The enzyme was added after 5 min of preincubation of the mixture at 37 °C to start the reaction. The first sample, corresponding to t = 0 min, was removed immediately afterwards. The reaction was kept in the dark at 37 °C. Subsequent samples were removed after appropriate time intervals. To stop the reaction the sample, aliquots were added to a prepared volume of trichloroacetic acid (TCA) to a final concentration of 2 % TCA.
The samples were centrifuged (13,000 x *g* for 2 min) and filtered with 0.2 μm regenerated cellulose syringe filters prior to to HPLC-MS analysis.

Table 3.9: Reaction mixture for the flavokinase/FAD synthetase activity assay.

	Stock Conc. (mM)	Volume for 2 ml (μl)	Final Conc. (mM)
Buffer	100	1000	50.0
Flavin[a]	20	1 – 25	0.01 – 0.25
ATP	10	200	1.0
$MgCl_2$	60	200	6.0
NaF	120	200	12.0
$Na_2S_2O_4$[b]	240	200	24.0
Enzyme[c]	200 – 300	10	1.0 – 1.5
H_2O		ad 2000	

[a] Flavin for FK-activity assay, flavin mononucleotide for FADS-activity assay
[b] prepared fresh before use
[c] Enzyme concentrations given in $\mu g/ml$

3.12 Determination of Intracellular Flavin Concentrations

For the determination of the intracellular flavin concentration in *L. monocytogenes*, cells from 10 ml of a liquid culture were harvested by centrifugation (8000 x g, 10 min, 4 °C). The cells were washed three times with 1 ml washing buffer (50 mM NaCl, 50 mM Tris-HCl, pH 7.5) to remove all residual flavins contained in the media.
The cells were resuspended in 50 μl ultrapure water, OD_{600} of an appropriate dilution was determined and correlated to a cell count. 100 μl GES buffer (5 M guanidinium thiocyanate, 0.1 M EDTA, 0.5 % (m/v) laurylsarkosin, pH 8) were prewarmed to 70 °C using a heatblock (Thermomixer Comfort, Eppendorf). To the preheated GES buffer, 40 μl of the sample were added and mixed immediately for 5 s. The mixture was then incubated for 1 min at 70 °C. The reaction was stopped by addition of 860 μl ice-cold water. The mixture was then centrifuged and the supernatant was subject to flavin quantification via HPLC-MS (von Canstein et al., 2007; Takemoto et al., 2014).

3.13 High-Performance Liquid Chromatography-Mass Spectrometry (HPLC-MS)

For the identification and quantification of flavins in cell free extracts and assay preparations an Agilent 1220 Infinity LC system (Agilent Technologies, Waldbronn, Germany) using reverse-phase columns was applied. Detection of flavins and cofactors was carried out with a diode array detector (1260 DAD) and a quadrupole mass spectrometer (6130 Quadrupole MS).
Throughout this work two columns with different methods were applied:

HPLC-MS Method1 was used for analysis of riboflavin and the cofactors FAD and FMN. The absorption at 445 nm was recorded for detection.
Column: ReproSil-Pur C18-AQ column (5 μm; 250 mm x 2.0 mm; Dr. Maisch GmbH, Ammerbich-Entringen, Germany)
Liquid phase: methanol (40% v/v) / 20 mM formic acid and 20 mM ammonium formate (pH 3.7; 60% v/v). Flow rate: 0.6 $^{ml}/_{min}$.
Retention times: FAD (4.45 min), FMN (5.64 min), riboflavin (7.19 min)

HPLC-MS Method2 was applied for separation of riboflavin, roseoflavin, 8-amino riboflavin and their respective cofactors and cofactor analogs. The development of this method was based on the work of Aliverti et al. (1999). Since each group of analytes exhibits a unique absorption spectrum, the detection was carried out at three wavelengths in parallel to utilize the respective absorption maximum. Riboflavin, FAD and FMN were detected at 445 nm, 8-amino riboflavin, AFAD and AFMN were detected at 480 nm and roseoflavin, RoFAD and RoFMN were detected at 503 nm.
Column: ReproSil-Pur C18-AQ column (5 μm; 250 mm x 4.6 mm; Dr. Maisch GmbH, Ammerbuch-Entringen, Germany).
Liquid phase: A solvent ratio of 15% v/v methanol / 20 mM formic acid and 20 mM ammonium formate (pH 3.7; 85% v/v) was used for equilibration of the column. After 2.5 min the methanol concentration was increased in a linear gradient over 8 min to 42% v/v. This concentration was maintained for 2 min. That was followed by an increase of the methanol concentration up to 100% v/v and re-equilibration to the conditions in the beginning, in order to remove excess flavins when samples with high concentrations were analyzed. A diagram of the solvent ratios throughout the method is depicted in figure 3.3. Flow rate: 1.0 $^{ml}/_{min}$.

Retention times: AFAD (9.26 min); AFMN (10.33 min); AF (11.51 min); FAD (11.45 min); FMN (12.77 min); RF (14.31 min); RoFAD (12.15 min); RoFMN (13.63 min); RoF (15.14 min).

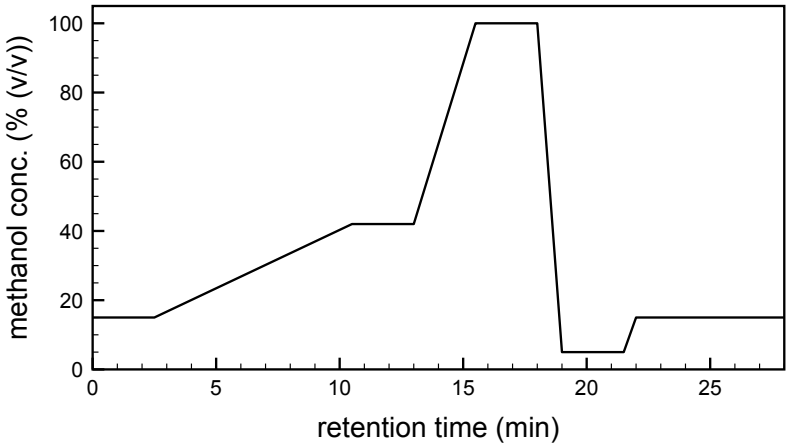

Figure 3.3: Solvent profile of HPLC-MS Method2. The diagram shows the methanol concentration throughout the HPLC-MS Method2. Column: ReproSil-Pur C18-AQ column (5 μm; 250 mm x 4.6 mm). Flow rate: 1 $^{\mathrm{ml}}/_{\mathrm{min}}$.

3.14 Determination of the pH Optimum

For the determination of the optimal pH of enzymatic reactions, a buffer system with a broad range spanning the relevant interval from pH 6 to 10 was desired. The BIS-Tris propane (BTP) buffer system with its two pK_{a} values being 6.8 and 9.0 at 25 °C fulfilled this requirement. The necessary ratios of BTP and hydrochloric acid for certain buffer pH values were determined by titration of a 50 mM BTP solution with 1 M HCl (see figure 3.4).

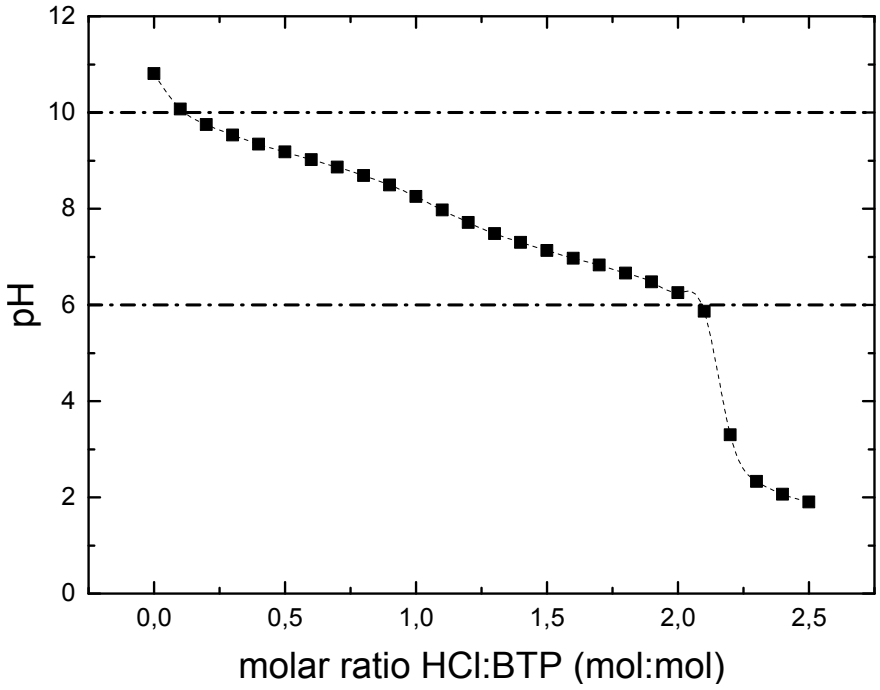

Figure 3.4: pH range of the BIS-Tris propane buffer system. Titration of 50 mM BIS-Tris propane with 1 M HCl. Measured pH values plotted against the molar ratio of HCl:BTP. The relevant pH range for the buffer system is marked with dashed lines.

By reading off the molar ratio at the desired pH values from the diagram in figure 3.4 the volumes given in table 3.10 were determined. Each combination was tested to verify its final pH in a 50 mM BTP solution.

Table 3.10: Volumes used for 1 ml 100 mM BIS-Tris propane buffer with various pH.

pH	$V_{BTP\ 1M}$ [μl]	$V_{HCl\ 1M}$ [μl]	V_{H_2O} [μl]	molar ratio
7.0	100	161	739	1.61
7.5	100	137	763	1.37
8.0	100	114	786	1.14
8.5	100	91	809	0.91
9.0	100	67	833	0.67
9.5	100	44	856	0.44

The 100 mM BTP solutions were used as 2 x buffer to perform the flavokinase/FAD synthetase activity assay as described in section 3.11.6 at different pH values. For each pH value, 50 μM FMN were used as substrate in triplicate assays. The FAD concentration was determined at 0, 3 and 6 min to calculate the initial reaction velocity which corresponds to the enzyme activity. The

resulting FAD synthetase activities for Lmo0728 and Lmo1329 plotted against the respective pH values are shown in figure 4.24.

3.15 Determination of the Kinetic Parameters for Flavokinase and FAD synthetase Activity

The numeric values of the the Michaelis constant K_{m} and the maximal reaction rate $v_{\max}$ are constant for an enzymatic reaction that follows the kinetic equation formulated originally by Michaelis and Menten (equation 3.2) with the molar substrate concentration $[S]$ (Michaelis and Menten, 1913; Kenneth and Goody, 2011).

$$v_0 = v_{\max} \cdot \frac{[S]}{[S] + K_m} \tag{3.2}$$

The initial reaction rate v_0 for each substrate concentration was determined by linear regression of the product formation at the start of the reaction, while the relationship $[S] \gg [P]$ holds true. Since the product formation of the flavokinase and FAD synthetase reactions had to be measured by HPLC, only a limited amount data points per reaction could be acquired. Several aspects regarding the sampling times as well as substrate and enzyme concentrations had to be considered. The time difference between samples had to be the same for all measurements of a kinetic plot to minimize the influence of the sampling process itself. The time points had to be chosen so that the product concentrations in the samples were above the detection limit for the product but the requirement of $[S] \gg [P]$ still held true. This requirements also determined the minimal substrate concentration that could be tested. The sampling times were determined to be 0, 3 and 6 min, while the enzyme concentration in the assay reaction was chosen to meet all the requirements mentioned above.

For each substrate concentration the reaction mixture according to table 3.9, excluding the enzyme, was set up and separated into three reaction volumes of 2 ml each. The parallel reactions were started by addition of the enzyme and the first sample for $t = 0\,\mathrm{min}$ was removed immediately. The assay was performed as described in section 3.11.6. From the nine collected samples per substrate concentration a mean initial reaction rate $v_{0,[S]}$ for the respective substrate concentration was calculated by linear regression of the product formation over time. By relating $v_{0,[S]}$ to the enzyme concentration in the

reaction the specific activity of the enzyme at the given substrate concentration was calculated.

$$k_{\text{cat}} = \frac{v_{\text{max}}}{[E]} \tag{3.3}$$

The specific activities were plotted against the substrate concentration and the apparent values for the Michaelis constant K_{m} and the maximal reaction rate v_{max} were determined through the best fit of the kinetic function given in equation 3.2 to the results of the experiment. Non-linear regression was performed with OriginPro® 9 (OriginLab, Wellesley Hills). From these two constants the turnover number k_{cat} and the kinetic efficiency $\frac{k_{\text{cat}}}{K_{\text{m}}}$ were calculated according to equation 3.3 with $[E]$ being the molar enzyme concentration.

4 Results

4.1 Growth of *L. monocytogenes* is Affected by Flavin Analogs

L. monocytogenes wild type and the mutant strain M1 (see section 2.5.2), featuring a deregulated FMN riboswitch upstream of the riboflavin transporter gene *lmo1945*, were grown in BHI liquid media supplemented with 100 μM riboflavin, roseoflavin or 8-amino riboflavin (DMSO as control).
To survey if the altered riboswitch sequence of *L. monocytogenes* M1 confers roseoflavin resistance, the mutant strain and the wild type of *L. monocytogenes* were grown under identical conditions (37 °C, 180 rpm, 100 μM flavin) in BHI. The optical density of the cultures was recorded over 7 h, until they reached the stationary growth phase (figure 4.1).

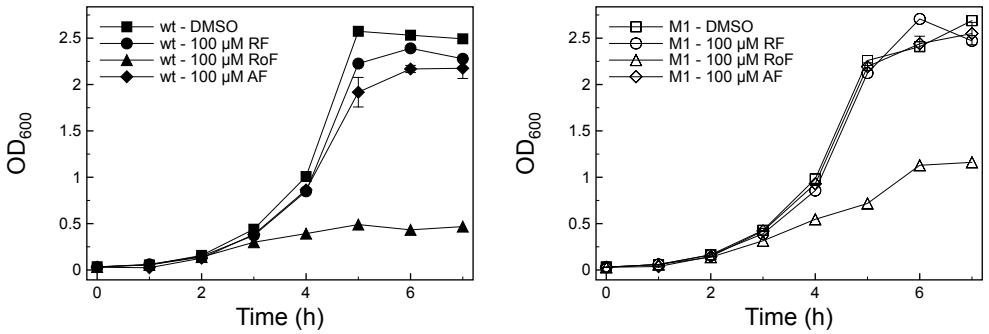

Figure 4.1: Deregulation of *lmo1945* confers increased roseoflavin tolerance. Growth curves of *L. monocytogenes* wild type (left panel) and mutant strain M1 (right panel) in BHI supplemented with 100 μM riboflavin (RF), roseoflavin (RoF) and 8-amino riboflavin (AF). DMSO was used as a control.

The growth data shown in figure 4.1 confirmed the finding of Mansjö and Johansson (2011), who reported the M1 strain to grow significantly better in the presence of 100 μM roseoflavin, when compared to the wild type. However, the performance of the M1 strain, grown in media supplemented with roseoflavin, was not restored to the level of the controls treated with riboflavin and DMSO. The growth of cultures treated with 8-amino riboflavin was only slightly reduced for the wild type, while growth of the M1 strain was not affected under the tested conditions. It was, however, reported that 8-amino riboflavin concentrations as high as 267 μM did significantly impair the growth of *L. monocytogenes* (unpublished data, personal communication with Jörgen Johansson, Laboratory for Molecular Infection Medicine Sweden, Department of Molecular Biology, Umeå University, Umeå, Sweden).

4.2 Intracellular Concentration of Flavins and Cofactors in *L. monocytogenes*

The following experiments were done to evaluate if the flavin analogs roseoflavin and 8-amino riboflavin are taken up into the cell and whether they are present as flavin or if they are converted to the respective cofactor analogs. Also, a comparison of the intracellular flavin and cofactor concentrations found in the wild type with those found in the mutant strain M1 were of interest, as they might reflect the effect of deregulated expression of the riboflavin transporter gene *lmo1945*. The qualitative HPLC analysis of cell free extracts from *L. monocytogenes* wild type and M1 is shown in figure 4.2. The cultures were grown in BHI supplemented with 100 μM riboflavin, roseoflavin and 8-amino riboflavin respectively (DMSO was added as a control). The HPLC analysis showed that both strains converted all three flavins into their respective mononucleotides and adenine dinucleotides.

The peak sizes in figure 4.2 do not directly correlate with intracellular concentrations, as the samples were taken at the end of the growth experiment described in section 4.1. Due to the treatment with roseoflavin and 8-amino riboflavin, the cultures did grow to the different final cell densities, however, the sample preparation for the HPLC measurement was done identically for all samples. The differences in cell counts of the respective cultures were taken into account when the intracellular concentrations given in table 4.1 were calculated from the chromatograms shown in figure 4.2.

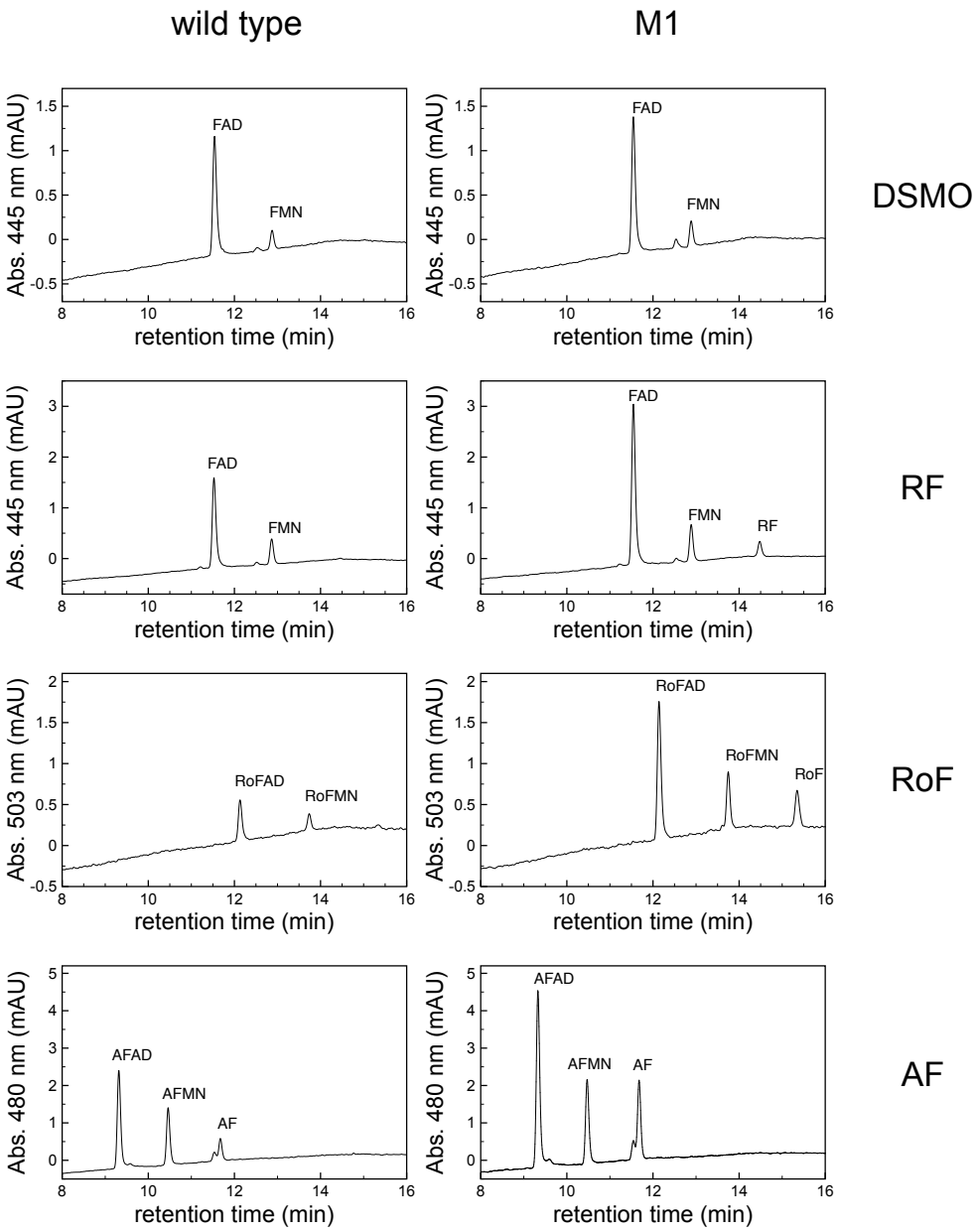

Figure 4.2: Flavin analogs are converted into cofactor analogs in *L. monocytogenes*. HPLC analysis of cell free extracts from cultures of *L. monocytogenes* wild type (left) and the deregulated FMN riboswitch mutant strain M1 (right), grown to the stationary phase in brain heart infusion media (BHI) with flavin supplementation (100 μM). DMSO was used as a solvent for flavin stocks and was added to the untreated culture as a control. RF: riboflavin; RoF: roseoflavin; AF: 8-amino riboflavin.

Table 4.1: Intracellular flavin and cofactor concentrations calculated from the HPLC-data shown in Figure 4.2.

	RF[a]	FAD[a]	FMN[a]	RoF[a]	RoFAD[a]	RoFMN[a]	AF[a]	AFAD[a]	AFMN[a]
wt (DMSO)	0	60	7	0	0	0	0	0	0
wt (RF)	0	84	17	0	0	0	0	0	0
wt (RoF)	0	11	0[b]	4	63	7	0	0	0
wt (AF)	0	18	0[b]	0	0	0	35	64	26
M1 (DMSO)	0	74	11	0	0	0	0	0	0
M1 (RF)	14	140	24	0	0	0	0	0	0
M1 (RoF)	0	24	0[b]	20	113	16	0	0	0
M1 (AF)	0	29	0[b]	0	0	0	65	88	28

[a] μM cofactor for an assumed cell volume of 1 μm^3
[b] below detection limit

Regarding the calculated intracellular flavin and cofactor concentrations, given in table 4.1, the mutant strain M1 appears to contain generally higher levels of the measured cofactors. This observation supports the hypothesis of increased flavin import due to constitutive and unregulated expression of *lmo1945*. Notably, the FAD and FMN concentrations found in the cells that were treated with roseoflavin and 8-amino riboflavin were decreased compared to the controls, treated with DMSO exclusively. This finding suggested a possible competition of riboflavin and its analogs as substrates for the generation of the cofactors.

Since the applied concentration of 100 μM was already in a range where passive uptake of riboflavin and roseoflavin through diffusion effects had to be considered over the transporter mediated active uptake (section 4.7.1), *L. monocytogenes* ild type and M1 cultures were treated with roseoflavin concentrations as low as 10 μM prior to determination of intracellular cofactor concentrations.
Figure 4.3 shows the intracellular concentrations after the cultures were treated with flavins and grown to the stationary phase. Panels A-D give a direct comparison of *L. monocytogenes* wild type and M1 cells. The previous finding of elevated cofactor levels in the cells of the M1 strains was confirmed. The difference is supposed to be a result of the mutation in *Rli96*.

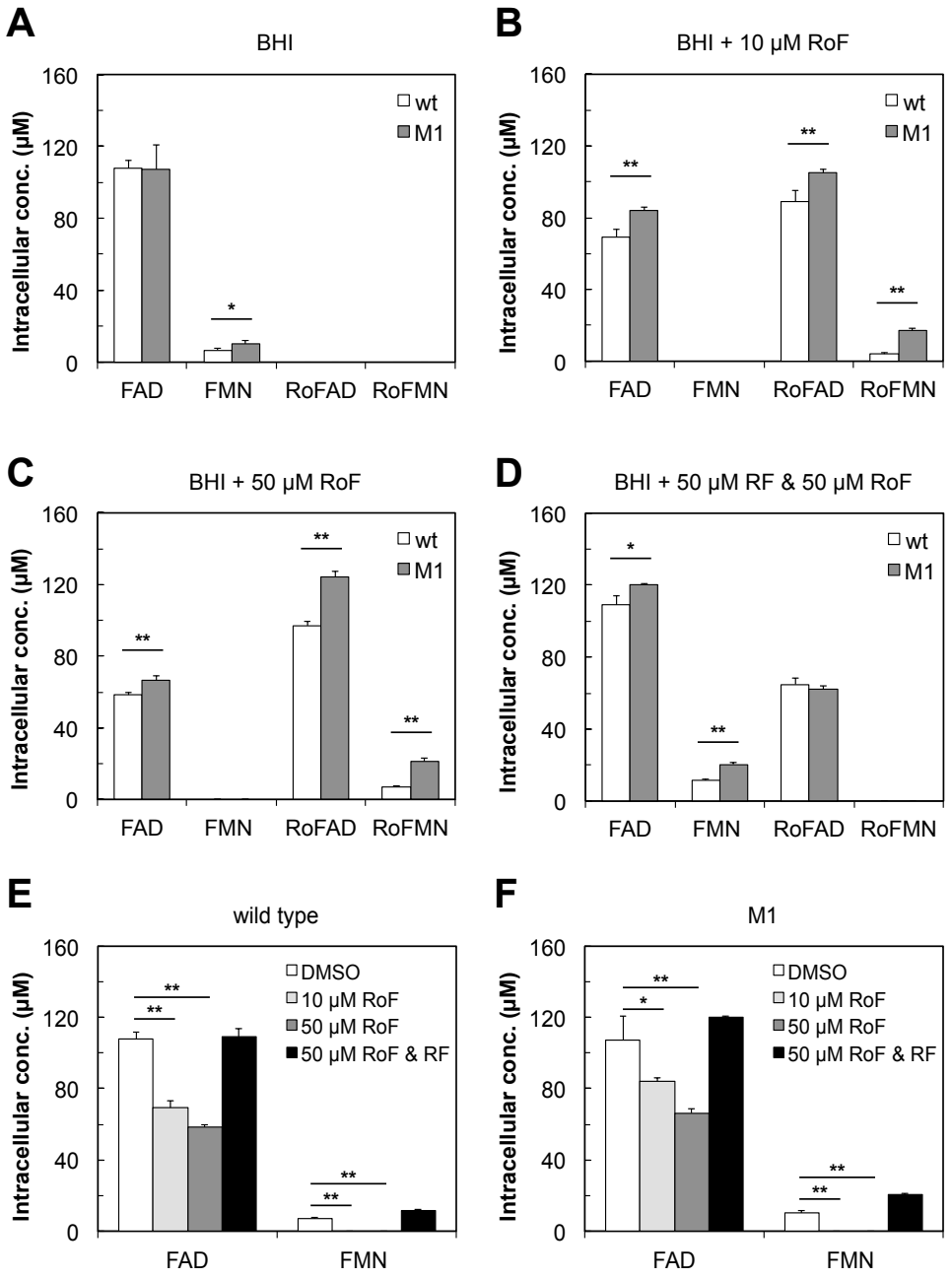

Figure 4.3: Intracellular cofactor concentrations of *L. monocytogenes* wild type and mutant strain M1. The cultures were grown to the stationary phase in BHI medium supplemented with various flavin concentrations. A: DMSO control; B: 10 μM roseoflavin; C: 50 μM roseoflavin; D: 50 μM riboflavin and 50 μM roseoflavin; E: FAD and FMN concentrations in wild type cells; F: FAD and FMN concentrations in M1 cells. Level of significance: * $p \leq 0.05$; ** $p \leq 0.01$.

Notably the FAD and FMN concentrations were reduced when only roseoflavin was added to the medium. When, in addition to 50 μM roseoflavin, also riboflavin in a concentration of 50 μM was added to the medium, the FAD and FMN concentrations were brought back the levels of the untreated cultures (figure 4.3-D). For a better comparison the FAD and FMN concentrations are displayed side by side for either strain in panels E and F of figure 4.3 respectively. The fact that this effect could be observed not only in the wild type but in the mutant strain as well, indicated that it was not a result of the mutation in the FMN riboswitch *Rli96*.

4.3 Identification of Flavokinase/FAD synthetase Genes in *L. monocytogenes*

As a riboflavin auxotrophic bacterium, *L. monocytogenes* does not posses genes coding for enzymes involved in riboflavin biosynthesis and relies solely on transporter mediated uptake of the vitamin. However, the metabolic active, phosphorylated forms of riboflavin are the cofactors FMN and FAD. In bacteria, these cofactors are typically synthesized by bifunctional enzymes, which exhibit flavokinase activity (EC 2.7.1.26.) as well as FAD synthetase activity (EC 2.7.7.2.).

A BLAST search at `http://blast.ncbi.nlm.nih.gov/` based on the amino acid sequence of the bifunctional flavokinase/FAD synthetase RibC from *B. subtilis* (UniProtKB accession number: P54575) in a database containing translated nucleotide sequences from *L. monocytogenes* EGD-e (Taxonomy ID: 169963) resulted in two sequences producing significant alignments. Those two sequences corresponded to the two loci annotated as *lmo1329* (nucleotides 1357753 to 1358697, GenBank accession number: WP_009925599) and *lmo0728* (nucleotides 758656 to 759396, GenBank accession number: WP_003721848) in the genome of *L. monocytogenes* EGD-e.

Since the genesis of cofactors appeared to play an important role in the toxic effect of flavin analogs on *L. monocytogenes*, both proteins (Lmo1329 and Lmo0728) were produced in recombinant *E. coli* strains and purified by affinity chromatography to study their catalytic flavokinase/FAD synthetase activities *in vitro*.

4.4 Recombinant Production and Purification of Lmo1329

The gene *lmo1329* was amplified from genomic DNA of *L. monocytogenes*, using the modyfying oligonucleotides F-lmo1329atg.NheI and R-lmo1329.NotI. The product of the PCR was inserted into the plasmid pET-24a(+) after digest with *NheI* and *NotI*. The gene was placed under the control of the IPTG inducible P_{T7} promoter, in frame with the sequence coding for a C-terminal His-Tag. The plasmid pET-24_lmo1329 was used to transform the expression strain *E. coli* BL21(DE3). Expression of *lmo1329-his* was induced with 1 mM IPTG in a culture volume of 250 ml and protein production was carried out for 5 h at 37 °C. The cells were harvested by centrifugation and lysed with a high pressure cell disruptor. The crude extract was applied to a *HisTrap*^{TM} *HP* column, packed with nickel-sepharose (see section 3.10.1). The column bound proteins were eluted from the column with a gradient of imidazole and collected in fractions of 5 ml each.

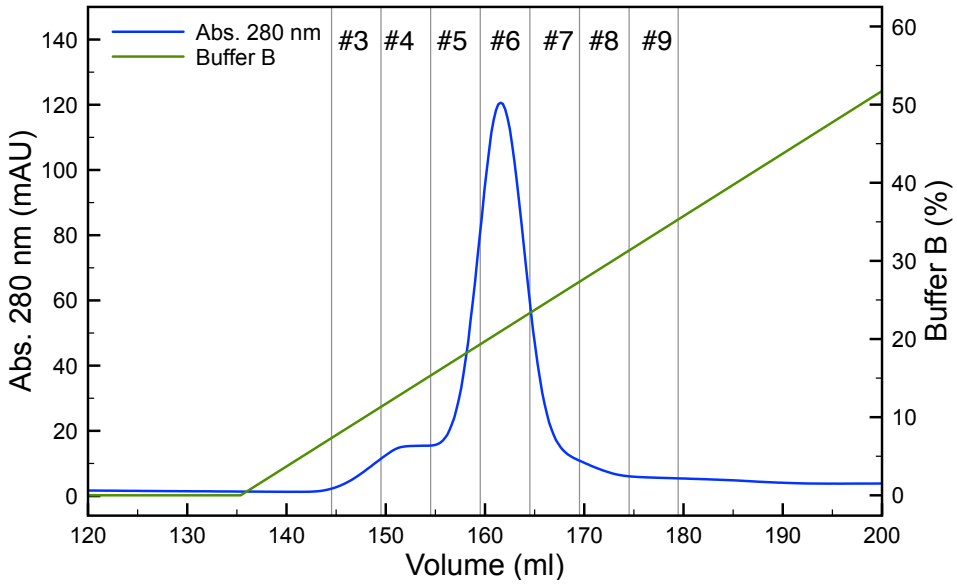

Figure 4.4: Purification of Lmo1329-His. FPLC chromatogram of the elution of recombinantly produced Lmo1329-His from a *HisTrap*^{TM} *HP* column with a linear gradient of imidazole. Blue: absorption at 280 nm; green: ratio (v/v) of elution buffer (Buffer B for IMAC, 200 mM imidazole) and loading buffer (Buffer A for IMAC, 20 mM imidazole). Collected fractions are numbered and indicated by vertical lines.

The chromatogram of the purification (figure 4.4) shows a single peak during the elution, led by a shoulder. The collected samples were applied to an SDS gel and separated electrophoretically, to verify the purity of the eluates. The resulting gel is displayed in figure 4.5. The gel shows a dominant band of with the expected size of Lmo1329-His. For the use in subsequent activity assays, Sample#6 was desalted via gel filtration and stored at -20 °C in 50 mM potassium phosphate buffer (pH 7.5). All other samples were discarded as they appeared to contain less Lmo1329-His and more contaminating proteins.

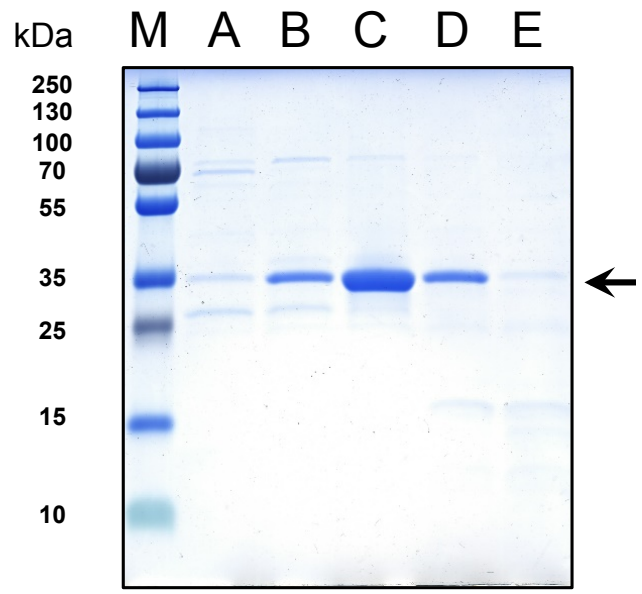

Figure 4.5: Purified Lmo1329-His. SDS-PAGE after HisTrap purification of Lmo1329-His. Sizes in kDa corresponding to the bands of the marker are given on the left. The arrow on the right marks the expected position of Lmo1329-His (36.8 kDa). Sample numbers according to figure 4.4. M: Marker (PageRuler^{TM} Plus); A: Sample#4; B: Sample#5; C: Sample#6; D: Sample#7; E: Sample#8.

4.5 Recombinant Production and Purification of Lmo0728

The initial approach of expression of *lmo0728* from pET-24a(+) and pET28 derivates in *E. coli* BL21(DE3) as C- and N-termnially His-tagged versions of Lmo0728, resulted in an accumulation of insoluble recombinant protein in the debris fraction after disruption of the cells. The absence of His-tagged Lmo0728

in the cell free extract, as well as its accumulation in the insoluble debris was confirmed through western blot analysis with an anti-His primary antibody.

To modulate the speed of protein production during induction, in order to ease correct folding of the produced protein and prevent aggregation, *E. coli* Rosetta(DE3) was used as host strain for protein production. *E. coli* Rosetta(DE3) allowed for adjustable levels of expression throughout all cells in a culture. By adjusting the concentration of the inducer IPTG, gene expression could be modulated from very low expression levels up to the fully induced expression levels of *E. coli* BL21(DE3). According to the manufacturer's recommendations, low-level expression may enhance the solubility and activity of difficult target proteins (Novagen, 2002). In addition to reduced IPTG concentrations the incubation temperature during protein production was reduced to 20 °C and the production phase was extended to 24 h.

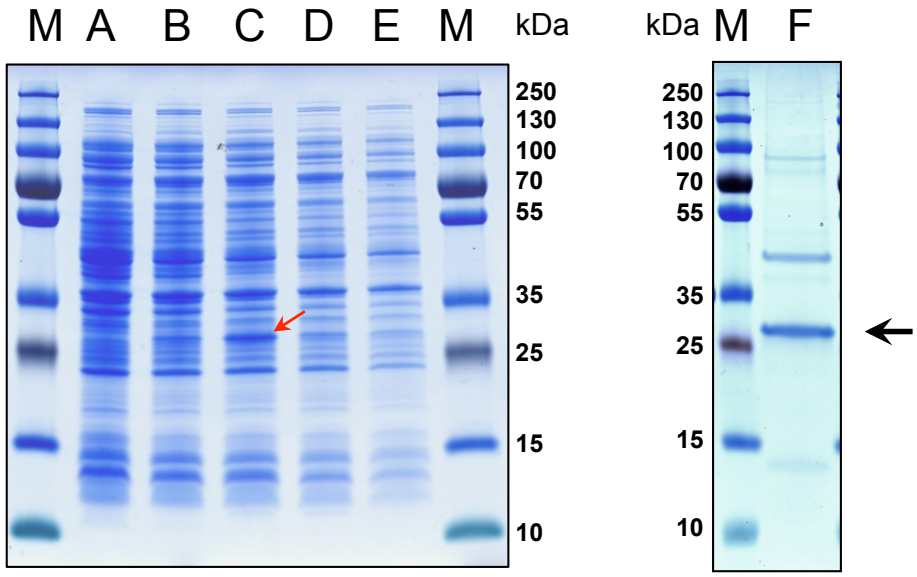

Figure 4.6: Expression and purification of inactive Lm0728-His. left: SDS-PAGE of cell free extracts from *E. coli* Rosetta(DE3) containing the expression plasmid pET-24_lmo0728 induced with varying IPTG concentrations at 20 °C for 24 h. M: Marker (PageRuler^{TM} Plus); A: 0 μM IPTG; B: 25 μM IPTG; C: 100 μM IPTG; D: 250 μM IPTG; E: 1 mM IPTG.
right: SDS-PAGE of the elution fraction after FPLC purification with a *HisTrap^{TM} HP* column. M: Marker (PageRuler^{TM} Plus); F: Elution fraction containing purified Lmo0728 from a culture induced with 100 μM IPTG at 20 °C for 24 h.
Sizes in kDa corresponding to the bands of the marker. The red arrow marks the band that is assumed to be soluble Lmo0728. Expected position of Lmo0728-His (black arrow, 27.8 kDa).

To test whether reduced IPTG concentrations in combination with lower temperatures during the protein production phase were beneficial for the solubility of Lmo0728-His, expressed from pET-24_lmo0728, three intermediate IPTG concentrations, i.e. 25 μM, 100 μM and 250 μM were applied to induce gene expression. The cell free extracts of these cultures were analyzed by SDS-PAGE and compared to an uninduced (no IPTG) and a fully induced (1 mM IPTG) culture. The result of the electrophoresis is shown in the left panel of figure 4.6. From the tested IPTG concentrations 100 μM appeared to yield the maximal amount of soluble Lmo0728-His (red arrow). The cell free extract of the culture was applied to a *HisTrap^{TM} HP* column packed with nickel-sepharose to purify the protein. The SDS-PAGE analysis displayed in the right panel of figure 4.6, shows the fraction that was eluted from the column with imidazole concentrations above 128 mM (60% *Buffer B for IMAC*). In addition to the dominant band with the approximate size of Lmo0728-His, at least four contaminating proteins were present in the eluate. The eluate was desalted and subject of a flavokinase/FAD synthetase activity assay. Since neither flavokinase nor FAD synthetase activity of the eluate could be detected, further purification of Lmo0728-His from the mixture was not pursued.

4.5.1 Maltose Binding Protein Fusions with Enhanced Solubility

A new approach to produce a soluble and active form of Lmo0728 was to produce a fusion protein with the highly soluble maltose binding protein (MBP) from *E. coli*, encoded by the gene *malE*, N-terminally fused to Lmo0728. For this approach the commercially available *pMAL^{TM} Protein Fusion and Purification System* (New England BioLabs) was applied. The coding sequence of *lmo0728* was introduced into the expression plasmid pMAL-c5x that provides the genetic information, necessary to produce a fusion of MBP connected to the protein of interest via a linker, that contains a protease recognition sequence, which facilitates the separation of the two parts of the fusion protein with the protease FactorXa subsequent to the purification of the fusion protein. Since the fusion protein MBP-Lmo0728 did not feature a His-tag, a *MBPTrap^{TM}* column (GE Healthcare), packed with amylose resin that binds the MBP portion of the fusion protein was used for affinity purification. Column bound proteins were eluted from the column with a buffer containing 10 mM maltose. The purification of MBP-fusion proteins with the FPLC system is described in more detail in section 3.10.2.

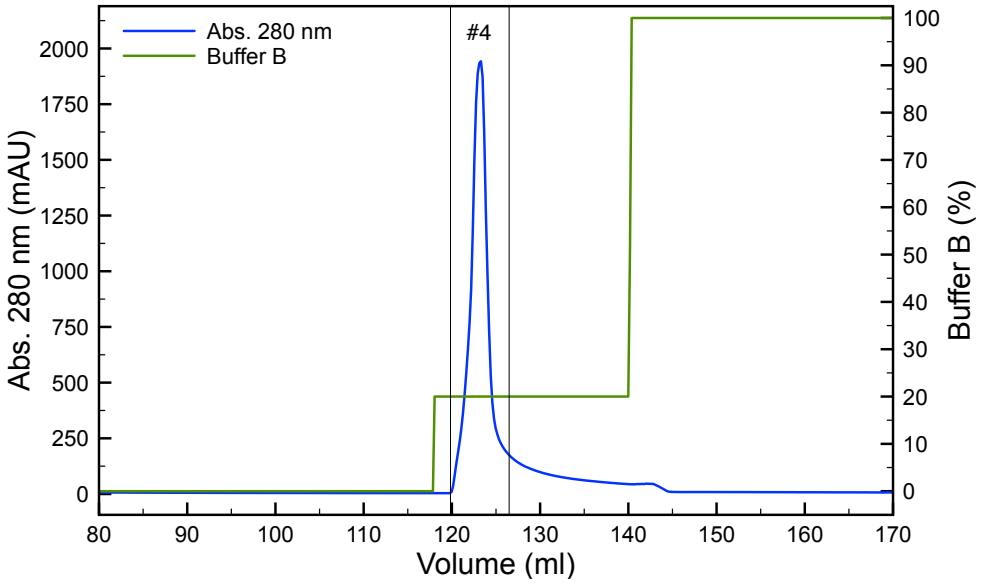

Figure 4.7: Purification of active MBP-Lmo0728 fusion protein. FPLC chromatogram of the elution of recombinantly produced MBP-Lmo0728 from a *MBPTrap*^{TM} *HP* column with a one step elution profile. Blue: absorption at 280 nm; green: ratio (v/v) of elution buffer (Buffer B for MBPTrap, 10 mM maltose) and loading buffer (Buffer A for MBPTrap). Collected fractions are numbered and indicated by vertical lines.

The production of MBP-Lmo0728 from pMAL_lmo0728 was carried out in *E. coli* ER2523. Gene expression was induced at OD_{600} = 0.4 with 0.3 mM IPTG and the culture was incubated for protein production for 3 h at 37 °C. After lysis of the cells, the cell free extract was clarified by centrifugation and was subsequently applied to a *MBPTrap*^{TM} *HP* column (GE Healthcare) with a column volume of 5 ml. The FPLC chromatogram of the elution of the column bound proteins is shown in figure 4.7. A single peak eluted from the column after the a maltose concentration was raised in a step profile to 2 mM (20% (v/v) *Buffer B for MBPTrap*). The cell free extract, a sample collected from the flow through of the column and the elution peak were subject to SDS-PAGE analysis. The gel is depicted in figure 4.8.

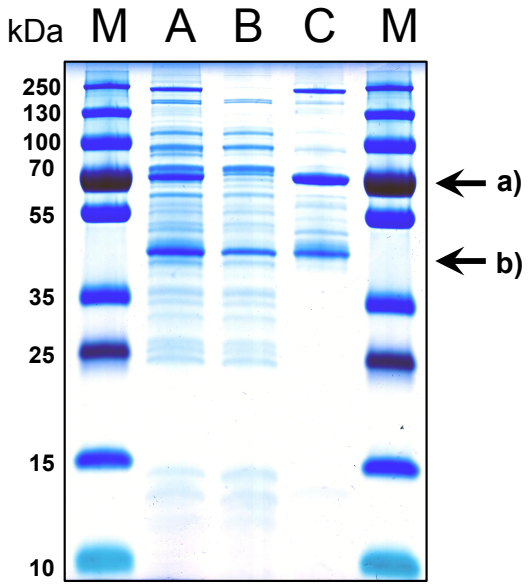

Figure 4.8: Purified MBP-Lmo0728 fusion protein. SDS-PAGE after MBPTrap purification of MBP-Lmo0728. Sizes in kDa corresponding to the bands of the marker are given on the left. The arrows on the right indicate the expected positions of a) the MBP-Lmo0728 fusion protein (71.5 kDa) and b) MBP (42.5 kDa). M: Marker (PageRuler^{TM} Plus); A: cell free extract that was loaded to the column; B: flow through; C: elution peak (sample #4, figure 4.7).

The SDS-PAGE analysis of the peak, eluted from the MBPTrap column (figure 4.8 lane C) showed that in addition to the two expected bands of MBP (a) and MBP-Lmo0728 fusion protein (b), several other proteins co-purify on the MBPTrap column. The eluate was tested for flavokinase and FAD synthetase activity. When riboflavin was used as substrate in the assay, no flavokinase activity could be detected. However, when FMN was used as a substrate in the activity assay, FAD was produced (figure 4.9) proving that the MBP-Lmo0728 fusion protein is an active FAD synthetase.

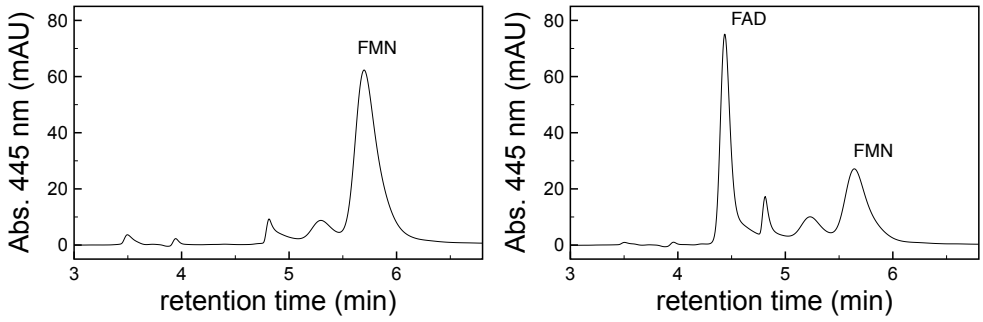

Figure 4.9: FAD synthetase activity of MBP-Lmo0728. HPLC chromatograms of an FAD synthetase activity assay, performed with 10 μM FMN as substrate and 170 $\mu g/ml$ of the desalted elution fraction (sample #4, figure 4.7) from the MBPTrap column. The reaction was stopped immediately after enzyme addition (left) and after 7 h incubation at 37 °C (right).

For further characterization, especially for the determination of kinetic parameters, it was desired to cleave the fusion protein and purify the protein of interest (i.e. Lmo0728) to apparent homogeneity. The user's instructions for the *pMAL™ Protein Fusion and Purification System* suggested to use the protease FactorXa that was supplied with the kit, followed by a separation of the target protein from the cleaved off MBP through anion exchange chromatography (AEX). The proteolytic digest was performed within the specifications of the manufacturer's recommendations (NEB, 8200).

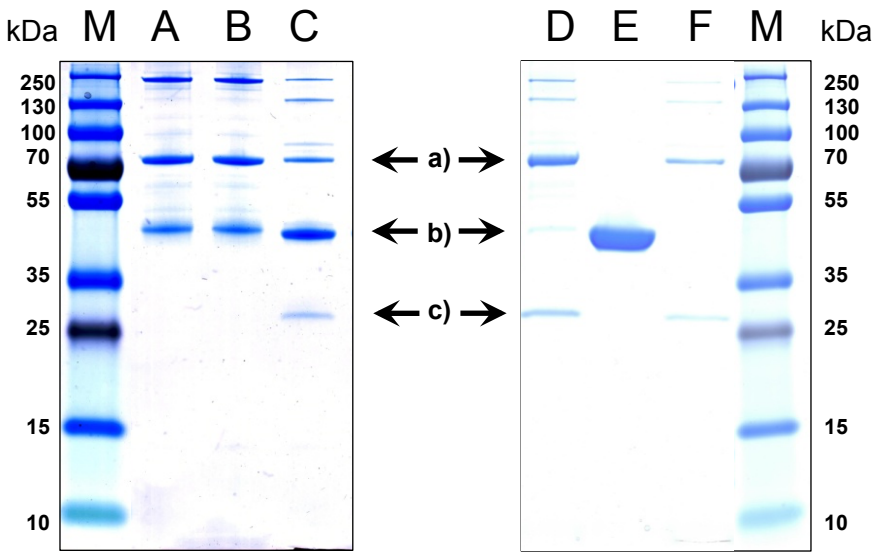

Figure 4.10: Incomplete digest and AEX purification of MBP-Lmo0728. SDS-PAGE after FactorXa digest of the MBPTrap eluate (left) and after AEX chromatography of the digested sample (right). Sizes in kDa corresponding to the bands of the markers. The arrows indicate the expected position of a) MBP-Lmo0728 fusion protein (71.5 kDa); b) MBP (42.5 kDa); c) Lmo0728 (27.8 kDa).
M: Marker (PageRuler™ Plus); A: Undigested eluate from MBPTrap column (sample #4, figure 4.7); B: Mock digest (8 h at room temperature without protease) of the MBPTrap eluate; C: FactorXa digest (8 h at room temperature) of the MBPTrap eluate; D: AEX flow through (sample #1, figure 4.11); E: AEX elution peak1 (sample #3, figure 4.11); F: AEX elution peak2 (sample #4, figure 4.11).

The SDS-PAGE analysis of the digested eluate (figure 4.10 lane C) revealed that the digestion of the fusion protein was incomplete after 8 h at room temperature. An extended incubation time of 18 h at 4 °C did not result in a complete digestion of the fusion protein (gel not shown). The reaction, although incomplete, resulted in the formation of cleaved Lmo0728. The separation of Lmo0728 from MBP and the remaining fusion protein was approached by loading the digest reaction to a *HiTrap™ Q FF* (GE Life Sciences) anion exchange column. The bound protein was eluted with a gradient of sodium chloride in the buffer (detailed information on AEX chromatography see section 3.10.3).

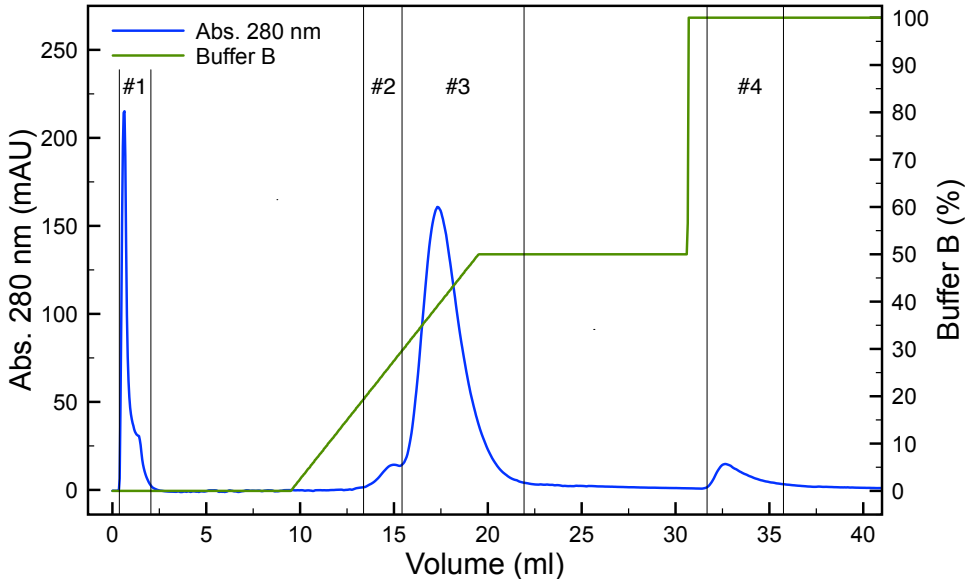

Figure 4.11: AEX chromatography after Factor Xa digest of MBP-Lmo0728. FPLC chromatogram of the separation of the FactorXa digest (8 h at room temperature) of the eluate fraction (sample #4, figure 4.11) of the MBPTrap purification with a *HiTrap™ Q FF* (CV = 1 ml) AEX column. Blue: absorption at 280 nm; green: ratio (v/v) of elution buffer (*Buffer B for AEX*, 500 mM NaCl) and loading buffer (*Buffer A for AEX*), 25 mM NaCl). Collected fractions are numbered and indicated by vertical lines.

The chromatogram of the anion exchange chromatography of the digested MBPTrap eluate with a *HiTrap™ Q FF* (figure 4.11) shows the separation of the sample into three fractions: the flow through, a main peak eluting from the column as the salt concentration rises and a smaller peak eluted with a step profile from 50% to 100% *Buffer B for AEX*, to focus the peak and counteract further dilution. The fractions collected during the AEX chromatography were analyzed by SDS-PAGE. The resulting gel (figure 4.10 right gel) shows that the

main elution peak contained purified MBP but it was, however, not possible to separate Lmo0728 from the uncleaved fusion protein, as both are present in the flow through as well as in the secondary elution peak (samples #1 and #4 in figure 4.11).

4.5.2 His-MBP-Lmo0728 Fusion Proteins Digested with His-tagged TEV Protease

Since the strategy of producing a MBP-Lmo0728 fusion protein with subsequent proteolytic digest seemed to be the most promising approach, considering the previous issues of solubility and activity of Lmo0728. Instead of optimizing the separation of cleaved Lmo0728 via AEX, a His-tagged MBP-Lmo0728 fusion was produced. On the pET-24d derived expression plasmid pET-MBP-1a the genetic information for *egfp* was replaced with the coding sequence *lmo0728* to form the plasmid pET-MBP-lmo0728.

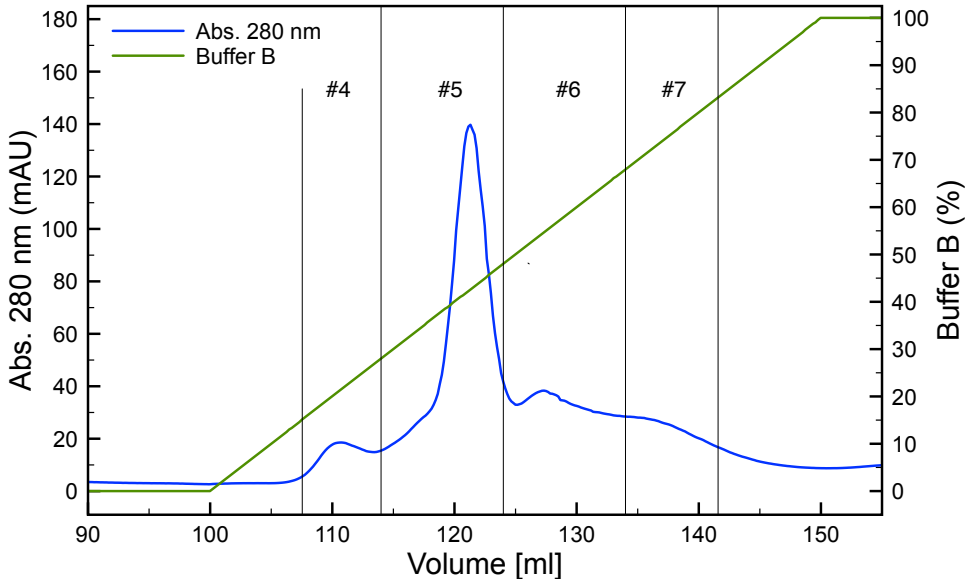

Figure 4.12: Purification of His-MBP-Lmo0728 fusion protein. FPLC chromatogram of the elution of recombinantly produced His-MBP-Lmo0728 from a *HisTrap^{TM} HP* column with a linear gradient of imidazole. Blue: absorption at 280 nm; green: ratio (v/v) of elution buffer (Buffer B for IMAC, 200 mM imidazole) and loading buffer (Buffer A for IMAC, 20 mM imidazole). Collected fractions are numbered and indicated by vertical lines.

The fusion protein His-MBP-Lmo0728 could be purified on a *HisTrap^{TM} HP* column while the MBP portion of the fusion still provides enhanced solubil-

ity. Additionally the fusion protein featured a recognition sequence for the highly specific tobacco etch virus (TEV) protease between MBP and Lmo0728. After the proteolytic digest was performed with a His-tagged TEV protease (expressed from the plasmid pTH24 and purified via IMAC) the His tagged MBP, potentially uncleaved fusion protein and the Protease could be captured on a *HisTrap^{TM} HP* column while the, now untagged, Lmo0728 remains in the flow through.

The His-MBP-Lmo0728 fusion protein was produced in BL21(DE3) from the expression plasmid pET-MBP-lmo0728. The expression was induced with 1 mM IPTG and carried out for 3 h at 37 °C. The cleared cell free extract was applied to a *HisTrap^{TM} HP* column and proteins bound to the column were eluted with a linear gradient of imidazole. The elution profile of the purification is shown in figure 4.12.

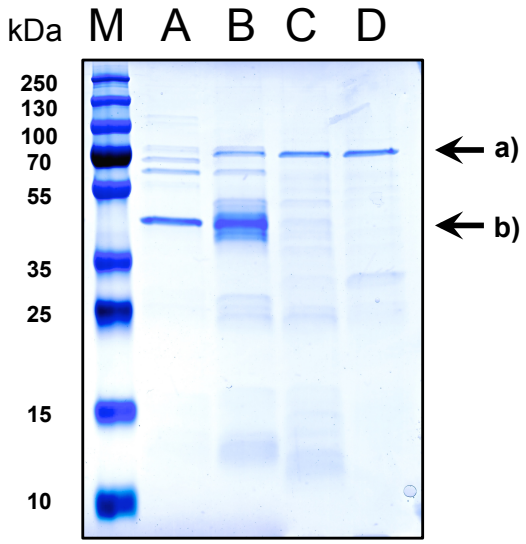

Figure 4.13: Purified His-MBP-Lmo0728 fusion protein. SDS-PAGE analysis of the HisTrap purification of the His-MBP-Lmo0728 fusion protein. Sizes in kDa corresponding to the bands of the marker are given on the left. The arrows on the right mark the expected position of a) His-MBP-Lmo0728 (70.8 kDa); b) His-MBP (42 kDa). Sample numbers corresponding to the chromatogram in figure 4.12. M: Marker (PageRuler^{TM} Plus); A: sample #4; B: sample #5; C: sample #6; D: sample #7.

The SDS-PAGE analysis of the collected samples (figure 4.13) showed that the main peak of the elution profile (sample #5) did contain a major band which corresponded in size to His-tagged MBP (42 kDa), however, a band with the expected size of the His-MBP-Lmo0728 fusion (70.8 kDa) eluted in the

collected samples #5 – #7. These three samples were pooled and concentrated using a *Vivaspin® 20* centrifugal concentrator (MWCO 10 kDA, Satorius) for subsequent incubation with His-tagged TEV protease. The introduction of His-MBP into the sample was accepted, since it was formed as a side product during the digest and had to be removed together with TEV-His and possibly remaining, uncleaved fusion protein subsequently to the digest reaction.

The pooled elution fractions (samples #5 – #7) were incubated with TEV-His over night at room temperature. A preparation of purified His-MBP-EGFP, purified after expressed from pET-MBP-1a was digested as a control to verify the proteolytic activity of the used TEV-His protease. A mock setup, that was incubated side by side with the digest but without addition of TEV-His, was also included in the subsequent SDS-PAGE analysis. The mock was done to check the stability of the fusion proteins under the chosen conditions. From the gel, that is shown in figure 4.14, the general proteolytic activity of TEV-His can be recognized, as the His-MBP-GFP fusion protein was clearly digested (figure 4.14 lane C). The His-MBP-Lmo0728 fusion protein, however, was not affected by the protease present in the mixture (figure 4.14 lane A).

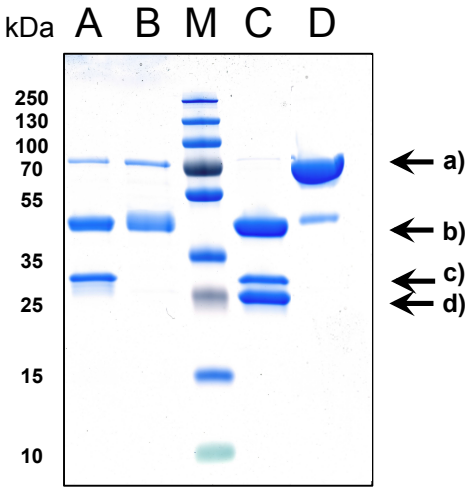

Figure 4.14: Incomplete digest of His-MBP-Lmo0728 with TEV-His. SDS-PAGE analysis after TEV-His digest of His-MBP-Lmo0728 and His-MBP-EGFP. A: TEV-His digest of His-MBP-Lmo0728; B: Mock digest of His-MBP-Lmo0728; M: Marker (PageRuler™ Plus); C: TEV-His digest of His-MBP-EGFP; D: Mock digest of His-MBP-EGFP. The arrows indicate the expected position of a)His-MBP-Lmo0728/-EGFP fusion protein (71.5/70.6 kDa); b) MBP (42.5 kDa); c) TEV-His (33.5 kDa); d) Lmo0728/EGFP (27.7/26.9 kDa).

To improve the accessibility of the protease recognition site between the N-terminal MBP portion and the C-terminal Lmo0728 domain of the fusion protein, a linker sequence was introduced. The linker consisting of five glycine residues was chosen to improve the structural flexibility of the fusion protein with minimal influence on the activity of Lmo0728 as it remained on the N-terminus of Lmo0728 after successful cleavage.

Figure 4.15: Glycine linker improves proteolytic accessibility of His-MBP-Lmo0728. Detail of the DNA sequence of the plasmid pET-MBP-pG-lmo0728. The plasmid was derived from pET-MBP-lmo0728 by introduction of a 25 nt long linker into the unique *NcoI* restriction site, directly upstream of *lmo0728* (see section 2.4.3). The translated amino acid sequence is shown below.

A 25 nt long linker sequence featuring the the codons GGT and GGC, both coding for glycine, in an alternating manner was introduced into the unique *NcoI* restriction site present of pET-MBP-lmo0728 between the TEV recognition sequence and the Lmo0728 domain of the fusion protein. The resulting plasmid, pET-MBP-pg-lmo0728, was used to produce the fusion protein MBP-pg-Lmo0728 in *E. coli* BL21(DE3). The expression was carried out for 16 h after it was induced with 1 mM IPTG at OD_{600} = 0.8. The incubation temperature for the protein production phase was reduced to 25 °C. This optimization was necessary since the introduction of the pGly-linker appeared to increase the amount of the by-product His-MBP. Especially if the expression was induced at lower OD_{600} (0.4) and carried out at higher temperatures (37 °C). The cell free extract was applied to a *HisTrap^{TM} HP* column and an imidazole gradient was used for the elution of column bound proteins. The chromatogram in figure 4.16 shows one major elution peak that was collected in several fractions. The subsequent SDS-PAGE analysis of the fractions collected during the elution process is shown in figure 4.17.

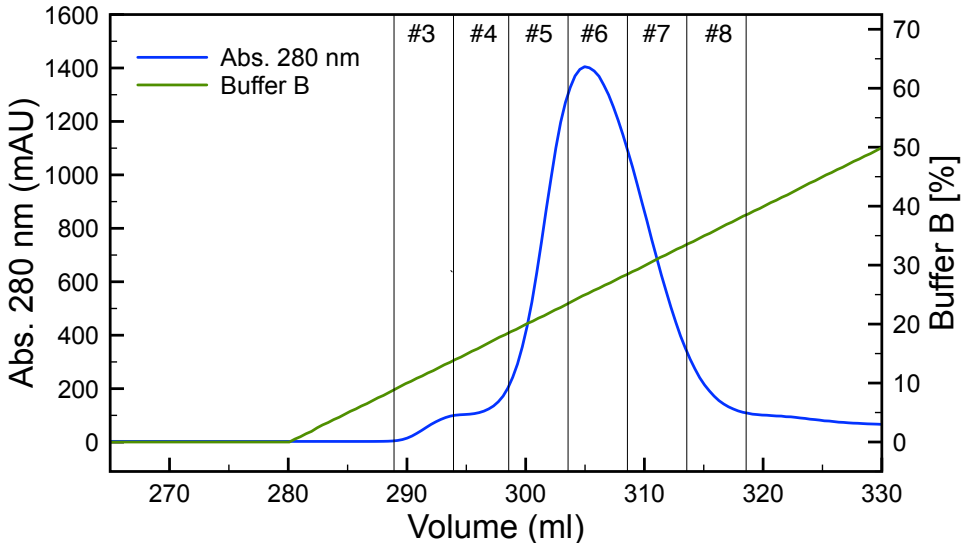

Figure 4.16: Purification of the His-MBP-pg-Lmo0728 fusion protein. FPLC chromatogram of the elution peak His-MBP-pg-Lmo0728 from a *HisTrap™ HP* column with a linear gradient of imidazole. Blue: absorption at 280 nm; green: ratio (v/v) of elution buffer (Buffer B for IMAC, 200 mM imidazole) and loading buffer (Buffer A for IMAC, 20 mM imidazole). Collected fractions are numbered and indicated by vertical lines.

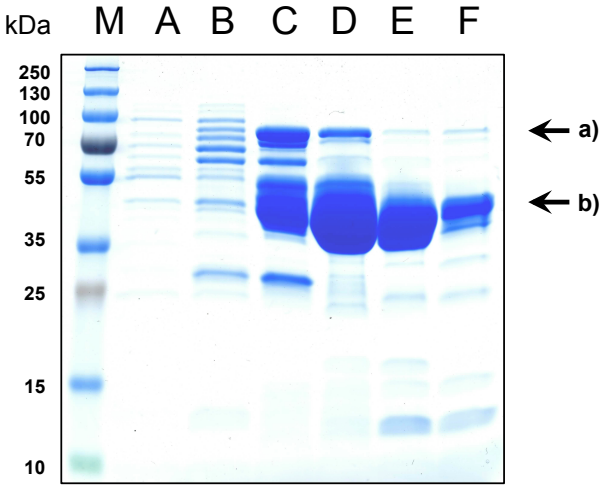

Figure 4.17: Purified His-MBP-pg-Lmo0728 fusion protein. SDS-PAGE analysis of the samples collected during the HisTrap purification of His-MBP-pg-Lmo0728. The arrows on the right mark the expected positions of a) His-MBP-pg-Lmo0728 (71.5 kDa); b) His-MBP (42.5 kDa). Sample numbers corresponding to figure 4.16. M: Marker (PageRuler™ Plus); A: sample #3; B: sample #4; C: sample #5; D: sample #6; E: sample #7; F: sample #8.

The gel revealed that different fractions contained varying amounts of the expected proteins as well as contaminating proteins, which elute mainly at lower imidazole concentrations (figure 4.17 lane A-C). Since fraction #6 (figure 4.17 lane D) appeared to have the best ratio of His-MBP-pg-Lmo0728 fusion protein to His-MBP and other contaminations, this fraction was used for the proteolytic digest with TEV-His.

The digest reaction was incubated at 4 °C for 16 h. The whole reaction mixture was then applied to a *HisTrap™ HP* column (CV = 1 ml). The flow through was collected and all column bound protein was was eluted with a single step elution profile to 100% Buffer B for IMAC. The FPLC chromatogram is shown in figure 4.18.

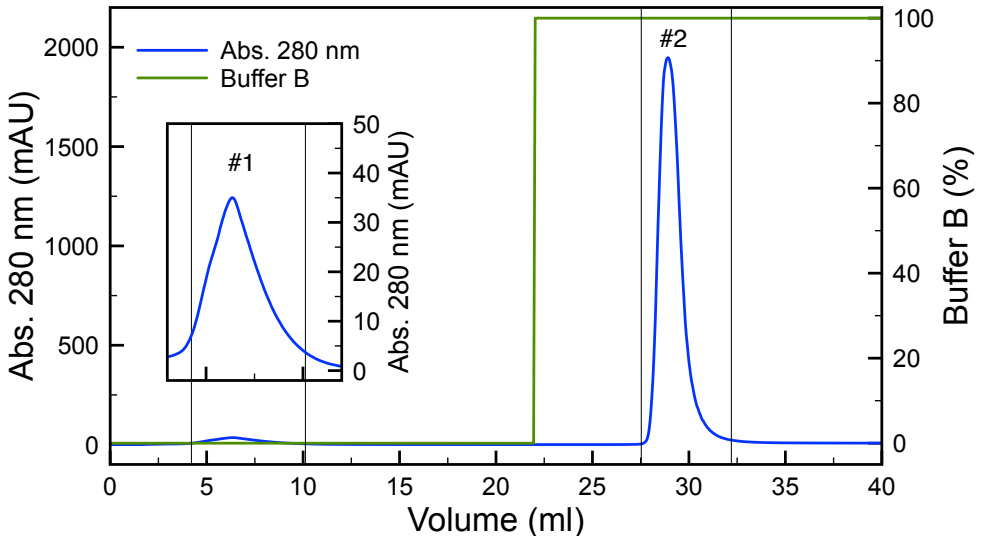

Figure 4.18: Separation of His-MBP and pg-Lmo0728 after TEV-His digest. FPLC chromatogram after the TEV-His digest reaction of sample #6 from the HisTrap purification of His-MBP-pg-Lmo0728 (figure 4.16). The Digest mixture was applied to a *HisTrap™ HP* column (CV = 1 ml). Inset graph shows the flow through peak with amplified scale for the absorption. Blue: absorption at 280 nm; green: ratio (v/v) of elution buffer (Buffer B for IMAC, 200 mM imidazole) and loading buffer (Buffer A for IMAC, 20 mM imidazole). Collected fractions are numbered and indicated by vertical lines.

In the FPLC chromatogram in figure 4.18 an approximately 50-fold lower UV absorption of the flow through compared to the elution peak was observed. This was consistent with a very low protein concentration in the flow through fraction, when compared to the elution fraction. Prior to the subsequent SDS-PAGE analysis (figure 4.19), the flow through fraction was concentrated

approximately 6-fold to a volume of about 1 ml with a *Vivaspin® 6* centrifugal concentrator (MWCO 10 kDa, Satorius). The final protein concentration in the concentrate was determined to be 0.3 $^{mg}/_{ml}$.

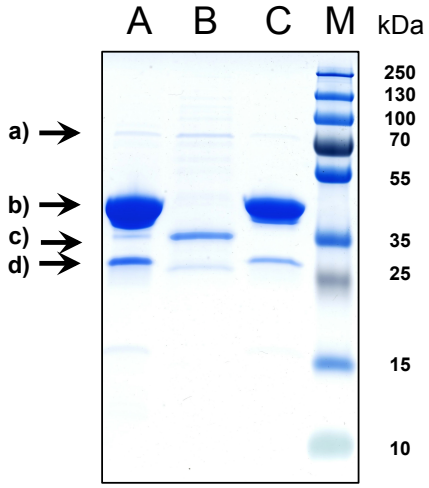

Figure 4.19: Purified pg-Lmo0728. SDS-PAGE analysis of the TEV-His digest reaction of His-MBP-pg-Lmo0728. The arrows on the left mark the expected positions of a) His-MBP-pg-Lmo0728 (71.5 kDa); b) His-MBP (42.5 kDa); c) pg-Lmo0728 (27.7 kDa); d) TEV-His (33.5 kDa) Sample numbers corresponding to figure 4.18. A: Digest reaction mixture, that was loaded to the column; B: concentrated flow through (sample #1); C: elution peak (sample #2); M: Marker (PageRuler^{TM} Plus).

A sample of the digest reaction, the concentrated flow through fraction and the eluate fraction were analyzed by SDS-PAGE (figure 4.19). Notably, the dominant protein band of the concentrated flow through fraction was found on the same height as the 35 kDa band of the marker. Western blot analysis confirmed that the dominant band on lane B in figure 4.19 did not react with the anti-His primary antibody and thus was considered to be the C-terminal part (pg-Lmo0728) of the cleaved fusion protein. The concentrated flow through fraction was tested for flavokinase/FAD synthetase activity (section 4.6.2) and found to contain an active FAD synthetase.

4.6 Flavokinase/FAD synthetase Activity of Lmo1329 and Lmo0728

To test the recombinantly produced proteins Lmo1329 and Lmo0728 for flavokinase (EC 2.7.1.26) and FAD synthetase (EC 2.7.7.2) activity, the purified proteins

were subject to the flavokinase/FAD synthetase activity assay described in section 3.11.6. For qualitative evaluation of the enzymes' flavokinase activity, the assay was supplied with riboflavin as a substrate. Samples were taken immediately after addition of the respective enzyme and after 10 min an 60 min of incubation at 37 °C from the same reaction mixture. The FAD synthetase activity was tested alike with FMN added as the substrate in the assay reaction instead of riboflavin. The assays were repeated to test for enzyme activity with the riboflavin analogs 8-amino riboflavin and roseoflavin as well as the cofactor analogs AFMN and RoFMN. All samples were analyzed by HPLC-MS (Method2) to monitor the the potential reduction of the substrate and the formation of the reaction products over time.

4.6.1 Lmo1329 is a Bifunctional Flavokinase/FAD synthetase

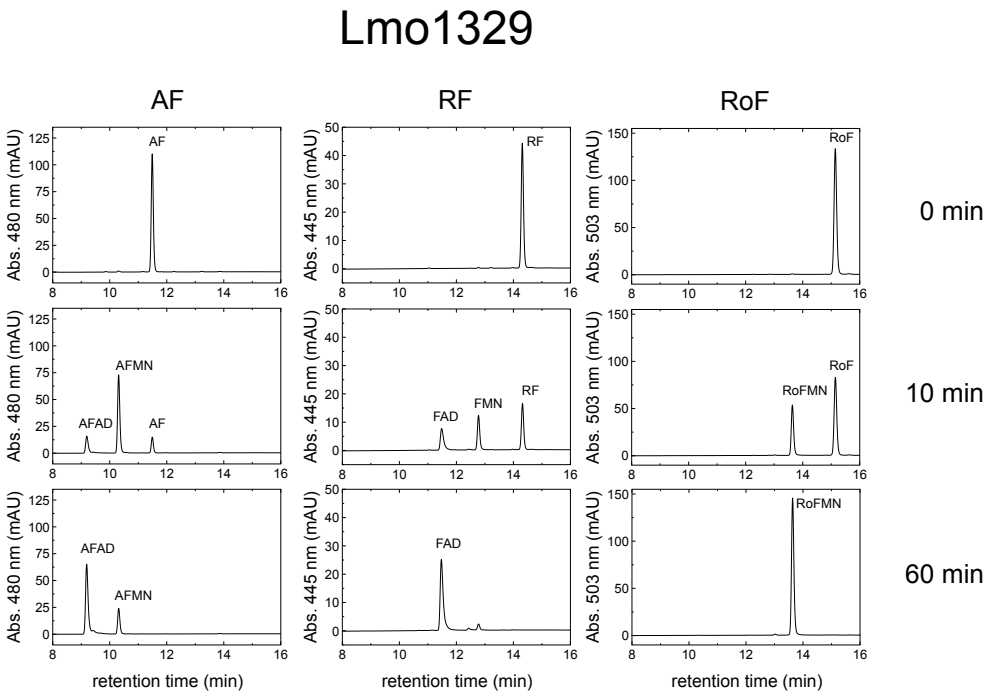

Figure 4.20: Flavokinase activity assay of Lmo1329. HPLC Chromatograms of flavokinase/FAD synthetase activity assays performed with Lmo1329. 8-amino riboflavin (AF, left), riboflavin (RF, middle) and roseoflavin (RoF, right) as substrates. The reactions were stopped after 0 min (top), 10 min (middle) and 60 min (bottom) of incubation.

The results of the HPLC-MS analysis in the middle column of Figure 4.20 confirmed that Lmo1329 is a bifunctional enzyme, that has flavokinase and

FAD synthetase activity. If riboflavin was provided as substrate, FMN was formed as an intermediate reaction product which was further converted into FAD. If 8-amino riboflavin was used as substrate, the two corresponding reaction products AFMN and AFAD could be detected (Figure 4.20 left column). In contrast to these findings, when roseoflavin was used as substrate for the reaction, only the formation of RoFMN could be observed. After 60 min the roseoflavin present in the reaction mixture has been completely converted into RoFMN but no RoFAD formation could be detected (Figure 4.20 right column).

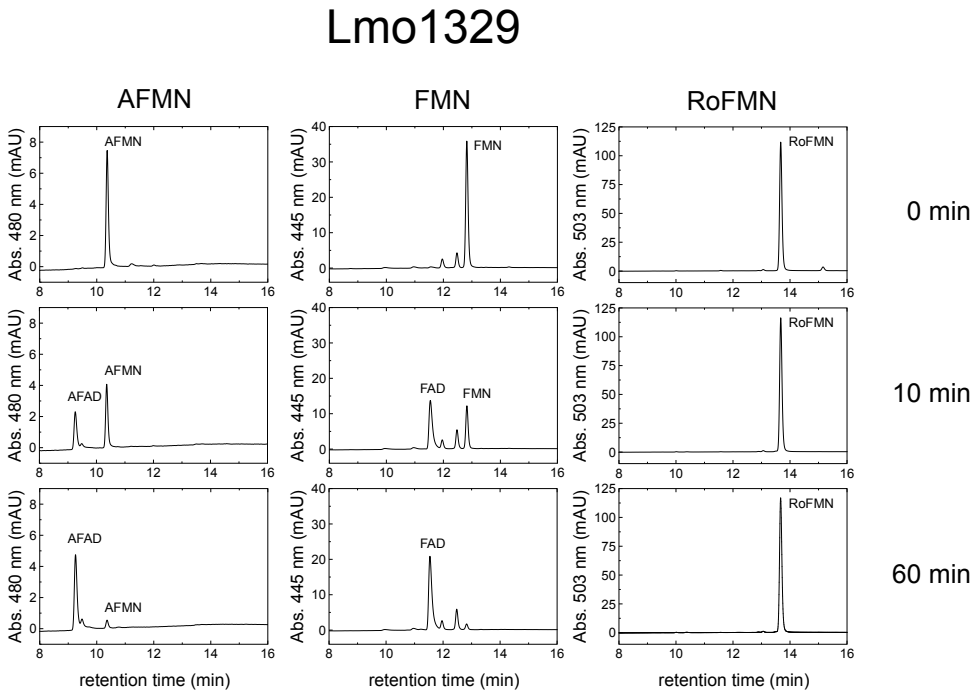

Figure 4.21: FAD synthetase activity assay of Lmo1329. HPLC Chromatograms of flavokinase/FAD synthetase activity assays performed with Lmo1329. AFMN (left), FMN (middle) and RoFMN (right) as substrates. The reactions were stopped after 0 min (top), 10 min (middle) and 60 min (bottom) of incubation.

When the respective flavin mononucleotides (AFMN, FMN and RoFMN) were used as substrates in the flavokinase/FAD synthetase activity assay, no FAD synthetase activity of Lmo1929 could be detected with RoFMN in contrast to the other two substrates (figure 4.21).

4.6.2 Lmo0728 is a Monofunctional FAD synthetase

The recombinantly produced enzyme Lmo0728, did not convert any of the substrate within 60 min, when it was tested in the flavokinase/FAD synthetase activity assay with 8-amino riboflavin, riboflavin and roseoflavin as substrates (figure 4.22). Also extended incubation times up to 18 h did not lead to any substrate consumption or cofactor formation (data not shown).

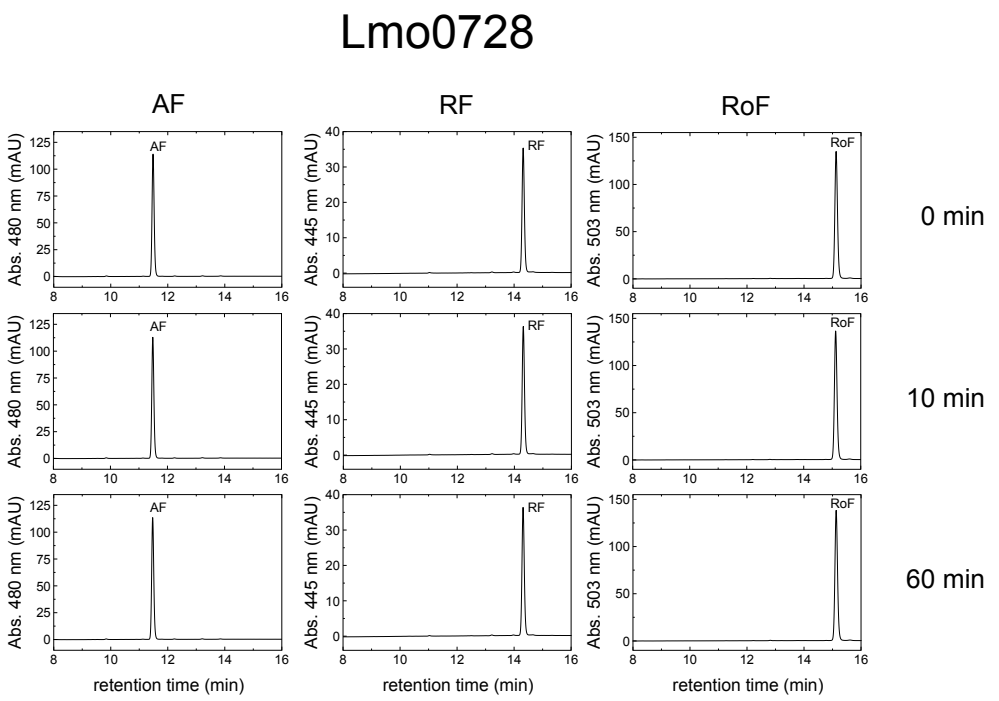

Figure 4.22: Flavokinase activity assay of Lmo0728. HPLC Chromatograms of flavokinase/FAD synthetase activity assays performed with Lmo0728. 8-amino riboflavin (AF, left), riboflavin (RF, middle) and roseoflavin (RoF, right) as substrates. The reactions were stopped after 0 min (top) 10 min (middle) and 60 min (bottom) of incubation.

When the respective flavin mononucleotides (AFMN, FMN and RoFMN) were applied as substrates in the flavokinase/FAD synthetase activity assay with Lmo0728, FAD synthetase activity was observed for all three substrates (Figure 4.23). Notably, in contrast to Lmo1329, Lmo0728 showed FAD synthetase activity also when RoFMN was used as substrate. RoFAD was formed in this reaction (figure 4.23 right column).

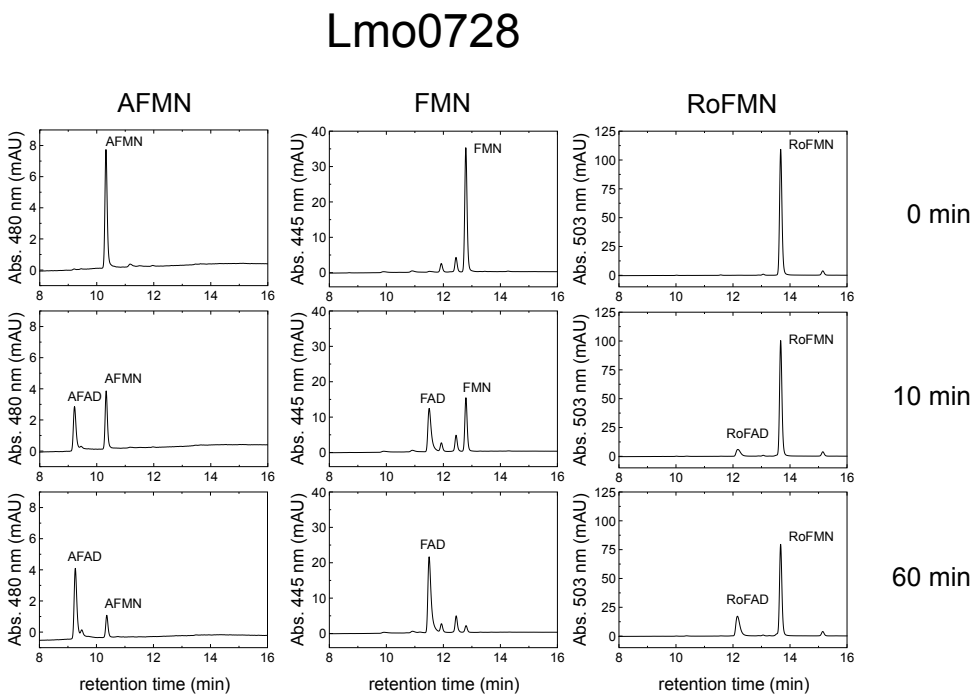

Figure 4.23: FAD synthetase activity assay of Lmo0728. HPLC Chromatograms of flavokinase/FAD synthetase activity assays performed with Lmo0728. AFMN (left), FMN (middle) and RoFMN (right) as substrates. The reactions were stopped after 0 min (top) 10 min (middle) and 60 min (bottom) of incubation.

The results of the flavokinase/FAD synthetase activity assays presented in figures 4.22 and 4.23 show that Lmo0728 is a monofunctional FAD synthetase without detectable flavokinase activity. Further the presence of RoFAD in the cell free extract of *L. monocytogenes* grown in the presence of roseoflavin can be attributed to the cooperation of Lmo1329, producing RoFMN from roseoflavin and ATP, and Lmo0728, converting it into RoFAD.

4.6.3 Optimal pH for FAD synthetase Activity of Lmo0728 and Lmo1329

Throughout the qualitative experiments presented in section 4.6.2 a high dependence of the FADS activity, particularly of Lmo0728, to the pH of the reaction buffer was noticed. Several BIS-Tris propane (BTP) buffer compositions (given in Table 3.10) with a pH range from 7.0 to 9.5 were used in the flavokinase/FAD synthetase activity assays to identify the pH with maximal enzyme activity.

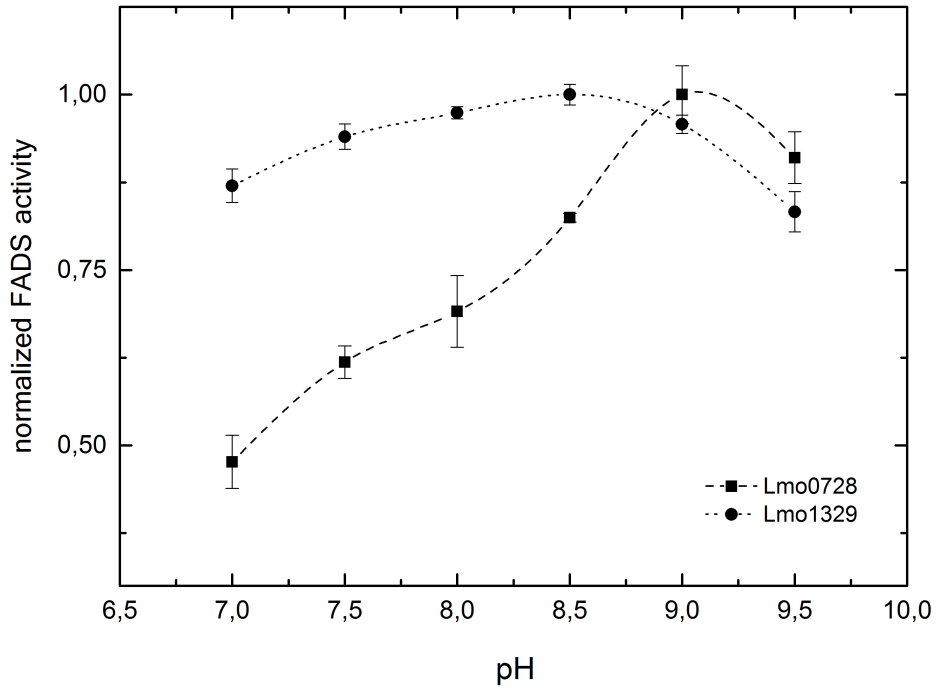

Figure 4.24: Determination of the optimal pH for FAD synthetase activity. Normalized FAD synthetase activities of Lmo0728 (■) and Lmo1329 (●) in 50 mM BIS-TRIS propane buffer with varying pH.

The specific FAD synthetase activities plotted in figure 4.24 were normalized to the maximal activity obtained for the respective enzyme to ease the comparison between both enzymes. The optimal pH for the FAD synthetase reaction of each enzyme was determined by reading off the pH corresponding to the enzyme's maximal activity. Thus pH 8.5 was determined to be the optimum for Lmo1329 while pH 9.0 was found to be the optimum for Lmo0728. All further characterizations of the enzymes were carried out in BTP buffer at the optimal pH for the respective enzyme.

4.6.4 Kinetic Characterization of the Flavokinase and FAD synthetase Activity of Lmo0728 and Lmo1329

To determine the apparent kinetic parameters for the enzyme-substrate combination, the Michaelis constant K_m and the maximal reaction rate v_max were calculated from the best fit of the Michaelis-Menten kinetic (equation 3.2 on page 65) to the experimental data. From these two constants, the turnover number k_cat and the kinetic efficiency $\frac{k_\mathrm{cat}}{K_\mathrm{m}}$ for each enzyme-substrate combination were calculated.

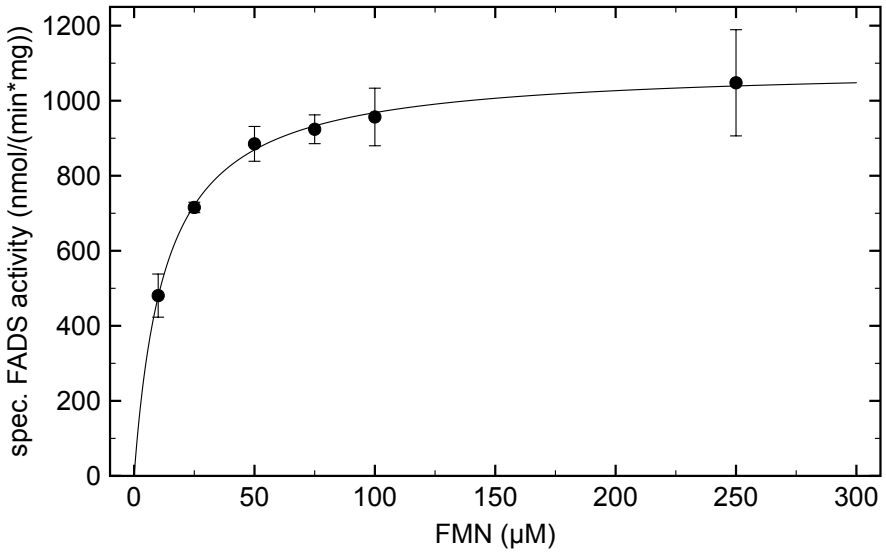

Figure 4.25: FAD synthetase kinetic of Lmo0728. Specific FAD synthetase activities of Lmo0728 plotted against the corresponding substrate (FMN) concentration. Solid line gives the non-linear regression according to the kinetic model of Michaelis-Menten. K_{m} = 12.9 μM; $v_{\max}$ = 1093 $^{\mathrm{nmol}}/_{\mathrm{min \cdot mg}}$.

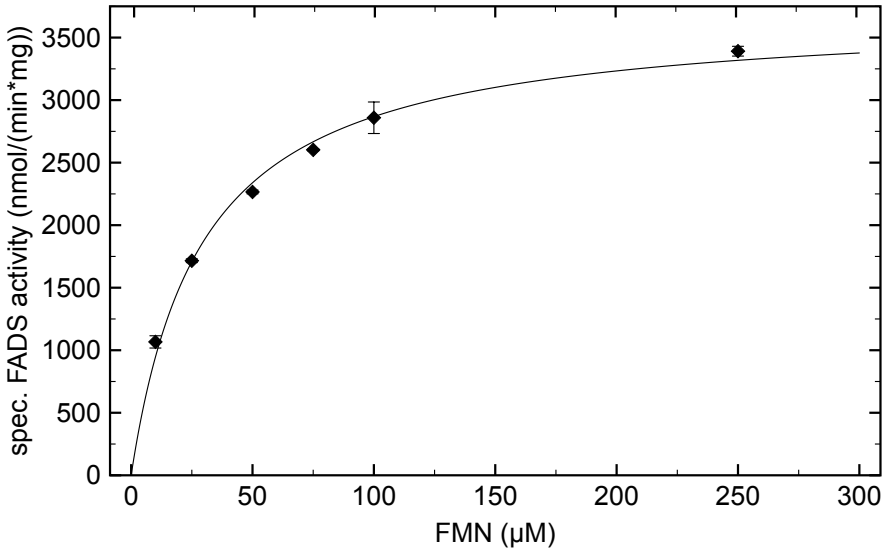

Figure 4.26: FAD synthetase kinetic of Lmo1329. Specific FAD synthetase activities of Lmo1329 plotted against the corresponding substrate (FMN) concentration. Solid line gives the non-linear regression according to the kinetic model of Michaelis-Menten. K_{m} = 29.2 μM; $v_{\max}$ = 3706 $^{\mathrm{nmol}}/_{\mathrm{min \cdot mg}}$.

For the determination of the kinetic parameters of the enzymes, their specific activity for various substrate concentrations was measured and plotted against

the corresponding substrate concentration. From these data pairs the kinetic function described by the Michaelis-Menten equation could be derived through non-linear regression. The method is described in more detail in section 3.15.

Figures 4.25 and 4.26 show the specific FAD synthetase activities of Lmo0728 and Lmo1329, respectively. The specific activities were plotted against the corresponding FMN concentrations. Figure 4.27 shows the specific flavokinase activities of Lmo1329 plotted against the corresponding riboflavin concentrations. The apparent kinetic parameters for each enzyme-substrate pair were derived from the best fit according to the kinetic model of Michaelis-Menten and are summarized in table 4.2.

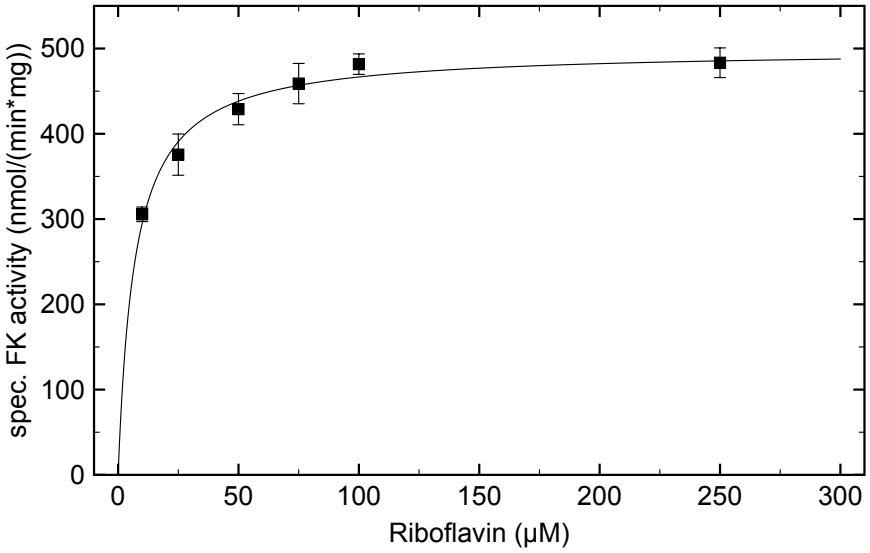

Figure 4.27: Flavokinase kinetic of Lmo1329. Specific flavokinase activities of Lmo1329 plotted against the corresponding substrate (RF) concentration. Solid line gives the non-linear regression according to the kinetic model of Michaelis-Menten. K_{m} = 6.9 μM; $v_{\max}$ = 668 $^{\mathrm{nmol}}/_{\mathrm{min\cdot mg}}$.

Table 4.2: Apparent kinetic parameters of Lmo0728 and Lmo1329, calculated from the results of flavokinase/FAD synthetase assays.

Enzyme	Substrate	K_{m} (μM)	$v_{\max}(\frac{\mathrm{nmol}}{\mathrm{min\cdot mg}})$	k_{cat} (s^{-1})	$\frac{k_{\mathrm{cat}}}{K_{\mathrm{m}}}(\frac{1}{\mathrm{s\cdot\mu M}})$
Lmo0728	FMN	12.9	1093	0.51	0.040
Lmo1329	FMN	29.2	3706	4.39	0.150
Lmo1329	RF	6.9	668	0.40	0.057

4.7 Characterization of the Gene Product of *lmo1945* from *L. monocytogenes* and its 5′–UTR *Rli96*

Mansjö and Johansson were able to show that, if riboflavin or roseoflavin was added to the growth medium, transcription was terminated between *Rli96* and *lmo1945* in a *L. monocytogenes* wild type strain indicating that the expression of *lmo1945* is regulated by the transcriptional FMN riboswitch *Rli96*. The nothern-blot data presented by Mansjö and Johansson are merely qualitative and give no information about the level of regulation regarding the expression level of the gene downstream of *Rli96* (Mansjö and Johansson, 2011).

The crystal structure of Lmo1945 has been solved recently by Karpowich et al.. They show that Lmo1945 is a a membrane-embedded substrate-binding subunit (EcfS) of an energy-coupling factor (ECF) riboflavin transporter. However, physiological experiments showing that Lmo1945 indeed is involved in riboflavin uptake were not carried out (Karpowich et al., 2015). In the context of this work, the question whether Lmo1945 is involved in the uptake of the flavin analogs roseoflavin was of great interest. Although the findings of Mansjö and Johansson (2011) suggest that roseoflavin is incorporated by *L. monocytogenes*, it remained unclear if the uptake is facilitated by Lmo1945.

4.7.1 The Gene Product of *lmo1945* from *L. monocytogenes* is Responsible for Riboflavin and Roseoflavin Uptake

To show that the FMN riboswitch controlled gene *lmo1945* from *L. monocytogenes* indeed codes for the substrate binding domain Lmo1945 of an ECF riboflavin importer, similar to RibU from *B. subtilis*, the expressed in the specialized *B. subtilis* test strain BsΔribUB (Hemberger et al., 2011). The coding sequence of *lmo1945* was introduced into the riboflavin auxotrophic double mutant (Δ*ribB::Erm*^{r} Δ*ribU::Kan*^{r}) *B. subtilis* strain BsΔribUB, deficient in riboflavin synthesis (Δ*ribB*) and also deficient with respect to riboflavin uptake (Δ*ribU*) on the IPTG inducible plasmid pHT01_lmo1945.

The strain BsΔribUB (pHT01_lmo1945) was streaked next to the control strain BsΔribUB (pHT01), carrying the empty plasmid, on LA plates, containing 0.1 mM IPTG to induce expression. The agar plates were supplemented with increasing amounts of riboflavin and incubated over night at 37 °C. The photographs in figure 4.28 show that the expression of *lmo1945* restored the ability of BsΔribUB to grow on unsupplemented LA, which contains approximately

4 μM riboflavin (figure 4.28-A). The control strain was able to grow on LA supplemented with 100 μM riboflavin, since the flavin can enter the cells passively as a result of the high riboflavin concentration in the growth medium.

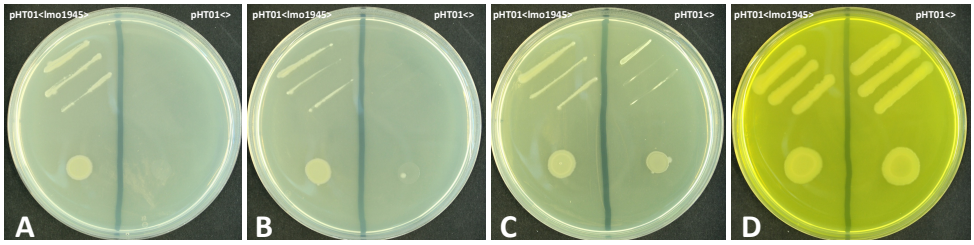

Figure 4.28: Lmo1945 is a functional riboflavin transporter - plate assay. Streaks (top) and 10 μl drop of an overnight culture OD_{600} = 2.0 (bottom) of BsΔribUB expressing *lmo1945* from pHT01_lmo1945 (left) and empty vector control (right) were applied to LA plates supplemented with additional amounts of riboflavin (A: no supplementation, B: 1 μM, C: 10 μM, D: 100 μM) and 0.1 mM IPTG to induce gene expression.

A growth experiment on agar plates gives only a qualitative result whether or not a strain is able to grow on certain media but it does not yield information about parameters like growth rate, biomass concentration or overall performance of the culture. To gain a better understanding, the same BsΔribUB strains that were used in the experiment above, were grown in liquid cultures of Spizizen-Minimal-Medium (SMM). The medium was prepared without any riboflavin and was later supplemented with two defined concentrations of riboflavin (10 μM and 100 μM) and an equivalent volume of the solvent DMSO as a control. The recorded growth curves are depicted in figure 4.29.

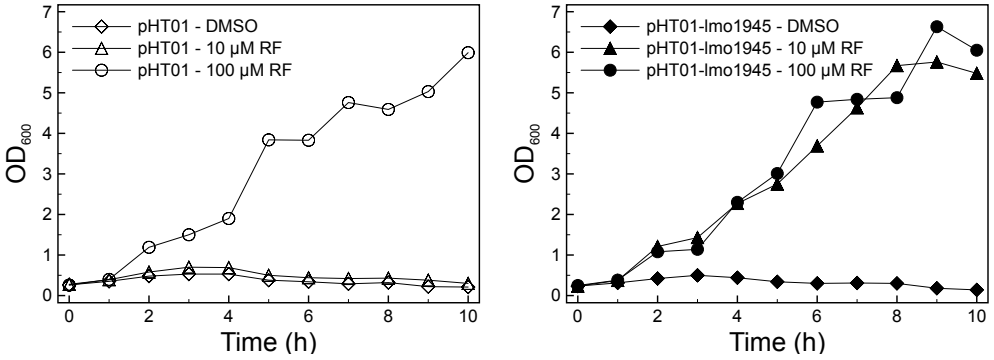

Figure 4.29: Lmo1945 is a functional riboflavin transporter - liquid culture growth assay. Growth curves of BsΔribUB expressing *lmo1945* of *L. monocytogenes* from pHT01_lmo1945 (right panel) and empty vector control (left panel). Cultures were grown in SMM supplemented with different amounts of riboflavin (♦: no supplementation, ▲: 10 μM, ●: 100 μM) and 0.1 mM IPTG.

In those cultures where no riboflavin was added to the medium, no growth was observed for both strains, since both are *ribB* deficient and thus are depending solely on riboflavin provided with the growth medium. In those cultures, grown with a riboflavin concentration of 10 μM, the control strain with the empty plasmid was still not able to grow, while the strain carrying the plasmid pHT01_lmo1945 could grow to a final $OD_{600} > 5.0$ within 8 h. If the medium was supplemented with riboflavin concentrations as high as 100 μM both strains were able grow with no significant difference in growth rate or final cell density.

To find out if Lmo1945 also functions as a transporter for the toxic riboflavin analog roseoflavin, a similar experiment was performed. Instead of the riboflavin auxotrophic strain BsΔribUB, the *B. subtilis* strain BsΔribU was employed and the cultures were treated with roseoflavin instead. This strain features an undisrupted *ribB* gene and, hence, is riboflavin heterotrophic and does not rely exclusively on riboflavin import to survive, while it still does not express the native *ribU* gene coding for the substrate binding domain RibU, responsible for riboflavin import in *B. subtilis*.

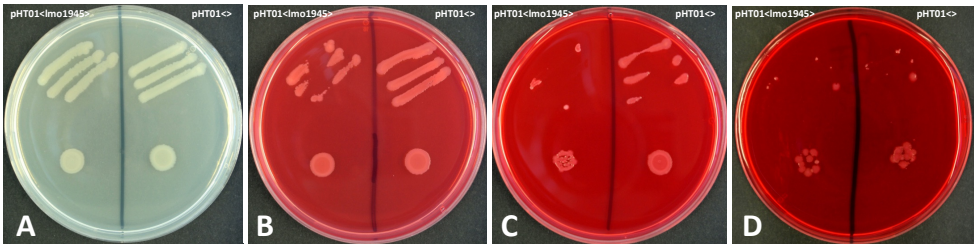

Figure 4.30: Lmo1945 is a functional roseoflavin transporter - plate assay. Streaks (top) and 10 μl drop of an overnight culture OD_{600} = 2.0 (bottom) of BSΔribU expressing *lmo1945* of *L. monocytogenes* from pHT01_lmo1945 (left) and empty vector control (right) were applied to LA plates supplemented with different amounts of roseoflavin (A: no supplementation, B: 50 μM, C: 100 μM, D: 250 μM) and 0.1 mM IPTG.

The strain BsΔribU (pHT01_lmo1945) was streaked side by side with the control strain BsΔribU (pHT01), carrying the empty plasmid, on LA plates supplemented with 0.1 mM IPTG to induce expression and various amounts of roseoflavin. The plates were incubated over night at 37 °C. The photographs in figure 4.30 show that the expression of *lmo1945* made BsΔribU more susceptible to the adverse effect of roseoflavin (figrue 4.30-B & 4.30-C). The difference in performance was not visible as clearly, since the empty plasmid control strain

also showed signs of diminished growth, if the media was supplemented with 100 μM roseoflavin (figure 4.30-C). On the other hand, both strains yielded resistant colonies, that were able to grow on LA with a roseoflavin concentration as high as 250 μM (figure 4.30-D).

To get a better understanding of the effect roseoflavin has on the growth rates of the two BsΔribU strains and in particular to show if the heterologous expression of *lmo1945* influences this effect, liquid cultures of BsΔribU (pHT01) and BsΔribU (pHT01_lmo1945) were grown in SMM supplemented with 50 μM and 100 μM roseoflavin. The recorded growth curves are depicted in figure 4.31.

The growth behavior of the empty plasmid control BsΔribU (pHT01) was not influenced by the addition of 50 μM roseoflavin to the medium when compared to the culture treated with DMSO only, while 100 μM roseoflavin clearly reduced the growth rate of the culture as well as the final cell density to which the culture grew within 10 h. The growth rate of the Lmo1945 producing strain BsΔribU (pHT01_lmo1945) was reduced already by 50 μM roseoflavin when compared to the DMSO treated culture and showed stagnation of growth for approximately 8 h if the growth medium was supplemented with 100 μM roseoflavin. Also, when compared to the empty vector control strain, BsΔribU (pHT01_lmo1945) exhibited slower growth and lower OD_{600} in the presence of roseoflavin.

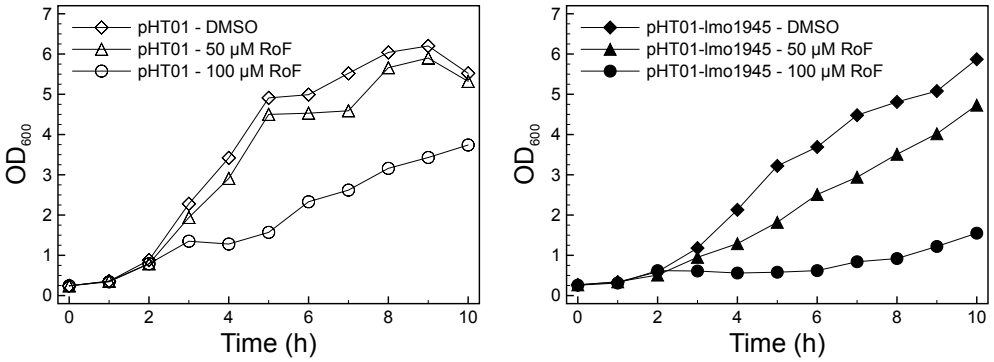

Figure 4.31: Lmo1945 is a functional roseoflavin transporter - liquid culture growth assay. Growth curves of BsΔribU expressing *lmo1945* of *L. monocytogenes* from pHT01_lmo1945 (right panel) and empty vector control (left panel) in SMM supplemented with different amounts of roseoflavin (♦: no supplementation, ▲: 50 μM, ●: 100 μM) and 0.1 mM IPTG.

4.7.2 Characterization of the FMN Riboswitch *Rli96*

To functionally characterize the FMN riboswitch *Rli96* from *L. monocytogenes*, it was evaluated with an *in vivo* β-galactosidase (LacZ) activity assay. The applied test system was already used by Ott et al. (2009) for the characterization of the FMN riboswitch of *B. subtilis* in the 5′–UTR of the *rib*-operon. The sequence of *Rli96* was placed upstream of the β-galactosidase gene *lacZ* from *E. coli* on the integrative plasmid pDG268. The strain Bs::Rli96 was created through integration of pDG268_Rli96 into the locus *amyE* of *B. subtilis* wild type. To prevent downregulation of the riboflavin transporter RibU in the host during the treatment, the *B. subtilis* gene *ribU* was expressed additionally from the IPTG inducible, non integrative plasmid pDG148_ribU. The Strain Bs::RFNbs featuring the FMN riboswitch from *B. subtilis* was used as a reference.

Both strains were grown with additional 50 μM and 100 μM riboflavin, as well as without supplementation as control. The expression of *ribU* from pDG148_ribU was induced in all cultures with 1 mM IPTG. LacZ activity assays were performed as described in section 3.11.3. The LacZ activities were normalized to the untreated control, to account for the different strengths of the promoters (figure 4.32).

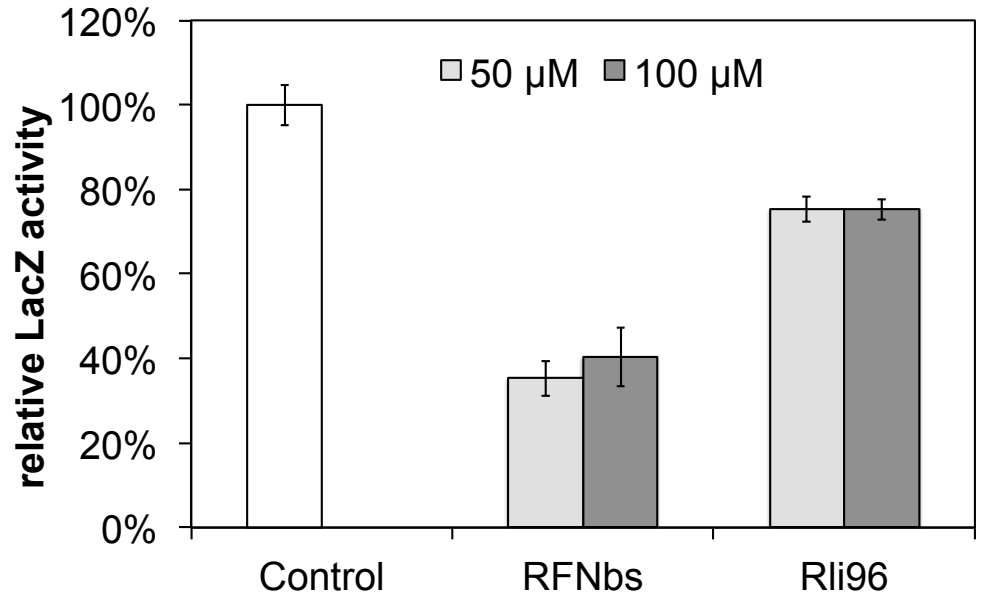

Figure 4.32: *Rli96* reduces reporter expression by 25% *in vivo*. Relative β-galactosidase (LacZ) activity of transcriptional riboswitch-*lacZ* fusions integrated into the *amyE*-locus of *B. subtilis* (pDG148_ribU). Cultures were treated with 50 μM and 100 μM riboflavin.

The relative LacZ activity of Bs::Rli96 (pDG148_ribU) cultures, treated with 50 μM and 100 μM riboflavin, was reduced to about 75% of the activity of the untreated control, while the reference strain Bs::RFNbs (pDG148_ribU) showed reduction to 35% and 40% of the untreated control, respectively.

To survey whether the flavin analogs roseoflavin and 8-amino riboflavin also effect the *lacZ* expression in Bs::Rli96 (pDG148_ribU) the above experiment was repeated with roseoflavin and 8-amino riboflavin treatments. The LacZ activity data collected in this experiment (figure 4.33) suggested that roseoflavin reduced LacZ activity in a similar manner as riboflavin, while cultures treated with 8-amino riboflavin, however, exhibited a slight increase of LacZ activity rather than the expected reduction.

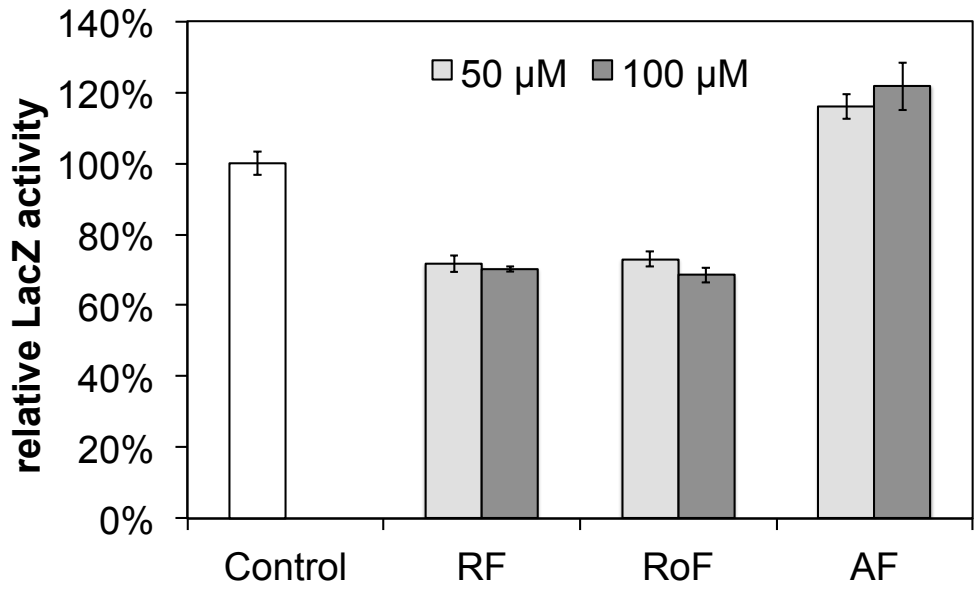

Figure 4.33: *Rli96* reduces reporter expression *in vivo* in the presence of riboflavin and roseoflavin. Relative LacZ activities of Bs::Rli96 (pDG148_ribU) after treatment with 50 μM and 100 μM of riboflavin (RF), roseoflavin (RoF) and 8-amino riboflavin (AF).

The unreduced LacZ activity in the cultures treated with 8-amino riboflavin could possibly be attributed to the lack of the FMN analog AFMN inside the cell, since there was no evidence whether RibU of *B. subtilis* did transport 8-amino riboflavin into the cell. Also, the further metabolization of 8-amino riboflavin to AFMN and possibly AFAD in *B. subtilis* remained unclear.
To address these drawbacks in the experimental design of an *in vivo* assay, *Rli96* was placed on the plasmid pT7luc_Rli96 between the P_{T7} promoter and

the reporter gene *luc* coding for firefly luciferase. The plasmid was used in a coupled *in vitro* transcription/translation assay. The effect of FMN, RoFMN and AFMN on the luciferase activity was assayed as described in section 3.11.5. The results shown in figure 4.34 support the hypothesis, of AFMN not hindering the expression of the gene downstream of *Rli96* and thus confirmed the results collected from the *in vivo* experiments.

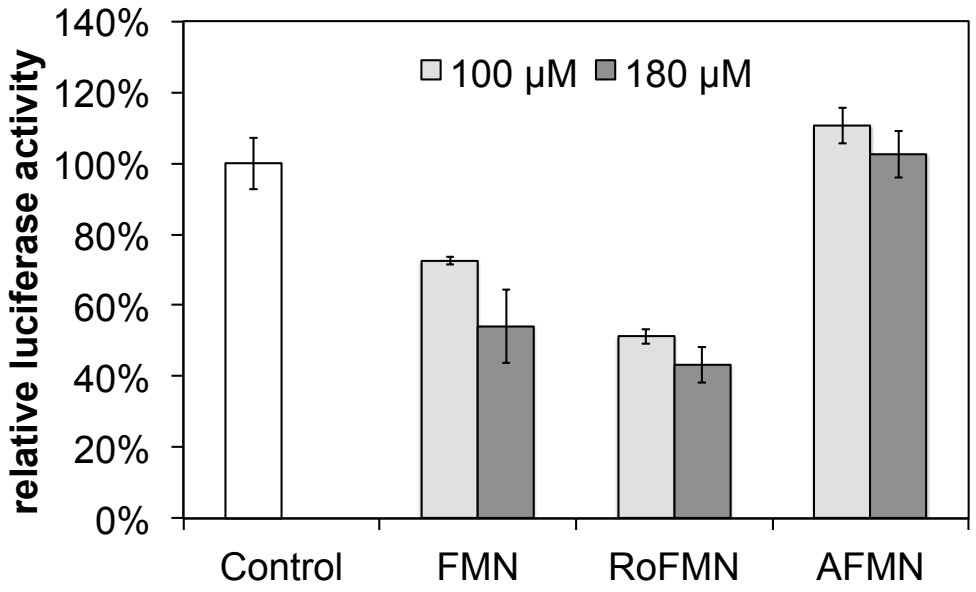

Figure 4.34: *Rli96* reduces reporter expression *in vitro* in the presence of FMN and RoFMN. Relative luciferase activities obtained in the presence of phosphorylated flavins FMN, RoFMN and AFMN in a coupled *in vitro* transcription/translation assays from the plasmid pT7luc_Rli96.

4.8 *In Vivo* Reporter System for the Characterization of Translational Riboswitches

FMN riboswitches are promising targets for antimicrobial compounds. In contrast to the transcriptional FMN riboswitch of *B. subtilis* that has been characterized *in vivo* earlier by Ott et al. (2009), the FMN riboswitches of many streptomycetes regulate gene expression of downstream genes by sequestration of the ribosomal binding site. In these translationally controlled riboswitches, the ribosomal binding site is part of the secondary structure and is obstructed in the "off"-state of the riboswitch (see figure 1.2 on page 8). *Streptomyces coelicolor* and *S. davawensis* were chosen as models, since they are closely related

while *S. davawensis* is resistant to the antibiotic roseoflavin but *S. coelicolor* is sensitive to the compound. The FMN riboswitches of these two species have been studied earlier *in vitro*, as described by Pedrolli et al. (2012). However, a functional characterization *in vivo* has, for the lack of a suitable reporter system, not been described.
The translational control of gene regulation required a highly specialized reporter system, where the open reading frame of the reporter gene is fused directly to a short leader (six codons) of the controlled gene downstream of the riboswitch. Furthermore the previously used reporter gene *lacZ*, coding for the enzyme β-galactosidase of *E. coli*, cannot be used as a reporter gene in *Streptomyces* spp. since these bacteria exhibit a high level of endogenous β-galactosidase activity (Ingram et al., 1989). For the *in vivo* characterization of the FMN riboswitches of *S. davawensis* and *S. coelicolor* the establishment of new reporter systems based on a translational fusion with the reporter genes *xylE*, coding for the catechol 2,3–dioxygenase from *Pseudomonas putida*, and *gusA*, coding for the β-glucuronidase from *E. coli*, were designed.

4.8.1 The XylE Reporter System is Not Suitable for the *In Vivo* Characterization of FMN Riboswitches

To compare the *rib*-promoters (P_{rib}) from *S. coelicolor* and *S. davawensis*, derivates of the *xylE* based promoter probe plasmid pIPP1, constructed by Jones (2011), were used to generate *S. coelicolor* strains with an integrated copy of *xylE* downstream of the respective P_{rib} promoter sequences. A schematic representation of the integrative promoter probe plasmid is given in figure 4.35.

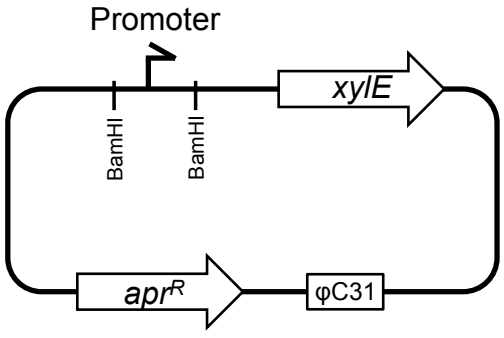

Figure 4.35: Integrative promoter probe plasmids. Schematic representation of the pIPP1 derived promoter probe plasmids. Putative promoter sequence cloned into unique *BamHI* restriction site upstream of the reporter gene *xylE*. Apramycine resistance gene apr^R and ϕC31 integration site.

Cell free extracts from liquid cultures of the test strains Sc::PribSd and Sc::PribSc showed XylE activity. The control strains Sc::PribSdAS and Sc::PribScAS with the same P_{rib} sequences inserted in anti sense (AS) orientation, however, did not exhibit specific XylE activities different to the background activity of the control strain Sc:pIPP1, with integrated empty plasmid pIPP1. Crude extract of *S. coelicolor* wild type did not show any XylE activity when tested in the same assay. The specific XylE activities are displayed in figure 4.36.

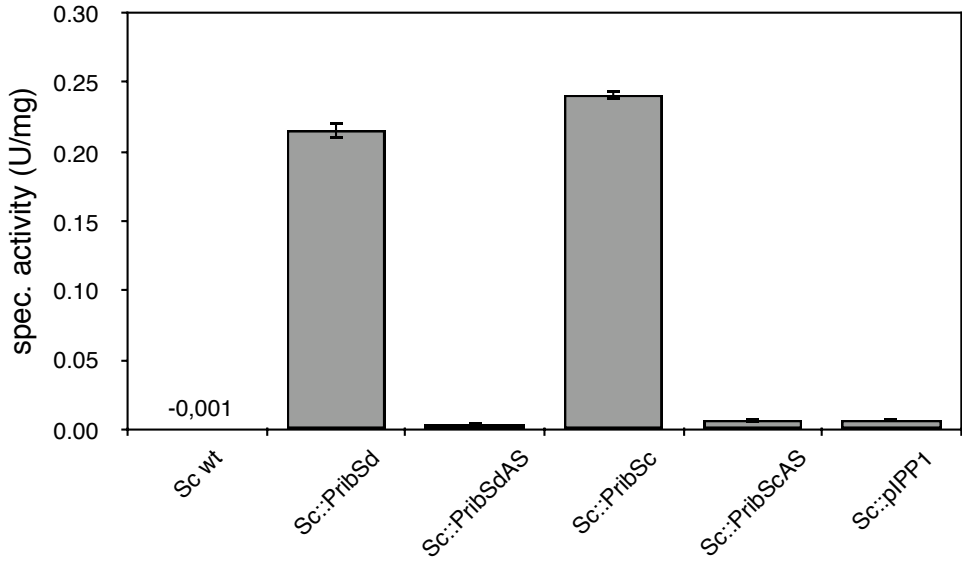

Figure 4.36: P_{rib} is an active promoter in *S. coelicolor*. Specific catechol 2,3–dioxygenase (XylE) activity measured for the cell free extract of *S. coelicolor* (Sc) wt and strains with integrated pIPP1 derivates. Strains with putative P_{rib} promoter sequences cloned in the correct orientation upstream of *xylE* show catechol 2,3–dioxygenase activity while anti-sense (AS) controls exhibit only background levels of activity.

To provide an *in vivo* reporter system that allows the characterization of riboswitches with translational attenuation, the original ribosomal binding site (RBS) has to remain unchanged and cannot be spaced out differently relative to the riboswitch sequence, since it is part of the sequester loop (see figure 1.6 on page 14). The strain Sc::SdxE features the reporter gene *xylE* in frame connected to the leading six codons of *ribB* forming a translational fusion of the promoter and riboswitch sequence from *S. davawensis* including the RBS and the reporter gene *xylE*.

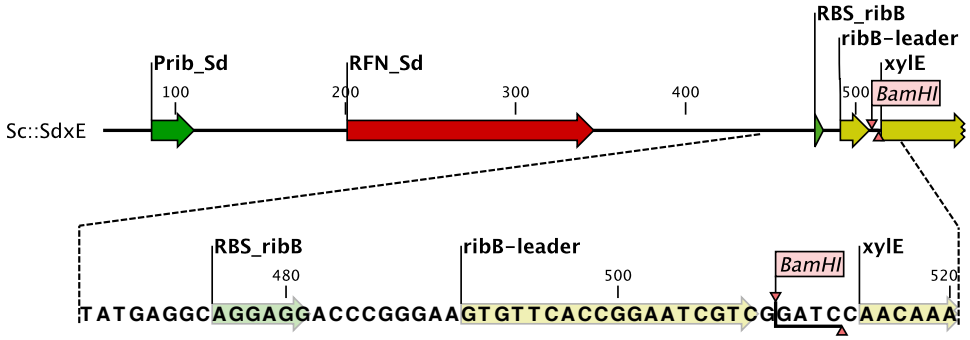

Figure 4.37: Translational fusion of the *ribB*-leader and *xylE*. Schematic representation of the translational fusion of the P_{rib} promoter, the FMN riboswitch and the *ribB*-leader with the reporter gene *xylE* in the strain Sc::SdxE (top). Sequence detail of the translational fusion (bottom).

As the specific XylE activity in cell free extracts of Sc:SdxE was only at about 10% of the activity level of the pIPP1 derived promoter test strain Sc::PribSd (see figure 4.38), the gene *xylT* was introduced into Sc::SdxE with the non integrative plasmid pAMxT. The gene *xylT* is coding for the soluble ferredoxin XylT which is reactivating inactive XylE by reducing an oxidized iron atom at the active center of XylE (Gonzalez-Ceron et al., 2001). The data obtained from activity measurements of cell free extracts from Sc::SdxE (pAMxT), constitutively expressing *xylT*, did not show the expected increase in XylE activity but rather a further decrease to one third of the specific activity observed for Sc::SdxE. This reduced level of XylE activity is not different to the background activities measured for the promoterless XylE construct Sc::pIPP1 (figure 4.36).

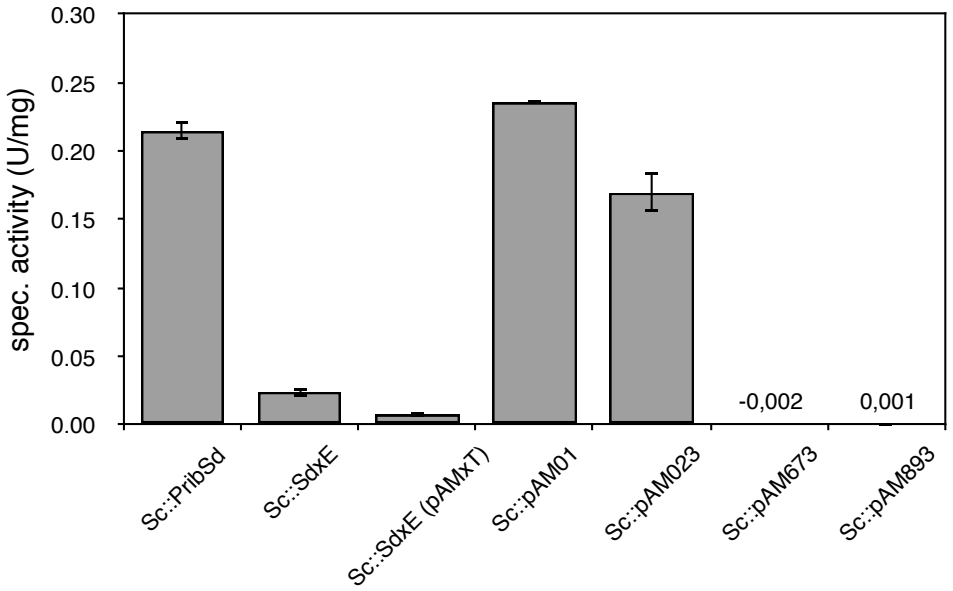

Figure 4.38: Coexpression of *xylT* does not restore activity of translational *xylE*-fusions. Specific catechol 2,3–dioxygenase (XylE) activity measured for the cell free extracts of *S. coelicolor* strains with integrated plasmids featuring different fusions of promoter and FMN riboswitch elements from *S. davawensis* controlling the expression of the reporter gene *xylE*.

The coding sequences of *xylT* and *xylE* on the original sequence derived from *Pseudomonas putida* overlap and they are transcribed in a shared message, driven by a single promoter. To ensure that the separation of *xylT* and *xylE* into two independent transcription units, where *xylT* is constitutively expressed from a non-integrative plasmid, and the riboswitch controlled expression of *xylE* occrus from a single integrated copy, is not the reason for the observed decrease in activity, the two genes were regrouped into a single transcription unit.

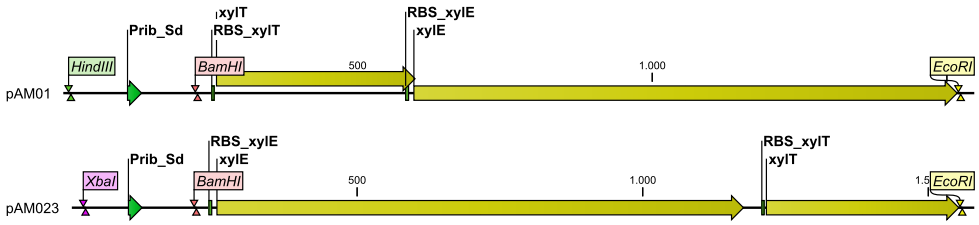

Figure 4.39: The pSET152 derived plasmids pAM01 and pAM023. The plasmids pAM01 and pAM023 were used to verify the rearrangement of the coding sequences does not impair XylE activity (see section 2.4.1).

Sc::pAM01 featuring the P_{rib} promoter upstream of the original overlapping *xylT-xylE* constellation, similar to Sc::PribSd, was used as a reference with a specific XylE activity comparable to the activity obtained from Sc:PribSd. To allow the translational fusion of *xylE* to the riboswitch sequence it was necessary to interchange the order of the two genes in the transcription unit and place *xylT* downstream of *xylE*. The XylE activity, measured from crude extracts of the strain Sc::pAM023, featuring *xylE* and *xylT* separately and in reversed order in one transcription unit downstream of the P_{rib} promoter, proved that the permutation of the two genes lead to specific XylE activities in the range of 75% compared to the reference strain Sc::pAM0 (figure 4.38).

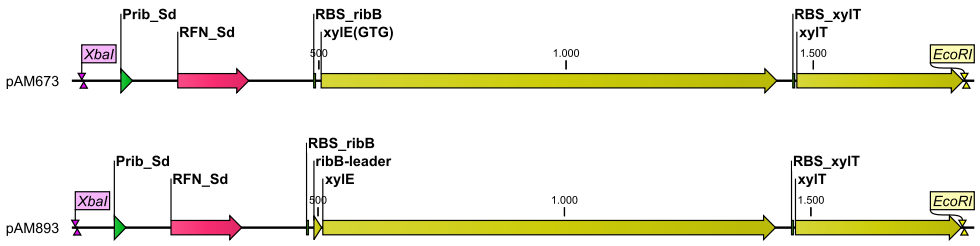

Figure 4.40: The pSET152 derived plasmids pAM673 and pAM893. The plasmids pAM673 and pAM893 were used to test translational fusions of the *S. davawensis ribB* FMN riboswitch and *xylE* (see section 2.4.1).

The two strains Sc::pAM673 and Sc::pAM893 with translational fusions of xylE to the riboswitch element directly after the RBS and to the *ribB*-leader sequence respectively, however, did not exhibit any XylE activity in their cell free extracts (figure 4.38).

A qualitative XylE plate assay revealed that the expression of functional XylE in *S. coelicolor* was restored by translational uncoupling of *xylE* from the RFN-RBS_{ribB} domain in Sc::pAM893.

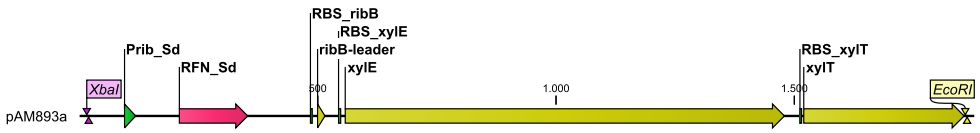

Figure 4.41: The pSET152 derived plasmid pAM893a. The plasmid pAM893a features the *S. davawensis ribB* FMN riboswitch, similar to pAM893, but translationally uncoupled from *xylE* (see section 2.4.1).

Spores of Sc::pAM01 (positive control), *S. coelicolor* wt (negative control), Sc::pAM893 (translational fusion of P_{rib} promoter, riboswitch, RBS_{ribB} and *ribB*-leader from *S. davawensis* with *xylE*) and Sc::pAM893a (translationally uncoupled *xylE* by insertion of RBS_{xylE} between *ribB*-leader and *xylE*) were streaked on a MS agar plate and incubated at 30 °C for 72 h. The plate was flooded with 1 ml freshly prepared 0.5 M pyrocatechol solution and incubated at room temperature for approx. 5 min. In contrast to *S. coelicolor* wt and Sc::pAM893, the positive control Sc::pAM01 and Sc::pAM893a exhibit a clearly visible, bright yellow halo around the edge of the colonies (see figure 4.42).

Figure 4.42: Translational uncoupling of *xylE* restores reporter activity. Qualitative XylE plate assay of Sc::pAM01 (top left), *S. coelicolor* wild type (top right), Sc::pAM893a (bottom left) and Sc::pAM893 (bottom right).

The restoration of XylE activity after uncoupling of *xylE* from the *ribB*-leader and its RBS through the introduction of RBS_{xylE} suggested that expression of functional XylE in Sc::pAM893 was hindered by the N-terminal fusion of of XylE to the RibB-leader and its upstream RBS. Since these sequences are part of the secondary structure that forms the sequester loop of the riboswitch, they could not be replaced or omitted without corrupting the test system.

4.8.2 The GusA Reporter System

Due to the fact that the XylE based test system described above was not suitable to characterize the *in vivo* behavior of FMN riboswitches under investigation, a GusA based reporter system, based on the work of Myronovskyi et al. (2011), was approached.

A transcriptional fusion placing the codon optimized reporter gene *gusA* under the control of the promoter P_{rib} (pAMgus01) and a translational fusion of *gusA* with the riboswitch domain of *S. davawensis* including the *ribB*-leader sequence (pAMgus04), similar to pAM893 were constructed and integrated into the chromosome of *S. coelicolor*.

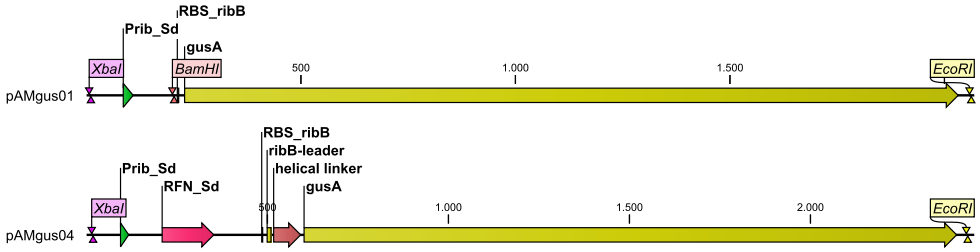

Figure 4.43: The pSET152 derived plasmids pAMgus01 and pAMgus04. Plasmids for transcriptional (pAMgus01) and translational (pAMgus04) fusions with *gusA*.

GusA activity was assayed as described in section 3.11.2. The strain Sc::pSETgus where *gusA* expression is controlled by the thiostrepton inducible promoter P_{tipA} was used as a positive control and reference of GusA activity. The results of the GusA activity assays are displayed in figure 4.44.

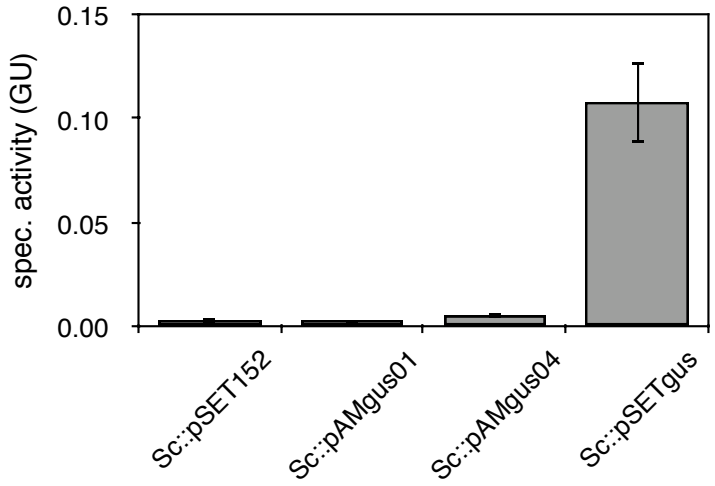

Figure 4.44: P_{rib} and P_{rib}-RFN fusions with *gusA* show no reporter activity. Specific GusA activity measured for the cell free extracts of *S. coelicolor* strains with integrated plasmids featuring a transcriptional fusion of the P_{rib} promoter (pAMgus01) and the *ribB* FMN riboswitch (pAMgus04) from *S. davawensis* controlling the expression of the reporter gene *gusA*.

While the positive control Sc::pSETgus reached GusA activity levels of approximately 0.1 GU, the strains carrying the transcriptional fusion of P_{rib} and *gusA* (Sc::pAMgus01) as well as the strain featuring the translational fusion of P_{rib}, FMN riboswitch, RBS and *ribB*-leader with *gusA* (Sc::pAMgus04) did not exhibit GusA activities significantly different from the negative control Sc::pSET152.

5 Discussion

The potential of flavin analogs as antimicrobial compounds, affecting the growth of bacteria which take up flavins from their environment, has been evaluated for several years (Mack and Grill, 2006). In particular, the antibiotic roseoflavin was reported to impair the growth of the human pathogen *L. monocytogenes* (Mansjö and Johansson, 2011). Since the metabolism of *L. monocytogenes* does not include a pathway for the biosynthesis of riboflavin, it relies entirely on the uptake of riboflavin from its environment. The lack of a riboflavin biosynthesis pathway in *L. monocytogenes* leaves a reduced number of enzymes involved in flavin metabolism, comprising only the functions of riboflavin uptake and cofactor synthesis. Thus *L. monocytogenes*is an ideal system to study the uptake and metabolism of flavin analogs. FMN riboswitches have been identified as target molecules for roseoflavin and other flavin analogs (Blount and Breaker, 2006; Lee et al., 2009; Ott et al., 2009; Howe et al., 2015).

5.1 Flavin Analogs Affect the Growth of *L. monocytogenes*

As previously reported by Mansjö and Johansson (2011), roseoflavin and 8-amino riboflavin inhibit the growth of *L. monocytogenes*. Growth experiments of *L. monocytogenes* in BHI liquid cultures supplemented with riboflavin and roseoflavin, respectively, confirmed this adverse effect of roseoflavin on the growth of *L. monocytogenes*. The deregulated mutant strain M1, featuring a mutation in the FMN riboswitch *Rli96*, was tolerant to roseoflavin in the medium to some extend. The growth inhibiting effect of roseoflavin on the deregulated mutant strain M1, was not as strong as on the *L. monocytogenes*

wild type. The fact that the mutant strain M1 still shows reduced growth, when compared to untreated controls or cultures treated with riboflavin, signifies that the FMN riboswitch *Rli96* is not the only target in *L. monocytogenes* that is affected by roseoflavin or one of its metabolites.
When *L. monocytogenes* wild type was grown in the presence of the riboflavin analog 8-amino riboflavin, a key intermediate of the roseoflavin biosynthesis, growth was reduced only slightly, while the mutant strain M1 did not show any signs of impaired growth. However, a stronger effect of 8-amino riboflavin on the growth of *L. monocytogenes* was reported by Jörgen Johansson (Laboratory for Molecular Infection Medicine Sweden, Department of Molecular Biology, Umeå University, Umeå, Sweden) in a personal communication, for 8-amino riboflavin concentrations as high as 267 μM. While these results could either be explained by reduced 8-amino riboflavin uptake into the cell, or 8-amino riboflavin not being metabolized to the riboswitch targeting cofactor analog AFMN inside the cell. Another possible explanation of the less pronounced effect of 8-amino riboflavin was that AFMN does not interact with the FMN riboswitch *Rli96*, which was confirmed to be the case through *in vivo* and *in vitro* assays throughout this work.

The analysis of the cell free extracts of *L. monocytogenes* wild type and M1 cultures, treated with riboflavin and the flavin analogs roseoflavin and 8-amino riboflavin revealed, that the two flavin analogs were present inside the cells and that they were converted to their respective cofactor analogs. The presence of 8-amino riboflavin inside the cells, as well as the cofactor analogs AFMN and AFAD, in similar concentrations as RoFMN and RoFAD, excluded possible explanations for the less distinct effect of 8-amino riboflavin on the growth of *L. monocytogenes*.

Higher concentrations of flavins and cofactors were found in cell free extracts of the mutant strain M1. This difference was attributed to the deregulated expression of *lmo1945* in the mutant strain. In cells, treated with the flavin analogs roseoflavin or 8-amino riboflavin, the concentrations of riboflavin derived cofactors was found to be reduced drastically when compared to the untreated controls. This observation, however, could not be attributed to a restrained riboflavin uptake due to insufficient amounts of the riboflavin transport protein Lmo1945, since the effect was observed in the wild type and the mutant strain M1 in a similar manner. A more likely explanation for this effect would be the competition of the substrates (i.e. riboflavin and the respective

flavin analog) for the cofactor producing flavokinase/FAD synthetase enzymes inside the cell. This hypothesis was further supported by the finding that a combined treatment of *L. monocytogenes* wild type and M1 cultures with both, riboflavin and roseoflavin, reduced the concentrations of roseoflavin derived cofactors found in the cell free extract, while it restored the concentrations of riboflavin derived cofactors to a level, that was not different from that in untreated cells. Since this effect was observed in a similar manner in wild type and M1 cells (see figure 4.3 D-F on page 71), it could not be attributed to the deregulation of *lmo1945*.

5.2 Metabolization of Flavins and Flavin Analogs

5.2.1 Identification of Two Enzymes with Flavokinase/FAD synthetase Activity in *L. monocytogenes*

Two genes, coding for enzymes with putative flavokinase/FAD synthetase activity, have been identified in *L. monocytogenes* through comparison of translated nucleotide sequences with the bifunctional flavokinase/FAD synthetase RibC from *B. subtilis*, a close relative of *L. monocytogenes*.

An alignment of the amino acid sequences of the two hypothetical proteins Lmo0728 and Lmo1329 (Lmo_RibC) with known bifunctional enzymes with flavokinase/FAD synthetase activity from other bacterial species (*Cornyebacterium ammoniagenes*, *E. coli*, *B. subtilis*, *S. coelicolor* and *S. davawensis*) was performed (figure 5.1). The alignment revealed that both amino acid sequences of the two hypothetical proteins feature all motifs that were reported by Serrano et al. (2012) to be involved in FAD synthetase activity (red boxes in figure 5.1), while only Lmo0728 lacks three out of five motifs (blue boxes in figure 5.1) that were reported by Serrano et al. (2013) to be responsible for the flavokinase activity of bifunctional enzymes. Especially the absence of the highly conserved "GxP-TAN" motif (amino acids 213 - 219 of the alignment) has been attributed to the lack of flavokinase activity in monofunctional FAD synthetases in plants, and is also present in flavokinase enzymes found in fungi and humans (Sandoval et al., 2008; Yruela et al., 2010; Herguedas et al., 2015).

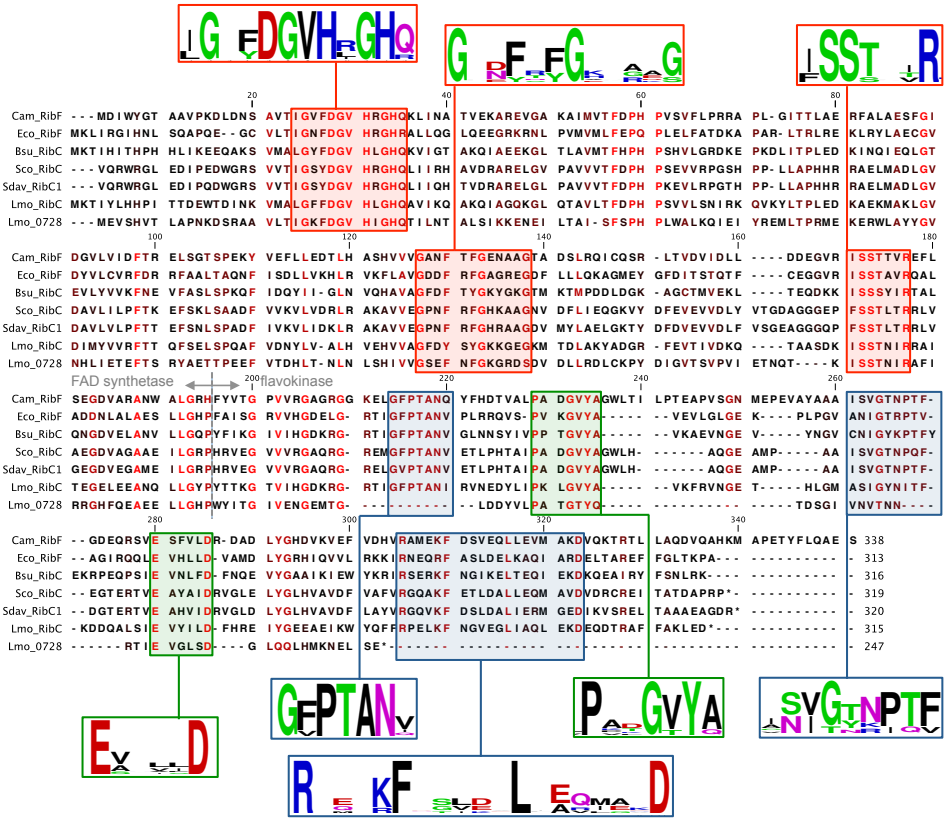

Figure 5.1: Multiple sequence alignment of representative primary structures of bacterial flavokinases/FAD synthetases (FK/FADS). Conserved residues are highlighted in red. UniProtKB accession numbers for proteins are as follows: Cam_RibF, bifunctional FK/FADS from *Cornyebacterium ammoniagenes*, Q59263; Eco_RibF, bifunctional FK/FADS from *E. coli*, P0AG40; Bsu_RibC, bifunctional FK/FADS from *B. subtilis*, P54575; Sco_RibC, bifunctional FK/FADS from *S. coelicolor*, Q9Z530; Sdav_RibC1, bifunctional FK/FADS from *S. davawensis*, K4R340; Lmo_RibC, bifunctional FK/FADS from *L. monocytogenes*, Q8Y7F2; Lmo_0728, monofunctional FAD synthetase from *L. monocytogenes*, Q8Y914. The amino acid motifs enclosed by blue and green boxes were reported to be relevant for the flavokinase function, whereas amino acid motifs in red boxes were reported to be relevant for the FAD synthetase function (Serrano et al., 2012, 2013; Frago et al., 2008).

The presence of two motifs associated with flavokinase activity (green boxes) in Lmo0728, however, indicates an evolutionary origin of the enzyme from a former bifunctional enzyme. Interestingly a phylogenetic representation (figure 5.2) of the N-terminal portion (amino acids 1 - 195) of the alignment suggests that Lmo0728 is more closely related to the bifunctional flavokinase/FAD synthetase RibF from *E. coli* than to Lmo1329. This leads to the assumption that the presence of two genes coding for an enzyme with FAD synthetase activity in the genome of *L. monocytogenes* is a result of horizontal gene transfer in the

gastrointestinal tract, rather than duplication and subsequent truncation of *lmo1329*.

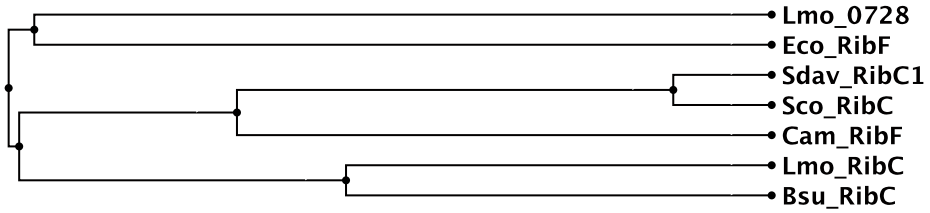

Figure 5.2: FAD synthetase domains of Lmo0728 and RibF from *E. coli* share a branch in the phylogenetic tree. Phylogenetic representation of the N-terminal portion (amino acids 1 - 195) of the multiple sequence alignment (see figure 5.1). The tree was created using the *Unweighted Pair Group Method using Arithmetic averages* (UPGMA) described by Sneath and Sokal (1973).

5.2.2 Production and Purification of Two Flavokinase/FAD synthetase Enzymes from *L. monocytogenes*

For the functional and kinetic characterization of the two enzymes Lmo0728 and Lmo1329, recombinant production and subsequent purification was necessary. An active, C-terminally His-tagged, version of Lmo1329 (Lmo1329-His) was recombinantly produced in *E. coli* BL21(DE3) and could be purified to apparent homogeneity in an affinity purification process, using a standard nickel-sepharose column.

The same approach of directly adding a His-tag, C- or N-terminal, to Lmo0728, resulted in the accumulation of insoluble recombinant protein in the production cells. Expression of soluble C-terminally His-tagged Lmo0728 (Lmo0728-His) was achieved by reducing the speed of protein production employing the specialized production strain *E. coli* Rosetta(DE3). An enriched fraction of Lmo0728-His, however, did not exhibit any activity when tested in a flavokinase/FAD synthetase activity assay.
The N-terminal fusion of the maltose binding protein MalE from *E. coli* (MBP) to Lmo0728 (MBP-Lmo0728) yielded a fusion protein that was soluble and could be enriched from the cell free extract with an amylose column in an FPLC system. The MBP-Lmo0728 fusion protein was found to be an active FAD synthetase when tested in a flavokinase/FAD synthetase activity assay. The proteolytic removal of the MBP-tag and subsequent purification of untagged Lmo0728 was challenging and required several iterations in the design of

the fusion protein as well as in the purification strategy, until a homogenous preparation of active, untagged Lmo0728 was obtained. This was possible by the cleavage of the fusion protein His-MBP-pg-Lmo0728 with a C-terminally His-tagged TEV protease (TEV-His) so that the cleaved off His-MBP part of the fusion protein and the TEV-His protease could be removed after a digest reaction by a single affinity chromatography step.

5.2.3 Functional and Kinetic Characterization of Two Flavokinase/FAD synthetase Enzymes from *L. monocytogenes*

To assay their flavokinase activity (EC 2.7.1.26) the two recombinantly produced proteins Lmo1329-His and Lmo0728 were tested with different flavin substrates, such as riboflavin, roseoflavin and 8-amino riboflavin in a flavokinase/FAD synthetase activity assay. The FAD synthetase activity (EC 2.7.7.2) of the two enzymes was tested with phosphorylated flavin substrates, such as FMN, RoFMN and AFMN.
HPLC analysis of the collected samples revealed, that Lmo1329 indeed is a bifunctional flavokinase/FAD synthetase, producing the cofactors FMN and FAD from riboflavin. A similar behavior was found when 8-amino riboflavin was used as substrate, the formation of AFMN and subsequently AFAD could be observed. Notably, the reaction of roseoflavin with Lmo1329 led to an accumulation of RoFMN whereas no RoFAD could be detected. These results were confirmed when the phosphorylated cofactor FMN and its analogs AFMN and RoFMN were used as substrates for Lmo1329 in the assay. No RoFAD was produced by Lmo1329 from roseoflavin or RoFMN respectively, under the tested conditions, which is different to what was reported for all other bifunctional flavokinases/FAD synthetases tested with this substrates so far (Grill et al., 2008; Pedrolli et al., 2011; Langer et al., 2013a).

When the flavokinase/FAD synthetase assays were performed with Lmo0728 instead of Lmo1329, the flavin substrates riboflavin, 8-amino riboflavin and roseoflavin remained unchanged in the reaction mixture. The phosphorylated forms FMN, AFMN and also also RoFMN were metabolized by Lmo0728 to the respective adenylated forms FAD, AFAD and RoFAD. The predicted lack of flavokinase activity of Lmo0728 was confirmed, while it was found to act as a monofunctional FAD synthetase that also accepts the FMN analogs AFMN and RoFMN as alternative substrates.

Prior to the kinetic characterization of the two enzymes, their optimal pH for the FAD synthetase reaction was determined experimentally. The pH optimum for both enzymes was found to be pH 8.5 for Lmo1329-His and pH 9.0 for Lmo0728. While Lmo1329-His was found to exhibit approximately 90% of its maximal FAD synthetase activity at pH 7.0, the FAD synthetase activity of Lmo0728 was reduced to only 50% of the maximum at pH 7.0. Hence, the activity assays for the kinetic characterization of the two enzymes were performed at the respective pH of maximal activity.

The kinetic model of first-order kinetics by Michaelis and Menten (1913) was fitted to the data obtained for the flavokinase and FAD synthetase reactions of Lmo1329-His and FAD synthetase reaction of Lmo0728, respectively. The Michaelis constant K_m and the maximal reaction rate v_max were derived directly from the fitted Michaelis-Menten equation, while the turnover number k_cat and the kinetic efficiency $\frac{k_\mathrm{cat}}{K_\mathrm{m}}$ were calculated according to equation 3.3 on page 66. The apparent kinetic parameters obtained for the tested enzyme-substrate pairs are summarized in tables 5.1 and 5.2, together with values published for other flavokinase/FAD synthetase enzymes for comparison.

Table 5.1: Apparent kinetic parameters for the FAD synthetase activity of Lmo0728 and Lmo1329 compared to values published for other enzymes.

Enzyme	Substrate	K_m (μM)	v_max ($\frac{\mathrm{nmol}}{\mathrm{min \cdot mg}}$)	k_cat (s^{-1})	$\frac{k_\mathrm{cat}}{K_\mathrm{m}}$ ($s^{-1} \cdot \mu M^{-1}$)	Reference
L. monocytogenes						
Lmo0728	FMN	12.9	1093	0.51	0.040	This work
Lmo1329	FMN	29.2	3706	4.39	0.150	This work
E. coli						
RibCF	FMN	3.6	110	0.06	0.017	Langer et al. (2013a)
C. ammoniagenes						
*Ca*FADS	FMN	1.2	–[a]	0.28	0.238	Serrano et al. (2013)
Homo sapiens						
hFADS2	FMN	68	88	0.08	0.0012	Pedrolli et al. (2011)

[a] not available

In direct comparison of the apparent K_{m} values for FMN, the value determined for Lmo0728 is lower when compared to Lmo1329-His, indicating a higher affinity of Lmo0728 to the substrate and the ability of Lmo0728 to produce FAD at lower FMN concentrations. Both K_{m} values lie within the range reported for other FAD synthetase enzymes. The maximal reaction rate v_{max} of the FAD synthetase reaction, however, is considerably higher for Lmo1329-His than for Lmo0728. This leads to the assumption that Lmo1329 is the dominant enzyme for FAD production in *L. monocytogenes*. This is also supported by the report of Wurtzel et al. who found Lmo1329 being expressed at a level more than 5-fold higher than Lmo0728 (Wurtzel et al., 2012). Notably, the turnover number k_{cat} for the FAD synthetase reaction of Lmo1329-His was determined to be 4.39 s^{-1}, which is about 15-fold higher than the turnover number reported by Serrano et al. for the bifunctional enzyme *Ca*FADS from *C. ammoniagenes*, the highest reported turnover number so far (Chang et al., 2009).

Table 5.2: Apparent kinetic parameters for the flavokinase activity of Lmo1329 compared to values published for other enzymes.

Enzyme	Substrate	K_{m} (μM)	v_{max} ($\frac{\mathrm{nmol}}{\mathrm{min \cdot mg}}$)	k_{cat} (s^{-1})	$\frac{k_{\mathrm{cat}}}{K_{\mathrm{m}}}$ ($s^{-1} \cdot \mu M^{-1}$)	Reference
L. monocytogenes						
Lmo1329	RF	6.9	668	0.40	0.057	This work
E. coli						
RibCF	RF	1.7	660	0.38	0.22	Langer et al. (2013a)
S. davawensis						
RibC	RF	40	500	0.3	0.0075	Grill et al. (2008)
B. subtilis						
RibC	RF	55	1200	0.7	0.013	Grill et al. (2008)
Homo sapiens						
Fmn1p	RF	36	1667	0.5	0.014	Pedrolli et al. (2011)

The kinetic parameters determined for the flavokinase activity of Lmo1329-His lie within the range of what was reported for other bacterial bifunctional flavokinase/FAD synthetase enzymes (table 5.2).

5.3 Transporter Mediated and Riboswitch Controlled Flavin Uptake in *L. monocytogenes*

Based on sequence analysis that identified an FMN riboswitch in the upstream region of Lmo1945, together with the high level of sequence similarity to the ECF riboflavin transport protein RibU from *B. subtilis*, Lmo1945 was considered being responsible for riboflavin import as well (Vitreschak et al., 2002; Mansjö and Johansson, 2011). The crystal structure of Lmo1945 was resolved recently by Karpowich et al. giving insight into the mechanism of ECF transporters. They also demonstrated binding of riboflavin to purified recombinantly produced Lmo1945 (Karpowich et al., 2015). Its physiological function as a riboflavin import protein, however, has not been demonstrated *in vivo* so far.

Proof of Lmo1945's functional role in riboflavin import could now be provided through this work. The recombinant expression of *lmo1945* in a riboflavin auxotrophic double mutant strain of *B. subtilis*, also lacking the gene coding for the substrate binding subunit RibU of the ECF riboflavin transporter, restored the ability of that strain to grow on LA without riboflavin addition, and in minimal medium with only 10 μM riboflavin supplementation. These results also suggest that the protein Lmo1945 is able to function as substrate binding subunit (EcfS) with the remaining, substrate independent, ECF transporter system of *B. subtilis*.

Since the FMN riboswitch *Rli96*, controlling expression of *lmo1945*, was suggested by Mansjö and Johansson (2011) as a target for the antibiotic flavin analog roseoflavin, it was of great interest to investigate whether Lmo1945 is also involved in the uptake of roseoflavin. The susceptibility to roseoflavin of the *ribU* deletion mutant *B. subtilis* strain, BSΔribU, was increased by heterologous expression of *lmo1945*, which indicated that Lmo1945 also facilitates roseoflavin uptake into the cell.

For the characterization of the FMN riboswitch *Rli96* an *in vivo* reporter system in *B. subtilis*, based on the work of Ott et al. (2009), was applied. The FMN riboswitch, together with its native promoter sequence was placed upstream of the reporter gene *lacZ* and integrated into the *amyE* locus into the chromosome of *B. subtilis*, forming the strain Bs::Rli96. Treatment of this modified strain with various concentrations of riboflavin, showed that *Rli96* reduced the reporter activity in the cell free extract only by 20%, which appears to be low when

compared to 60% reduction by the FMN *ribG* riboswitch of *B. subtilis*, which served as a reference.
The conclusion that the repression of the downstream gene of the FMN riboswitch *Rli96* in *L. monocytogenes* is regulated not as strictly as it is by other FMN riboswitches, agrees with its function of modulation of the expression of a transporter protein, providing the only source of riboflavin, an essential vitamin, to an auxotrophic organism. Indeed, tight regulation or even complete cessation of the expression of *lmo1945* could potentially cause a riboflavin deficiency for the cell. This assumption is further supported by the recent transcriptome analysis of *L. monocytogenes* that revealed that full-length transcripts of *lmo1945*, including *Rli96*, are present in all growth phases during growth of *L. monocytogenes* in BHI (Wurtzel et al., 2012).

When Bs::Rli96 was treated with the flavin analogs roseoflavin and 8-amino riboflavin, roseoflavin caused a reduction of reporter activity in a range similar to that caused by riboflavin. While, notably, treatment with 8-amino riboflavin even caused a slight increase of the reporter activity in the cell free extract.
Whether this effect was the result of the FMN analog AFM not affecting the FMN riboswitch *Rli96* or if it was the result of 8-amino riboflavin not being taken up into the cells by the riboflavin transporter RibU, was investigated with a coupled *in vitro* transcription/translation assay. In this assay the plasmid pT7luc_Rli96 was used as a template in the presence of various concentrations of FMN and its analogs RoFMN and AFMN. The results of the *in vitro* assay confirmed the previous finding of a slight increase of expression of the gene downstream of *Rli96* in the presence of AFMN. The reduction due to the presence of RoFMN was even more pronounced *in vitro*, when compared to FMN.
While the FMN riboswitch *Rli96* was confirmed as a target molecule for the roseoflavin derived FMN analog RoFMN, it was shown that *Rli96* was not affected by the 8-amino riboflavin derived cofactor analog AFMN. Therefore the antimicrobial effect of roseoflavin on *L. monocytogenes* can partially be attributed to RoFMN affecting the FMN riboswitch *Rli96*, while the adverse effect of 8-amino riboflavin very likely results from other targets, such as flavoenzymes, being affected by it or its metabolites.

5.4 Evaluation of Reporter Systems for the *In Vivo* Characterization of Translational Riboswitches in Streptomycetes

Expression of the riboflavin synthase RibB in *S. coelicolor* and *S. davawensis* is controlled by translationally acting FMN riboswitches. These two FMN riboswitches have been characterized *in vitro* using a coupled transcription/translation assay by Pedrolli et al. (2012). An *in vivo* characterization of these regulatory elements, however, was not performed since an appropriate reporter system was not available for streptomycetes. Establishment of such a system would provide a useful tool to study not only the regulatory mechanism underlying the roseoflavin resistance of *S. davawensis*, but also for the better comparison of translationally acting riboswitches from streptomycetes and other bacterial species with G+C rich genomes.

For the *in vivo* characterization of transcriptionally controlled FMN riboswitches the β-galactosidase based reporter system in *B. subtilis*, described by Ott et al. (2009) is available. The system was successfully applied for the *in vivo* characterization of the FMN riboswitch *Rli96* of *L. monocytogenes* throughout this work. The available system, however, was not suitable for the *in vivo* characterization of the translationally controlled FMN riboswitches of *S. coelicolor*, *S. davawensis* and other *Streptomyces* species. For the characterization of FMN riboswitches from streptomycetes, *B. subtilis* would not be an adequate host, due to the great difference in G+C content of the DNA. Especially the promoter sequences, found in streptomycetes are not recognized by the transcription machinery of *B. subtilis*. Also the available system only provides a test platform for transcriptionally controlled riboswitches that do not include the RBS of the regulated gene in their secondary structure (i.e. RBS sequestor). The adaption of the available β-galactosidase based reporter system to streptomycetes was not favorable, since the use of *lacZ* as a reporter gene in streptomycetes was reported to be impaired by their endogenous β-galactosidase activity, disqualifying it as a suitable reporter in *Streptomyces* species (King and Chater, 1986).

The catechol 2,3-dioxygenase XylE, encoded by the gene *xylE* from *Pseudomonas putida* was described as a suitable reporter enzyme in streptomycetes by Ingram et al. and was employed successfully in *S. coelicolor*, e.g. in promoter probe

plasmids created by Jones (Ingram et al., 1989; Jones, 2011). XylE was evaluated as a possible reporter in a reporter system suitable for the characterization of translationally regulating riboswitches in streptomycetes. For a translational fusion of the FMN riboswitch and the reporter gene *xylE*, rearrangement of the genetic elements on pIPP1 was necessary. The complete 5′–UTR, comprising the promoter region, the aptamer of the FMN riboswitch and the sequestor sequence, including the ribosomal binding site down to the actual start codon of the regulated gene had to be placed directly upstream of the reporter gene. Since the secondary structure of the RBS sequestor hairpin of the *ribB* FMN riboswitches of *S. coelicolor* and *S. davawensis* reaches up directly to the GTG start codon of *ribB* a short leader (18 nt) of the coding sequence of *ribB* was also included. This was necessary to prevent possible interference of the 5′ end of the *xylE* coding sequence with the stability of the RBS sequestor secondary structure.

5.4.1 The XylE Reporter System

The putative promoter regions upstream of the FMN riboswitch aptamer sequences from *S. davawensis* (P_{rib}Sd, 188 nt) and *S. coelicolor* (P_{rib}SC, 194 nt), were tested with the promoter probe plasmid pIPP1 with regard to their promoter activity in *S. coelicolor*. The assay of the specific XylE activity showed that both sequences contain promoters that are active in *S. coelicolor*. Due to the very high diversity in *Streptomyces* promoter sequences, which are recognized by various σ factors, there is no strong consensus in the -35 and -10 regions and the location of the transcription start simply by sequence analysis is not possible without additional experimental data (Strohl, 1992; Seghezzi et al., 2011; Luo et al., 2015).

For maximal activity, the enzyme XylE requires the soluble ferredoxin XylT, which reactivates inactive XylE by reduction of an oxidized iron atom at the active center of XylE (Gonzalez-Ceron et al., 2001). Since *xylT* is part of the transcription unit placed under the control of the putative promoter sequence on the plasmid pIPP1, both genes are transcribed if the promoter is active. For the use of *xylE* as reporter in a translational fusion, however, the coexpression of *xylT* requires attention, since the coding sequence of *xylT* lies upstream of *xylE* in the original configuration, derived from *P. putida*, and thus is not automatically included in a translational *xylE* fusion. The constitutive coexpression of *xylT* from a non integrative plasmid was approached, but did not result

in increased XylE activity from a strain carrying a translational fusion of the *ribB*-leader and *xylE* (Sc::SdxE (pAMxT)). Alternatively a coexpression of the two genes was attempted by changing their order in the transcription unit, placing *xylT* downstream of *xylE*. In this configuration a translational fusion of *xylE* was possible, while the two genes would still share the same transcription unit.
The strain Sc::pAM023, featuring the two genes in reversed order downstream of the P_{rib} promoter of *S. davawensis* yielded approximately 75% of specific XylE activity when compared to the strain Sc::pAM01, carrying the same promoter upstream the two coding sequences in their original configuration.

When the FMN riboswitch, including the ribosomal binding site RBS_{ribB} and the GTG start codon (Sc::pAM673) were introduced between the P_{rib} promoter and *xylE*, no XylE activity could be found in the cell free extract. The same effect was observed for the strain Sc::pAM893, including the six leading codons of *ribB* in the translational *xylE* fusion.
A reintroduction of the original ribosomal binding site RBS_{xylE} between the *ribB*-leader and *xylE* (Sc::pAM893a), translationally uncoupling *xylE* from the FMN riboswitch, led to a reconstitution of XylE activity in this strain, suggesting that the diminished XylE activity is a result of the translational fusion of *xylE* to the expression platform of the FMN riboswitch. Even small alternations of the N-terminus of XylE might prevent proper folding or could possibly interfere with the tetramerization of the enzyme, although N-terminally His-tagged XylE has been reported to be active after heterologous expression in *E. coli* (Winkler et al., 1995; Dong et al., 2009).

5.4.2 The GusA Reporter System

Since the ribosomal binding site RBS_{ribB} and the *ribB*-leader sequence are part of the expression platform of the FMN riboswitch they have to remain unaltered. To fulfill this requirement of the reporter system an alternative reporter was needed, that would tolerate N-terminal fusions. The gene *gusA*, coding for the β-glucuronidase enzyme GusA, which was used as a reporter in plants successfully over more than two decades, has been demonstrated by Myronovskyi et al. to be functional in N-terminal fusions. They constructed the plasmid pGUSHL4aadA containing *gusA* without a start codon and a short sequence coding for a helical linker intended to separate the N-terminally fused protein and GusA (Myronovskyi et al., 2011).

Based on the wok of Myronovskyi et al. a transcriptional fusion of the P_{rib} promoter, the ribosomal binding site RBS_{ribB} of *S. davawensis* and *gusA* (Sc::pAMgus01) and a translational fusion featuring the complete 5′–UTR, including the P_{rib} promoter, the FMN riboswitch, RBS_{ribB}, and the six codons of the *ribB*-leader of *S. davawensis* connected to *gusA* through the helical linker as it is present on the plasmid pGUSHL4aadA. Both constructs, however, did not yield GusA activity that was significantly higher than background levels found in a control strain.

With respect to the work of Rudolph et al., who successfully used a *gusA* based reporter system for the characterization of transcriptinally and translationally controlled artificial riboswitches in *S. coelicolor*, the further development of the reporter system throughout this work was suspended (Rudolph et al., 2013).

6 Conclusion

The riboflavin human pathogen *Listeria monocytogenes* relies exclusively on the uptake of riboflavin, since this bacterium is riboflavin auxotrophic. The production of the protein, facilitating the uptake of riboflavin from the environment is regulated by an FMN riboswitch. This FMN riboswitch represents a potential drug target, since a reduced expression of the riboflavin transporter gene *lmo1945* would consequently reduce the intracellular flavin level. Novel antibiotics based on flavin analogs have the potential to negatively interfere with FMN riboswitch function. The uptake and subsequent conversion of riboflavin analogs into cofactor analogs is supposedly a key part in the mechanism of how antimicrobial flavin analogs affect the metabolism of *L. monocytogenes*.

The riboflavin transporter Lmo1945 was confirmed to be responsible for the uptake, not only of riboflavin, but also of the toxic flavin analog roseoflavin. The FMN riboswitch *Rli96*, modulating expression of *lmo1945*, is negatively affected by FMN and RoFMN. However, it is not affected by the 8-amino riboflavin derived cofactor analog AFMN.
Two enzymes, involved in the conversion of riboflavin into the cofactors FMN and FAD in *L. monocytogenes* could be identified and were purified after heterologous expression in *E. coli*. The functional and kinetic characterization of these two enzymes showed that the bifunctional flavokinase/FAD synthetase Lmo1329 appears to be the dominant enzyme for FMN and FAD production in *L. monocytogenes*. Notably, it did not catalyze the synthesis of RoFAD. A second enzyme with FAD synthetase activity, Lmo0728 was identified in *L. monocytogenes*. This enzyme, however, was producing the cofactor analog RoFAD *in vitro* from RoFMN and ATP. Interestingly, Lmo0728 did not have any flavokinase activity and thus, is the first monofunctional FAD synthetase found in

bacteria to be functionally characterized.

The FMN riboswitch *Rli96* in *L. monocytogenes* was confirmed as a target for the roseoflavin derived cofactor analog RoFMN, which is synthesized by the bifunctional flavokinase/FAD synthetase Lmo1329. Growth experiments with a deregulated *L. monocytogenes* strain indicated that additional targets for cofactor analogs exist in this bacteria, since the deregulation of *Rli96* did not confer full roseoflavin resistance to *L. monocytogenes*.
Further insight into the metabolization of flavin analogs in *L. monocytogenes* could be gained through a more detailed characterization of the two flavokinase/FAD synthetases Lmo1329 and Lmo0728 with special attention to their activity in assays with riboflavin and flavin analogs as competing substrates. Also, the heterologous expression of flavoenzymes from *L. monocytogenes*, followed by activity assays in the presence of cofactor analogs could help to identify additional targets for flavin analogs in *L. monocytogenes*.

Bibliography

Abbas, C. A. and Sibirny, A. A. (2011). Genetic control of biosynthesis and transport of riboflavin and flavin nucleotides and construction of robust biotechnological producers. *Microbiol Mol Biol Rev*, 75(2):321–360.

Aliverti, A., Curti, B., and Vanoni, M. A. (1999). Identifying and quantitating FAD and FMN in simple and in iron-sulfur-containing flavoproteins. In *Flavoprotein protocols*, pages 9–23. Springer.

Antoniewski, C., Savelli, B., and Stragier, P. (1990). The spoIIJ gene, which regulates early developmental steps in Bacillus subtilis, belongs to a class of environmentally responsive genes. *Journal of Bacteriology*, 1(172):86–93.

Bacher, A., Eberhardt, S., Fischer, M., Kis, K., and Richter, G. (2000). Biosynthesis of vitamin b2 (riboflavin). *Annu Rev Nutr*, 20:153–167.

Barrick, J. E. and Breaker, R. R. (2007). The distributions, mechanisms, and structures of metabolite-binding riboswitches. *Genome Biol*, 8(11):R239.

Bennett, P. M., Grinsted, J., and Richmond, M. H. (1977). Transposition of TnA does not generate deletions. *Mol Gen Genet*, 154(2):205–211.

Bentley, S. D., Chater, K. F., Cerdeño-Tárraga, A.-M., Challis, G. L., Thomson, N. R., James, K. D., Harris, D. E., Quail, M. A., Kieser, H., Harper, D., Bateman, A., Brown, S., Chandra, G., Chen, C. W., Collins, M., Cronin, A., Fraser, A., Goble, A., Hidalgo, J., Hornsby, T., Howarth, S., Huang, C.-H.,

Kieser, T., Larke, L., Murphy, L., Oliver, K., O'Neil, S., Rabbinowitsch, E., Rajandream, M.-A., Rutherford, K., Rutter, S., Seeger, K., Saunders, D., Sharp, S., Squares, R., Squares, S., Taylor, K., Warren, T., Wietzorrek, A., Woodward, J., Barrell, B. G., Parkhill, J., and Hopwood, D. A. (2002). Complete genome sequence of the model actinomycete Streptomyces coelicolor A3(2). *Nature*, 417(6885):141–147.

Bierman, M., Logan, R., O'Brien, K., Seno, E. T., Nagaraja Rao, R., and Schoner, B. E. (1992). Plasmid cloning vectors for the conjugal transfer of DNA from Escherichia coli to Streptomyces spp. *Gene*, 116(1):43–49.

Blaesing, F., Mühlenweg, A., Vierling, S., Ziegelin, G., Pelzer, S., and Lanka, E. (2005). Introduction of DNA into Actinomycetes by bacterial conjugation from E. coli—An evaluation of various transfer systems. *Journal of Biotechnology*, 120(2):146–161.

Blount, K. F. and Breaker, R. R. (2006). Riboswitches as antibacterial drug targets. *Nature Biotechnology*, 24(12):1558–1564.

Bradford, M. M. (1976). A rapid and sensitive method for the quantitation of microgram quantities of protein utilizing the principle of protein-dye binding. *Analytical biochemistry*, 72(1):248–254.

Breaker, R. R. (2012). Riboswitches and the RNA world. *Cold Spring Harb Perspect Biol*, 4(2).

Brizio, C., Galluccio, M., Wait, R., Torchetti, E. M., Bafunno, V., Accardi, R., Gianazza, E., Indiveri, C., and Barile, M. (2006). Over-expression in Escherichia coli and characterization of two recombinant isoforms of human FAD synthetase. *Biochem Biophys Res Commun*, 344(3):1008–1016.

Burgess, C. M., Slotboom, D. J., Geertsma, E. R., Duurkens, R. H., Poolman, B., and van Sinderen, D. (2006). The riboflavin transporter RibU in Lactococcus lactis: molecular characterization of gene expression and the transport mechanism. *J Bacteriol*, 188(8):2752–2760.

Chang, A., Scheer, M., Grote, A., Schomburg, I., and Schomburg, D. (2009).

BRENDA, AMENDA and FRENDA the enzyme information system: new content and tools in 2009. *Nucleic Acids Res*, 37(Database issue):D588–D592.

Cohen, S. N., Chang, A. C., and Hsu, L. (1972). Nonchromosomal antibiotic resistance in bacteria: genetic transformation of Escherichia coli by R-factor DNA. *Proceedings of the National Academy of Sciences*, 69(8):2110–2114.

Coppins, R. L., Hall, K. B., and Groisman, E. A. (2007). The intricate world of riboswitches. *Curr Opin Microbiol*, 10(2):176–181.

Cutting, S. M., editor (1990). *Molecular Biological Methods for Bacillus*. John Wiley, Chichester.

Deka, R. K., Brautigam, C. A., Biddy, B. A., Liu, W. Z., and Norgard, M. V. (2013). Evidence for an ABC-type riboflavin transporter system in pathogenic spirochetes. *MBio*, 4(1):e00615–e00612.

Demerec, M. and Hartman, P. E. (1959). Complex loci in microorganisms. *Annual Reviews in Microbiology*, 13(1):377–406.

Dong, X., Xin, Y., Ye, L., and Ma, Y. (2009). Using Pseudomonas putida xylE gene to teach molecular cloning techniques for undergraduates. *Biochem Mol Biol Educ*, 37(6):339–343.

Efimov, I., Kuusk, V., Zhang, X., and McIntire, W. S. (1998). Proposed Steady-State Kinetic Mechanism for Corynebacterium ammoniagenes FAD Synthetase Produced by Escherichia coli. *Biochemistry*, 37(27):9716–9723.

Elvin, S. and Bingham, A. (1991). Electroporation-induced transformation of Escherichia coli: evaluation of a square waveform pulse. *Letters in applied microbiology*, 12(2):39–42.

Engler, C., Kandzia, R., Marillonnet, S., and El-Shemy, H. A. (2008). A One Pot, One Step, Precision Cloning Method with High Throughput Capability. *PLoS ONE*, 3(11):e3647.

Farber, J. M. and Peterkin, P. I. (1991). Listeria monocytogenes, a food-borne pathogen. *Microbiol Rev*, 55(3):476–511.

Fischer, M. and Bacher, A. (2005). Biosynthesis of flavocoenzymes. *Natural Product Reports*, 22(3):324.

Flärdh, K. and Buttner, M. J. (2009). Streptomyces morphogenetics: dissecting differentiation in a filamentous bacterium. *Nat Rev Microbiol*, 7(1):36–49.

Fraaije, M. W. and Mattevi, A. (2000). Flavoenzymes: diverse catalysts with recurrent features. *Trends Biochem Sci*, 25(3):126–132.

Frago, S., Martínez-Júlvez, M., Serrano, A., and Medina, M. (2008). Structural analysis of FAD synthetase from Corynebacterium ammoniagenes. *BMC Microbiology*, 8(1):160.

García Angulo, V. A., Bonomi, H. R., Posadas, D. M., Serer, M. I., Torres, A. G., Zorreguieta, Á., and Goldbaum, F. A. (2013). Identification and characterization of RibN, a novel family of riboflavin transporters from Rhizobium leguminosarum and other proteobacteria. *J Bacteriol*, 195(20):4611–4619.

Gelfand, M. S., Mironov, A. A., Jomantas, J., Kozlov, Y. I., and Perumov, D. A. (1999). A conserved RNA structure element involved in the regulation of bacterial riboflavin synthesis genes. *Trends Genet*, 15(11):439–442.

Gerdes, S. Y., Scholle, M. D., D'Souza, M., Bernal, A., Baev, M. V., Farrell, M., Kurnasov, O. V., Daugherty, M. D., Mseeh, F., Polanuyer, B. M., Campbell, J. W., Anantha, S., Shatalin, K. Y., Chowdhury, S. A. K., Fonstein, M. Y., and Osterman, A. L. (2002). From genetic footprinting to antimicrobial drug targets: examples in cofactor biosynthetic pathways. *J Bacteriol*, 184(16):4555–4572.

Glaser, P., Frangeul, L., Buchrieser, C., Rusniok, C., Amend, A., Baquero, F., Berche, P., Bloecker, H., Brandt, P., Chakraborty, T., Charbit, A., Chetouani, F., Couvé, E., de Daruvar, A., Dehoux, P., Domann, E., Domínguez-Bernal, G., Duchaud, E., Durant, L., Dussurget, O., Entian, K. D., Fsihi, H., García-del Portillo, F., Garrido, P., Gautier, L., Goebel, W., Gómez-López, N., Hain, T., Hauf, J., Jackson, D., Jones, L. M., Kaerst, U., Kreft, J., Kuhn, M., Kunst, F., Kurapkat, G., Madueno, E., Maitournam, A., Vicente, J. M., Ng, E., Nedjari, H., Nordsiek, G., Novella, S., de Pablos, B., Pérez-Diaz, J. C., Purcell, R.,

Remmel, B., Rose, M., Schlueter, T., Simoes, N., Tierrez, A., Vázquez-Boland, J. A., Voss, H., Wehland, J., and Cossart, P. (2001). Comparative genomics of Listeria species. *Science*, 294(5543):849–852.

Gonzalez-Ceron, G., Licona, P., and Servin-Gonzalez, L. (2001). Modified xylE and xylTE reporter genes for use in Streptomyces: analysis of the effect of xylT. *FEMS Microbiology Letters*, 196(2):229–234.

Griffiths-Jones, S., Bateman, A., Marshall, M., Khanna, A., and Eddy, S. R. (2003). Rfam: an RNA family database. *Nucleic acids research*, 31(1):439–441.

Griffiths-Jones, S., Moxon, S., Marshall, M., Khanna, A., Eddy, S. R., and Bateman, A. (2005). Rfam: annotating non-coding RNAs in complete genomes. *Nucleic Acids Res*, 33(Database issue):D121–D124.

Grill, S., Busenbender, S., Pfeiffer, M., Köhler, U., and Mack, M. (2008). The bifunctional flavokinase/flavin adenine dinucleotide synthetase from Streptomyces davawensis produces inactive flavin cofactors and is not involved in resistance to the antibiotic roseoflavin. *J Bacteriol*, 190(5):1546–1553.

Grill, S., Yamaguchi, H., Wagner, H., Zwahlen, L., Kusch, U., and Mack, M. (2007). Identification and characterization of two Streptomyces davawensis riboflavin biosynthesis gene clusters. *Archives of Microbiology*, 188(4):377–387.

Gutiérrez-Preciado, A., Torres, A. G., Merino, E., Bonomi, H. R., Goldbaum, F. A., and García-Angulo, V. A. (2015). Extensive Identification of Bacterial Riboflavin Transporters and Their Distribution across Bacterial Species. *PLoS One*, 10(5):e0126124.

Hanahan, D. (1983). Studies on transformation of Escherichia coli with plasmids. *J Mol Biol*, 166(4):557–580.

Hansen, J. M., Gerner-Smidt, P., and Bruun, B. (2005). Antibiotic susceptibility of Listeria monocytogenes in Denmark 1958-2001. *APMIS*, 113(1):31–36.

Haubert, L., Mendonça, M., Lopes, G. V., de Itapema Cardoso, M. R., and da Silva, W. P. (2016). Listeria monocytogenes isolates from food and food

environment harbouring tetM and ermB resistance genes. *Lett Appl Microbiol*, 62(1):23–29.

Hemberger, S., Pedrolli, D. B., Stolz, J., Vogl, C., Lehmann, M., and Mack, M. (2011). RibM from Streptomyces davawensis is a riboflavin/roseoflavin transporter and may be useful for the optimization of riboflavin production strains. *BMC Biotechnology*, 11(1):119.

Herguedas, B., Lans, I., Sebastián, M., Hermoso, J. A., Martínez-Júlvez, M., and Medina, M. (2015). Structural insights into the synthesis of FMN in prokaryotic organisms. *Acta Crystallogr D Biol Crystallogr*, 71(Pt 12):2526–2542.

Hodgson, D. A. (2000). Primary metabolism and its control in streptomycetes: a most unusual group of bacteria. *Adv Microb Physiol*, 42:47–238.

Hopwood, D. A. (2006). Soil to genomics: the Streptomyces chromosome. *Annu Rev Genet*, 40:1–23.

Howe, J. A., Wang, H., Fischmann, T. O., Balibar, C. J., Xiao, L., Galgoci, A. M., Malinverni, J. C., Mayhood, T., Villafania, A., Nahvi, A., Murgolo, N., Barbieri, C. M., Mann, P. A., Carr, D., Xia, E., Zuck, P., Riley, D., Painter, R. E., Walker, S. S., Sherborne, B., de Jesus, R., Pan, W., Plotkin, M. A., Wu, J., Rindgen, D., Cummings, J., Garlisi, C. G., Zhang, R., Sheth, P. R., Gill, C. J., Tang, H., and Roemer, T. (2015). Selective small-molecule inhibition of an RNA structural element. *Nature*, 526(7575):672–677.

Ingram, C., Brawner, M., Youngman, P., and Westpheling, J. (1989). xylE functions as an efficient reporter gene in Streptomyces spp.: use for the study of galP1, a catabolite-controlled promoter. *Journal of Bacteriology*, 171(12):6617–6624.

Jacob, F. and Monod, J. (1961). Genetic regulatory mechanisms in the synthesis of proteins. *J Mol Biol*, 3:318–356.

Jankowitsch, F., Kuhm, C., Kellner, R., Kalinowski, J., Pelzer, S., Macheroux, P., and Mack, M. (2011). A Novel N,N-8-Amino-8-demethyl-D-riboflavin Dimethyltransferase (RosA) Catalyzing the Two Terminal Steps of Rose-

oflavin Biosynthesis in Streptomyces davawensis. *Journal of Biological Chemistry*, 286(44):38275–38285.

Jankowitsch, F., Schwarz, J., Rückert, C., Gust, B., Szczepanowski, R., Blom, J., Pelzer, S., Kalinowski, J., and Mack, M. (2012). Genome sequence of the bacterium Streptomyces davawensis JCM 4913 and heterologous production of the unique antibiotic roseoflavin. *J Bacteriol*, 194(24):6818–6827.

Jones, A. C., Gust, B., Kulik, A., Heide, L., Buttner, M. J., and Bibb, M. J. (2013). Phage p1-derived artificial chromosomes facilitate heterologous expression of the FK506 gene cluster. *PloS one*, 8(7):e69319.

Jones, G. H. (2011). Integrative, xylE-based promoter probe vectors for use in Streptomyces. *Plasmid*, 65(3):219–225.

Karpowich, N. K., Song, J. M., Cocco, N., and Wang, D.-N. (2015). ATP binding drives substrate capture in an ECF transporter by a release-and-catch mechanism. *Nature structural & molecular biology*, 22(7):565–571.

Karthikeyan, S., Zhou, Q., Mseeh, F., Grishin, N. V., Osterman, A. L., and Zhang, H. (2003). Crystal structure of human riboflavin kinase reveals a beta barrel fold and a novel active site arch. *Structure*, 11(3):265–273.

Kenneth, A. and Goody, R. S. (2011). The original Michaelis Constant: Translation of the 1913 Michaelis-Menten paper. *Biochemistry*, 50(39):8264–8269.

Kieser, T., Bibb, M. J., Buttner, M. J., Chater, K. F., and Hopwood, D. A. (2000). *Practical Streptomyces Genetics*. John Innes Foundation, Norwich.

Kil, Y. V., Mironov, V. N., Gorishin IYu, Kreneva, R. A., and Perumov, D. A. (1992). Riboflavin operon of Bacillus subtilis: unusual symmetric arrangement of the regulatory region. *Mol Gen Genet*, 233(3):483–486.

King, A. A. and Chater, K. F. (1986). The expression of the Escherichia coli lacZ gene in Streptomyces. *J Gen Microbiol*, 132(6):1739–1752.

Kreneva, R., Gelfand, M., Mironov, A., Iomantas, I., Kozlov, I., Mironov, A., and Perumov, D. (2000). Study of the phenotypic occurrence of *ypaA* gene inactivation in *Bacillus subtilis*. *Genetika*, 36(8):1166.

Langer, S., Hashimoto, M., Hobl, B., Mathes, T., and Mack, M. (2013a). Flavoproteins Are Potential Targets for the Antibiotic Roseoflavin in Escherichia coli. *Journal of Bacteriology*, 195(18):4037–4045.

Langer, S., Nakanishi, S., Mathes, T., Knaus, T., Binter, A., Macheroux, P., Mase, T., Miyakawa, T., Tanokura, M., and Mack, M. (2013b). The Flavoenzyme Azobenzene Reductase AzoR from Escherichia coli Binds Roseoflavin Mononucleotide (RoFMN) with High Affinity and Is Less Active in Its RoFMN Form. *Biochemistry*, 52(25):4288–4295.

Lee, E. R., Blount, K. F., and Breaker, R. R. (2009). Roseoflavin is a natural antibacterial compound that binds to FMN riboswitches and regulates gene expression. *RNA Biol*, 6(2):187–194.

Liu, D., editor (2008). *Handbook of Listeria monocytogenes*. CRC Press.

Luo, Y., Zhang, L., Barton, K. W., and Zhao, H. (2015). Systematic Identification of a Panel of Strong Constitutive Promoters from Streptomyces albus. *ACS Synth Biol*, 4(9):1001–1010.

Macheroux, P., Kappes, B., and Ealick, S. E. (2011). Flavogenomics - a genomic and structural view of flavin-dependent proteins. *FEBS Journal*, 278(15):2625–2634.

Mack, M. and Grill, S. (2006). Riboflavin analogs and inhibitors of riboflavin biosynthesis. *Appl Microbiol Biotechnol*, 71(3):265–275.

Mack, M., van Loon, A. P., and Hohmann, H. P. (1998). Regulation of riboflavin biosynthesis in Bacillus subtilis is affected by the activity of the flavokinase/flavin adenine dinucleotide synthetase encoded by ribC. *J Bacteriol*, 180(4):950–955.

MacNeil, D. J., Gewain, K. M., Ruby, C. L., Dezeny, G., Gibbons, P. H., and MacNeil, T. (1992). Analysis of Streptomyces avermitilis genes required for avermectin biosynthesis utilizing a novel integration vector. *Gene*, 111(1):61–68.

Mansjö, M. and Johansson, J. (2011). The Riboflavin analog Roseoflavin targets

an FMN-riboswitch and blocks Listeria monocytogenes growth, but also stimulates virulence gene-expression and infection. *RNA Biology*, 8(4):674–680.

Manstein, D. J. and Pai, E. F. (1986). Purification and characterization of FAD synthetase from Brevibacterium ammoniagenes. *J Biol Chem*, 261(34):16169–16173.

Mashhadi, Z., Xu, H., Grochowski, L. L., and White, R. H. (2010). Archaeal RibL: a new FAD synthetase that is air sensitive. *Biochemistry*, 49(40):8748–8755.

Massey, V. (1994). Activation of molecular oxygen by flavins and flavoproteins. *J Biol Chem*, 269(36):22459–22462.

Massey, V. (1995). Introduction: flavoprotein structure and mechanism. *FASEB J*, 9(7):473–475.

Michaelis, L. and Menten, M. L. (1913). Die Kinetik der Invertinwirkung. *Biochemische Zeitschrift*, 49:333–369.

Miller, E. M. and Nickoloff, J. A. (1995). Escherichia coli electrotransformation. In *Electroporation Protocols for Microorganisms*, pages 105–113. Springer.

Mironov, A. S., Gusarov, I., Rafikov, R., Lopez, L. E., Shatalin, K., Kreneva, R. A., Perumov, D. A., and Nudler, E. (2002). Sensing Small Molecules by Nascent RNAA Mechanism to Control Transcription in Bacteria. *Cell*, 111(5):747–756.

Mobitec (2012). *Bacillus subtilis Expression Vectors*. MoBiTec GmbH, Germany.

Myronovskyi, M., Welle, E., Fedorenko, V., and Luzhetskyy, A. (2011). -Glucuronidase as a Sensitive and Versatile Reporter in Actinomycetes. *Applied and Environmental Microbiology*, 77(15):5370–5383.

Nahvi, A., Sudarsan, N., Ebert, M. S., Zou, X., Brown, K. L., and Breaker, R. R. (2002). Genetic control by a metabolite binding mRNA. *Chem Biol*, 9(9):1043.

NEB (E8200). *pMAL Protein Fusion and Purification System - Instruction Manual*. New England Biolabs.

Neidhardt, F., editor (1994). *Escherichia coli and Salmonella. Cellular and Molecular Biology*, chapter Biosynthesis of Riboflavin, pages 657–664. American Society for Microbiology, Washington, DC.

Novagen (2002). *pET System Manual*. Novagen, 10th edition.

Novagen (2011). *His·Tag® Monoclonal Antibody. User Protocol TB283 Rev. D 0611JN*. Novagen.

O'Kane, C., Stephens, M., and McConnell, D. (1986). Integrable alpha-amylase plasmid for generating random transcriptional fusions in Bacillus subtilis. *Journal of bacteriology*, 168(2):973–981.

Otani, S., Matsui, K., and Kasai, S. (1997). Chemistry and biochemistry of 8-aminoflavins. *Osaka City Med J*, 43(2):107–137.

Otani, S., Takatsu, M., Nakano, M., Kasai, S., and Miura, R. (1974). Letter: Roseoflavin, a new antimicrobial pigment from Streptomyces. *J Antibiot (Tokyo)*, 27(1):86–87.

Ott, E., Stolz, J., and Mack, M. (2009). The RFN riboswitch of Bacillus subtilis is a target for the antibiotic roseoflavin produced by Streptomyces davawensis. *RNA Biology*, 6:276–280.

Overbeek, R., Fonstein, M., D'Souza, M., Pusch, G. D., and Maltsev, N. (1999). The use of gene clusters to infer functional coupling. *Proc Natl Acad Sci U S A*, 96(6):2896–2901.

Pedrolli, D. B., Jankowitsch, F., Schwarz, J., Langer, S., Nakanishi, S., and Mack, M. (2014). Natural riboflavin analogs. *Methods Mol Biol*, 1146:41–63.

Pedrolli, D. B., Kühm, C., Sévin, D. C., Vockenhuber, M. P., Sauer, U., Suess, B., and Mack, M. (2015a). A dual control mechanism synchronizes riboflavin and sulphur metabolism in Bacillus subtilis. *Proc Natl Acad Sci U S A*, 112(45):14054–14059.

Pedrolli, D. B., Langer, S., Hobl, B., Schwarz, J., Hashimoto, M., and Mack, M. (2015b). The ribB FMN riboswitch from Escherichia coli operates at the

transcriptional and translational level and regulates riboflavin biosynthesis. *FEBS J*, 282(16):3230–3242.

Pedrolli, D. B. and Mack, M. (2014). Bacterial flavin mononucleotide riboswitches as targets for flavin analogs. *Methods Mol Biol*, 1103:165–176.

Pedrolli, D. B., Matern, A., Wang, J., Ester, M., Siedler, K., Breaker, R., and Mack, M. (2012). A highly specialized flavin mononucleotide riboswitch responds differently to similar ligands and confers roseoflavin resistance to Streptomyces davawensis. *Nucleic Acids Research*, 40(17):8662–8673.

Pedrolli, D. B., Nakanishi, S., Barile, M., Mansurova, M., Carmona, E. C., Lux, A., Gärtner, W., and Mack, M. (2011). The antibiotics roseoflavin and 8-demethyl-8-amino-riboflavin from Streptomyces davawensis are metabolized by human flavokinase and human FAD synthetase. *Biochemical Pharmacology*, 82(12):1853–1859.

Perkins, J. B. and Pero, J. G. (2001). *Bacillus subtilis and Its Relatives: From Genes to Cells*, chapter Vitamin biosynthesis, pages 279–293. American Society for Microbiology, Washington, DC.

Poyart-Salmeron, C., Carlier, C., Trieu-Cuot, P., Courtieu, A. L., and Courvalin, P. (1990). Transferable plasmid-mediated antibiotic resistance in Listeria monocytogenes. *Lancet*, 335(8703):1422–1426.

Premaratne, R. J., Lin, W. J., and Johnson, E. A. (1991). Development of an improved chemically defined minimal medium for Listeria monocytogenes. *Appl Environ Microbiol*, 57(10):3046–3048.

Procópio, R. E. d. L., Silva, I. R. d., Martins, M. K., Azevedo, J. L. d., and Araújo, J. M. d. (2012). Antibiotics produced by Streptomyces. *Braz J Infect Dis*, 16(5):466–471.

Reihl, P. and Stolz, J. (2005). The monocarboxylate transporter homolog Mch5p catalyzes riboflavin (vitamin B2) uptake in Saccharomyces cerevisiae. *J Biol Chem*, 280(48):39809–39817.

Rudolph, M. M., Vockenhuber, M.-P., and Suess, B. (2013). Synthetic ri-

boswitches for the conditional control of gene expression in Streptomyces coelicolor. *Microbiology*, 159(Pt 7):1416–1422.

Sambrook, J. and Russell, D. (2001). *Molecular Cloning: A Laboratory Manual*. Cold Spring Harbor Laboratory Press.

Sandoval, F. J., Zhang, Y., and Roje, S. (2008). Flavin nucleotide metabolism in plants: monofunctional enzymes synthesize fad in plastids. *J Biol Chem*, 283(45):30890–30900.

Santos, M. A., Jimenez, A., and Revuelta, J. L. (2000). Molecular characterization of FMN1, the structural gene for the monofunctional flavokinase of Saccharomyces cerevisiae. *J Biol Chem*, 275(37):28618–28624.

Sauer, E., Merdanovic, M., Mortimer, A. P., Bringmann, G., and Reidl, J. (2004). PnuC and the utilization of the nicotinamide riboside analog 3-aminopyridine in Haemophilus influenzae. *Antimicrob Agents Chemother*, 48(12):4532–4541.

Schuppler, M. and Loessner, M. J. (2010). The Opportunistic Pathogen Listeria monocytogenes: Pathogenicity and Interaction with the Mucosal Immune System. *Int J Inflam*, 2010:704321.

Schwarz, J., Konjik, V., Jankowitsch, F., Sandhoff, R., and Mack, M. (2016). Identification of the Key Enzyme of Roseoflavin Biosynthesis. *Angewandte Chemie International Edition*. doi:10.1002/anie.201600581.

Seghezzi, N., Amar, P., Koebmann, B., Jensen, P. R., and Virolle, M.-J. (2011). The construction of a library of synthetic promoters revealed some specific features of strong Streptomyces promoters. *Appl Microbiol Biotechnol*, 90(2):615–623.

Serganov, A., Huang, L., and Patel, D. J. (2009). Coenzyme recognition and gene regulation by a flavin mononucleotide riboswitch. *Nature*, 458(7235):233–237.

Serganov, A. and Nudler, E. (2013). A decade of riboswitches. *Cell*, 152(1-2):17–24.

Serrano, A., Frago, S., Herguedas, B., Martínez-Júlvez, M., Velázquez-Campoy,

A., and Medina, M. (2013). Key Residues at the Riboflavin Kinase Catalytic Site of the Bifunctional Riboflavin Kinase/FMN Adenylyltransferase From Corynebacterium ammoniagenes. *Cell Biochemistry and Biophysics*, 65(1):57–68.

Serrano, A., Frago, S., Velázquez-Campoy, A., and Medina, M. (2012). Role of Key Residues at the Flavin Mononucleotide (FMN):Adenylyltransferase Catalytic Site of the Bifunctional Riboflavin Kinase/Flavin Adenine Dinucleotide (FAD) Synthetase from Corynebacterium ammoniagenes. *International Journal of Molecular Sciences*, 13(12):14492–14517.

Sklyarova, S. A. and Mironov, A. S. (2014). Bacillus subtilis ypaA gene regulation mechanism by FMN riboswitch. *Russ J Genet*, 50(3):319–322.

Sneath, P. H. A. and Sokal, R. R. (1973). *Numerical taxonomy. The principles and practices of numerical classification*. W.H. Freeman, San Francisco.

Solovieva, I. M., Kreneva, R. A., Leak, D. J., and Perumov, D. A. (1999). The ribR gene encodes a monofunctional riboflavin kinase which is involved in regulation of the Bacillus subtilis riboflavin operon. *Microbiology*, 145 (Pt 1):67–73.

Spizizen, J. (1958). Transformation of biochemically deficient strains of Bacillus subtilis by deoxyribonucleate. *Proceedings of the National Academy of Sciences*, 44(10):1072–1078.

Stragier, P., Bonamy, C., and Karmazyn-Campelli, C. (1988). Processing of a sporulation sigma factor in Bacillus subtilis: How morphological structure could control gene expression. *Cell*, 52(5):697–704.

Strohl, W. R. (1992). Compilation and analysis of DNA sequences associated with apparent streptomycete promoters. *Nucleic Acids Res*, 20(5):961–974.

Sudarsan, N., Hammond, M. C., Block, K. F., Welz, R., Barrick, J. E., Roth, A., and Breaker, R. R. (2006). Tandem riboswitch architectures exhibit complex gene control functions. *Science*, 314(5797):300–304.

Takemoto, N., Tanaka, Y., Inui, M., and Yukawa, H. (2014). The physiological

role of riboflavin transporter and involvement of FMN-riboswitch in its gene expression in Corynebacterium glutamicum. *Appl Microbiol Biotechnol*.

Tilney, L. G. and Portnoy, D. A. (1989). Actin filaments and the growth, movement, and spread of the intracellular bacterial parasite, Listeria monocytogenes. *J Cell Biol*, 109(4 Pt 1):1597–1608.

Toledo-Arana, A., Dussurget, O., Nikitas, G., Sesto, N., Guet-Revillet, H., Balestrino, D., Loh, E., Gripenland, J., Tiensuu, T., Vaitkevicius, K., Barthelemy, M., Vergassola, M., Nahori, M.-A., Soubigou, G., Régnault, B., Coppée, J.-Y., Lecuit, M., Johansson, J., and Cossart, P. (2009). The Listeria transcriptional landscape from saprophytism to virulence. *Nature*, 459(7249):950–956.

Troxler, R., von Graevenitz, A., Funke, G., Wiedemann, B., and Stock, I. (2000). Natural antibiotic susceptibility of Listeria species: L. grayi, L. innocua, L. ivanovii, L. monocytogenes, L. seeligeri and L. welshimeri strains. *Clin Microbiol Infect*, 6(10):525–535.

Tsakris, A., Papa, A., Douboyas, J., and Antoniadis, A. (1997). Neonatal meningitis due to multi-resistant Listeria monocytogenes. *J Antimicrob Chemother*, 39(4):553–554.

Tung, W. L. and Chow, K. C. (1995). A modified medium for efficient electrotransformation of E. coli. *Trends Genet*, 11(4):128–129.

Vázquez-Boland, J. A., Kuhn, M., Berche, P., Chakraborty, T., Domínguez-Bernal, G., Goebel, W., González-Zorn, B., Wehland, J., and Kreft, J. (2001). Listeria pathogenesis and molecular virulence determinants. *Clin Microbiol Rev*, 14(3):584–640.

Vitreschak, A. G., Rodionov, D. A., Mironov, A. A., and Gelfand, M. S. (2002). Regulation of riboflavin biosynthesis and transport genes in bacteria by transcriptional and translational attenuation. *Nucleic Acids Research*, 30(14):3141–3151.

Vogl, C., Grill, S., Schilling, O., Stulke, J., Mack, M., and Stolz, J. (2007). Charac-

terization of Riboflavin (Vitamin B2) Transport Proteins from Bacillus subtilis and Corynebacterium glutamicum. *Journal of Bacteriology*, 189(20):7367–7375.

von Canstein, H., Ogawa, J., Shimizu, S., and Lloyd, J. R. (2007). Secretion of Flavins by Shewanella Species and Their Role in Extracellular Electron Transfer. *Applied and Environmental Microbiology*, 74(3):615–623.

Waksman, S. A. and Henrici, A. T. (1943). The Nomenclature and Classification of the Actinomycetes. *J Bacteriol*, 46(4):337–341.

Walsh, C., Fisher, J., Spencer, R., Graham, D. W., Ashton, W. T., Brown, J. E., Brown, R. D., and Rogers, E. F. (1978). Chemical and enzymatic properties of riboflavin analogues. *Biochemistry*, 17(10):1942–1951.

Wickiser, J. K., Winkler, W. C., Breaker, R. R., and Crothers, D. M. (2005). The Speed of RNA Transcription and Metabolite Binding Kinetics Operate an FMN Riboswitch. *Molecular Cell*, 18(1):49–60.

Winkler, J., Eltis, L. D., Dwyer, D. F., and Rohde, M. (1995). Tetrameric structure and cellular location of catechol 2,3-dioxygenase. *Arch Microbiol*, 163(1):65–69.

Winkler, W. C., Cohen-Chalamish, S., and Breaker, R. R. (2002). An mRNA structure that controls gene expression by binding FMN. *Proc Natl Acad Sci U S A*, 99(25):15908–15913.

Wu, M., Repetto, B., Glerum, D. M., and Tzagoloff, A. (1995). Cloning and characterization of FAD1, the structural gene for flavin adenine dinucleotide synthetase of Saccharomyces cerevisiae. *Mol Cell Biol*, 15(1):264–271.

Wurtzel, O., Sesto, N., Mellin, J. R., Karunker, I., Edelheit, S., Bécavin, C., Archambaud, C., Cossart, P., and Sorek, R. (2012). Comparative transcriptomics of pathogenic and non-pathogenic Listeria species. *Mol Syst Biol*, 8:583.

Yao, Y., Yonezawa, A., Yoshimatsu, H., Masuda, S., Katsura, T., and Inui, K.-I. (2010). Identification and comparative functional characterization of a new human riboflavin transporter hRFT3 expressed in the brain. *J Nutr*, 140(7):1220–1226.

Yonezawa, A., Masuda, S., Katsura, T., and Inui, K.-i. (2008). Identification and functional characterization of a novel human and rat riboflavin transporter, RFT1. *Am J Physiol Cell Physiol*, 295(3):C632–C641.

Yruela, I., Arilla-Luna, S., Medina, M., and Contreras-Moreira, B. (2010). Evolutionary divergence of chloroplast FAD synthetase proteins. *BMC Evol Biol*, 10:311.

Zuker, M. (2003). Mfold web server for nucleic acid folding and hybridization prediction. *Nucleic acids research*, 31(13):3406–3415.

Zukowski, M. M., Gaffney, D. F., Speck, D., Kauffmann, M., Findeli, A., Wisecup, A., and Lecocq, J. P. (1983). Chromogenic identification of genetic regulatory signals in Bacillus subtilis based on expression of a cloned Pseudomonas gene. *Proceedings of the National Academy of Sciences*, 80(4):1101–1105.